Functional organization of vestibulospinal inputs to spinal neurons involved in autonomic and motor control

Doctoral Thesis by

Nedim Kasumacic

Department of Physiology

Institute of Basic Medical Sciences

Faculty of Medicine

University of Oslo

Norway

2012

Series of dissertations submitted to the
Faculty of Medicine, University of Oslo
No. 1366

ISBN 978-82-8264-475-4

Cover: Inger Sandved Anfinsen.
Printed in Norway: AIT Oslo AS.

Produced in co-operation with Unipub.
The thesis is produced by Unipub merely in connection with the
thesis defence. Kindly direct all inquiries regarding the thesis to the copyright
holder or the unit which grants the doctorate.

“It is easy to underrate the importance of a sensory system whose receptors are buried deep within the skull and of whose performance we are usually not aware. It is only when it malfunctions that we know we have a vestibular system!”

-Victor J. Wilson and Geoffrey Melvill Jones

TABLE OF CONTENTS

9. Data presentation and statistics
10. The advantages and limitations of calcium imaging as a tool to study neuronal circuits

AIMS OF THE STUDY

SUMMARIES OF INDIVIDUAL PAPERS

Paper I

Paper II

Paper III

LIST OF REFERENCES

PAPERS I-III

ACKNOWLEDGEMENTS

Work presented in this thesis was performed at the University of Oslo at the department of Physiology in the period 2007-2012.

I want to start by thanking my two supervisors Marie-Claude Perreault and Joel Glover for their guidance and support during my PhD. Thank you for giving me this opportunity and for all the time you have invested in me.

I also want to thank the Faculty of Medicine for the financial support for this thesis through their PhD stipend program.

Doing a PhD is a long and at times frustrating process filled with ups and downs. I have been fortunate to have had a lot of wonderful people around me who have made it so much easier to complete this work.
I want to thank my friends at the Glover lab for the great times we have had together. I am grateful to Dr. Gabor Halasi "Gibir" for being the best office mate anyone could wish for. With your openness and quirky since of humor, you have made this time unforgettable. I am also grateful to Karolina "Lina" Szokol for everything she has taught me and for being a great friend.
Thanks to all my other friends Magne, Francois, Åse-Marit, Mrinal, Kobra, Jean-Luc, Ushi, Marian and all the wonderful people at the Glover lab and the Department of Physiology.

Finally, I want to thank my family for their support and encouragement to finish this thesis.

Thanks to my wife Kristina for being my greatest supporter and best friend.

PAPERS INCLUDED IN THIS THESIS

Paper I **Nedim Kasumacic,** Joel C. Glover and Marie-Claude Perreault

Segmental patterns of vestibular-mediated synaptic inputs to axial and limb motoneurons in the neonatal mouse assessed by optical recording.

Journal of Physiology, 2010 588:4905-25

Paper II **Nedim Kasumacic,** Joel C. Glover and Marie-Claude Perreault

Vestibular-mediated synaptic inputs and pathways to sympathetic preganglionic neurons in the neonatal mouse.

Submitted to:

Paper III **Nedim Kasumacic,** Joel C. Glover and Marie-Claude Perreault

Vestibular inputs to descending commissural inter neurons in the thoracic and lumbar spinal cord of the neonatal mouse investigated with calcium imaging

Manuscript

ABBREVIATIONS

aCINs	acsending commissural interneurons
aCSF	artificial cerebrospinal fluid
aIINs	acsending ipsilateral inter neurons
BAPTA	(1,2-bis(o-aminophenoxy)ethane-N,N,N',N'-tetraacetic acid)
bCINs	bifurcating commissural interneurons
bIIN	bifurcating ipsilateral interneurons
CCD	charge-coupled device
CGDA	calcium green dextran amine
cMVST	contralateral medial vestibulospinal tract
CNS	central nervous system
dCINs	descending commissural interneurons
dIINs	descending ipsilateral interneurons
DVN	descending vestibular nucleus
E	embryonic day
EPSPs	excitatory postsynaptic potentials
FRET	fluorescence resonance energy transfer
GABA	gamma amino butyric acid
HMC	hypaxial motor column
HRP	horseradish peroxidase
iMVST	ipsilateral medial vestibulospinal tract
INs	interneurons
IPSPs	inhibitory postsynaptic potentials
IVN	inferior vestibular nucleus

LMC	lateral motor column
LVN	lateral vestibular nucleus
LVST	lateral vestibulospinal tract
mM	millimolar
MLF	medial longitudinal fascicle
MMC	medial motor column
MNs	motor neurons
MVN	medial vestibular nucleus
MVST	medial vestibulospinal tract
P	postnatal day
PGC	preganglionic motor column
PTX	picrotoxin
RDA	rhodamine dextran amine
ROI	region of interest
RVLM	rostral ventrolateral medulla
SEM	standard error
SPNs	sympathetic preganglionic neurons
STD	standard deviation
SVN	superior vestibular nucleus
V	trigeminal nerve
VIII	vestibulocochlear nerve

GENERAL INTRODUCTION

Overall organization of axonal tracts and neurons in the mammalian spinal cord

The mammalian spinal cord is composed of an inner grey matter containing the somata of spinal neurons, and an outer white matter, containing the axons of spinal neurons and of descending and ascending tract neurons. The white matter is roughly divided into three funiculi, the ventral funiculus, lateral funiculus and the dorsal funiculus. The dorsal funiculus contains predominantly axons that carry somatic sensory information to the brain, whereas the lateral and ventral funiculi contain axons that ascend to brain structures as well as those that descend from the brain to the spinal cord (Kandel et al 2000).

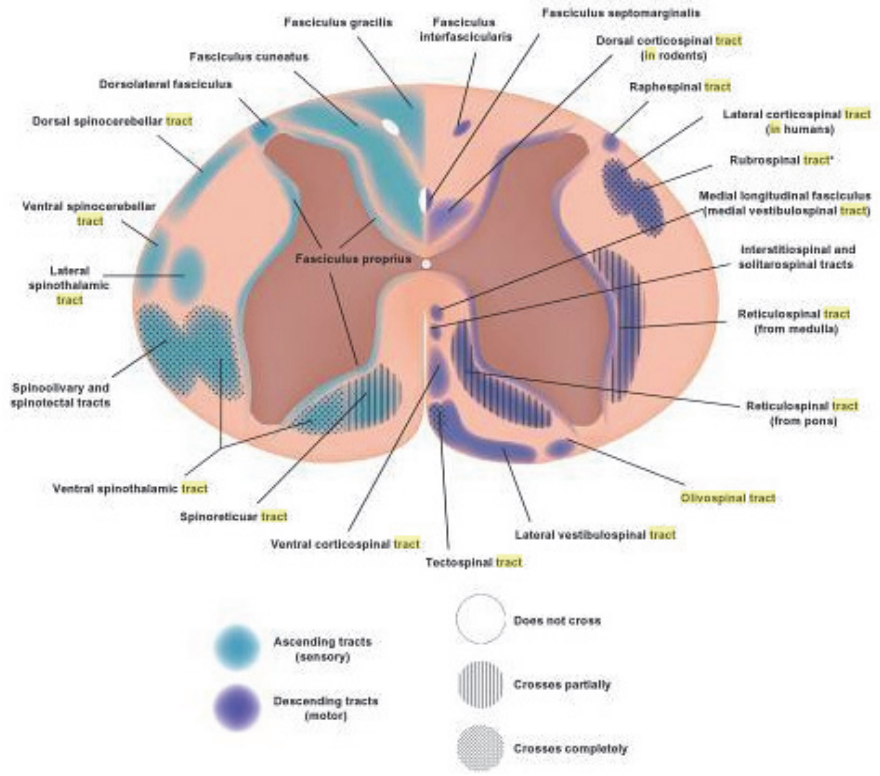

Figure 1. Organization of descending and ascending tracts in the spinal cord. Adapted from Comparative Anatomy and Histology: A Mouse and Human Atlas By Piper M. Treuting and Suzanne Dintzis.

The spinal cord contains three major types of neurons. The somatic motoneurons (MNs), whose axons project to the periphery and innervate striated musculature, are situated in the ventral horn through all segments of the spinal cord (Dasen and Jessell 2009). The sympathetic preganglionic neurons (SPNs) that innervate postganglionic sympathetic neurons are situated in the intermediolateral horn of the thoracic cord (Dasen and Jessell 2009). Finally the third group, the spinal interneurons distributed throughout the whole extent of the spinal cord, includes propriospinal neurons and ascending neurons.

Spinal MNs are organized at three levels. Firstly, there is a columnar division giving rise to four distinct motor columns, the medial (MMC), the lateral (LMC), the hypaxial (HMC) and the preganglionic (PGC). The MMC extends in the medial part of the ventral horn throughout the whole length of the spinal cord, whereas the LMC is found only in the brachial and lumbar enlargements. The HMC and the PGC are only found in thoracic segments. MNs within the MMC innervate axial and proximal limb musculature, whereas those of the LMC innervate predominantly limb musculature and those in the HMC innervate intercostal muscles (cat: Romanes 1951, human: Routal and Pal 1999, rat: Nicolopoulos-Stournaras and Iles 1983; McKenna et al 2000; Smith and Hollyday 1983). Secondly, the LMC and the MMC are subdivided further. This has been especially well described in the chicken embryo, where it is clear that the LMC divides into a medial and lateral part. The medial projects to ventral muscles in the limb, whereas the lateral projects to dorsal muscles of the limb

(Landmesser 1978). The MMC has a similar subdivision where the medial MMC neurons innervate dorsal axial muscles while the lateral MMC neurons (found at the thoracic level innervate body wall musculature). Finally, the third level of MN organization is the segregation of MNs into MN pools, each of which innervates a specific muscle (rabbit: Romanes 1941; cat: Romanes 1964; chicken embryo: Hollyday 1980). A single pool can consist of few or many MNs and may extend across a few spinal segments.

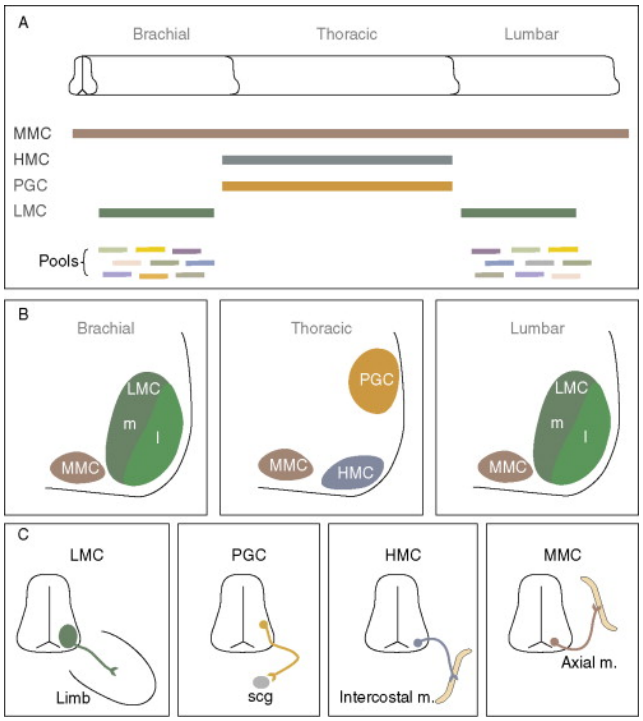

Figure 2. The levels of organization of spinal MNs
MNs in the brachial and lumbar enlargements are organized in two columns, the MMC (innervates axial musculature) and the LMC (innervates limb musculature). Efferent neurons in the thoracic cord are organized into three columns. Two of these are MN columns, the MMC and the HMC (hypaxial motor column, which innervates intercostal musculature), and the third is the PGC (preganglionic column) that innervates postganglionic sympathetic neurons. MNs are further subdivided into pools where MNs of a given pool innervate the same muscle.
A) Longitudinal view, **B)** transverse view, **C)** innervation patterns. scg.: sympathetic chain ganglion *Adapted from: Dasen and Jessell 2009.*

Spinal MNs are greatly outnumbered by the various types of inter neurons (INs) in the spinal grey matter. Anatomically, INs can be divided into different groups based on their axonal trajectories. Ipsilaterally and contralaterally projecting INs with ascending or descending axons (aIINs, dIINs, aCINs, and dCINs), ipsilaterally and contralaterally projecting INs with bifurcating axons (bIINs and bCINs) and short-range ipsilaterally and contralaterally INs with only intrasegmental projections (Eide et al 1999, Nissen et al 2005, Stokke et al 2002). Spinal INs have many functions because they can be part of different sensorimotor and autonomic networks. As major targets of sensory afferent terminals, they convey sensory information to other spinal INs, MNs and to supraspinal structures (Kandel 2000). As part of sensory-motor circuits they produce sensory-motor reflexes as well as more complex outputs such as locomotion (sensory reflexes: Kandel et al 2000, locomotion: Kiehn and Butt 2003; McCrea and Rybak 2008; Dougherty and Kiehn 2010). Finally, as targets of brainstem and higher order descending axons, they represent important components in descending motor control (Davies and Edgley 1994; Takakusaki et al 2001; Krutki et al 2003; Cabaj et al 2006; Szokol et al 2011).

The anatomy and physiology of the vestibulospinal system

For any animal, including humans, to survive, it is imperative to have the ability to successfully navigate through space. Even a simple task, such as holding our head straight up, requires an innate sense of position in space. The vestibular system has evolved to help us manage the challenge of maintaining body orientation and balance. The sensory organ of the vestibular system, the non-cochlear labyrinth, has the ability to detect linear and angular acceleration by virtue of its five specialized sensory end organs. Within these are located specialized hair cells equipped with cilia that become deflected during acceleration of the head. This in turn depolarizes the hair cells, which make synapses onto sensory neurons that translate the patterns of hair cell activation into patterns of action potentials that carry the information about head acceleration into the central nervous system. This information, when processed by the appropriate neuronal networks, helps us maintain balance, stabilize gaze and execute movements. In the following sections I will describe the anatomy and physiology of the vestibulo-spinal system, and how, in concert with other systems, it exerts its function within the body.

1. The vestibular labyrinth

The two vestibular labyrinths, buried deep within the temporal bones on each side of the head, are each made up of five sensory end organs. The saccule and utricle, commonly called the otolith organs, detect linear acceleration as well as static position of the head relative to gravity. The three semicircular canals detect angular acceleration. Sensory information deriving from the five sensory end organs is conveyed to the brainstem, by the sensory afferent fibers of the vestibular ramus of the VIIIth cranial nerve (vestibulocochlear nerve). The cell bodies of the primary vestibular sensory afferent fibers are situated in the vestibular ganglion (or Scarpa's

ganglion) adjacent to the labyrinth and the cochlea. The gross anatomy of the vestibular labyrinth and its relationship to different branches of the vestibular nerve is shown in figure 3.

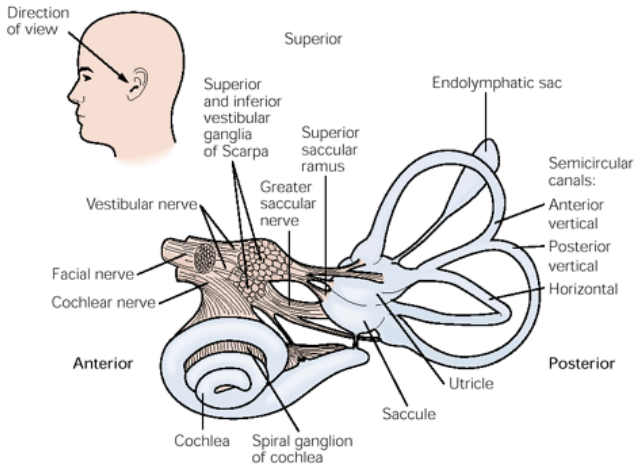

Figure 3.The labyrinth and its innervation. *Source: Kandel et al 2000.*

Vestibular hair cells

Hair cells, which form the basis for vestibular as well as cochlear function, have the ability to transduce mechanical stimuli into receptor potentials. They are located within a specialized sensory epithelium in the vestibular sensory end organs and are equipped with two types of cilia. Every hair cell has several stereocilia and one kinocilium. Movement of the cilia towards the kinocilium opens mechanically gated potassium channels, which depolarize the hair cells by virtue of an inward potassium current (because of the endolymph's high potassium concentration relative to the cerebrospinal fluid; Hudspeth 1985). By contrast, movement away from the kinocilium hyperpolarizes the hair cells (figure 4A). At rest, the hair cells activate vestibular afferent fibers by their tonic release of the neurotransmitter glutamate (Raymond et al 1988). Depolarization and hyperpolarization respectively increase and

decrease the amount of glutamate released, which thus increases or decreases the firing frequency of the vestibular sensory afferent fibers. Two types of hair cells exist, and they differ in their morphology and in the shape of their synaptic contacts with primary vestibular axons (figure 4 B). Type I cells, which are found only in higher vertebrates (mammals and birds), are pear-shaped and are innervated by a calyceal afferent terminal that entirely envelopes the cell. Type II cells, found in all vertebrates, have a cylindrical shape and are innervated by bud-shaped afferent terminals. A given end organ in mammals and birds contains both Type I and II cells. Although both semicircular canals and otolith organs have the same types of hair cells, the anatomical arrangement of the cells and the mechanics that lead to cilia deflection differ greatly.

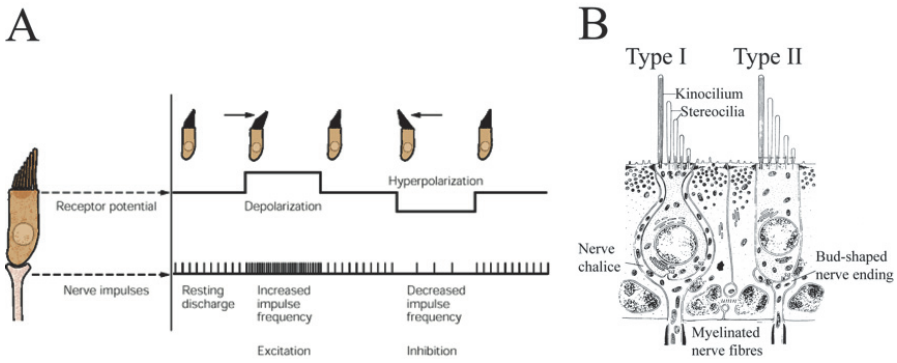

Figure 4. Physiology and anatomy of the hair cells in the inner ear. A) Cilia deflection towards the kinocilium depolarizes the hair cells and causes an increase in the firing rate of the vestibular sensory afferents. Deflection away from the kinocilim results in hyperpolarization of the hair cells and a decrease in the firing rate of the vestibular sensory afferents. *Source: Kandel et al 2000.* **B)** Structure of type I and type II hair cells. *Source: Benson et al 1982.*

Otolith organs

Hair cells of the saccule and utricle are found within structures called maculae. The distal ends of the hair cell cilia project into a gelatinous membrane, the otolithic membrane, which is embedded with calcium carbonate stones (otoconia, figure

5A).Static head tilts (because of gravitational acceleration) or linear accelerations of the head (because of the otolithic membrane's inertia) lead to deflection of the cilia(figure 5B). The macula of the saccule is oriented vertically whereas the macula of the utricle is oriented horizontally (figure 5C). The saccule is thus specialized for the detection of vertical movements, such as riding in an elevator, whereas the utricle is specialized for detection of horizontal movements, such is riding in a car. Furthermore, both organs have a continuous variation in the axis of polarization of the hair cells (relative locations of kinocilium and sterecilia),resulting in the ability to detect linear acceleration in virtually any direction. Finally, each macula is divided at the midline by a structure called the striola. Hair cells on either side of the striola have opposite polarities (Figure 5C).

In addition to detecting linear acceleration of the head, the otolith organs can detect absolute position of the head in space. Linear movement will lead to a transient deflection of the cilia during the acceleration period, and thus a transient change in afferent firing frequency, whereas continuous tilting of the head will lead to a continual deflection. Thus, as long as the head is tilted, the cilia of the hair cells that respond to the given direction of tilt will remain deflected as long as the tilt prevails.

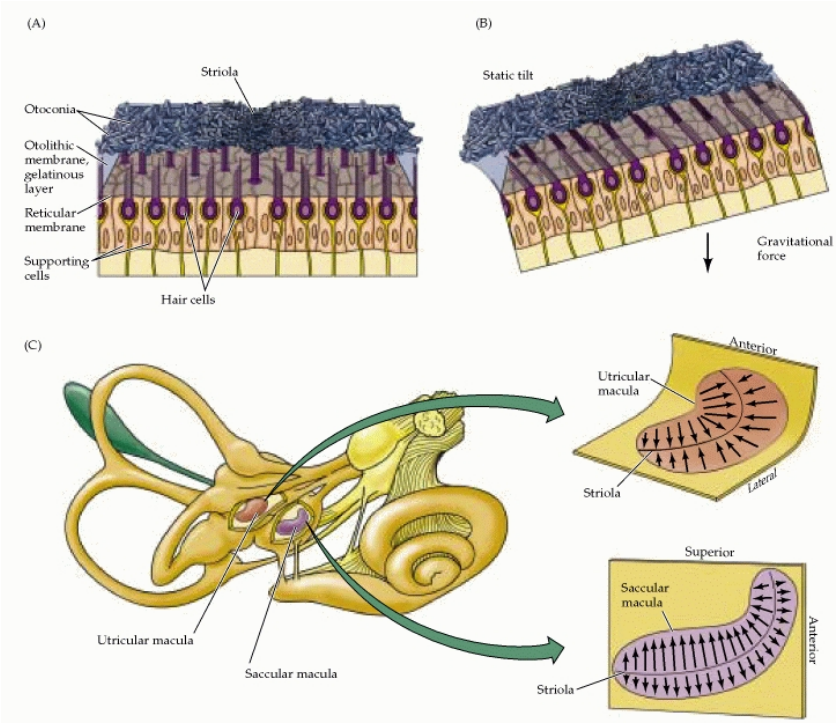

Figure 5. Physiology and anatomy of the otolith organs.
A) Hair cells within the utricular macula projecting into the gelatinous otolithic membrane, embedded with otoconia.

B) Deflection of hairs cells when the head is tilted.

C) ***Left:*** location of the otolith organs within the labyrinth. ***Right:*** the orientation of the hair cells in the utricular macula (upper) and saccular macula (lower).
Source: Purves et al 2008

Semicircular canals

Semicircular canals are equipped with the same type of hair cells as the otolith organs. However, unlike the otolith organs, which have hair cells oriented in many different directions, the hair cells within a semicircular canal are all oriented in the same direction. The ampulla, a specialized region of each semicircular canal, houses the

sensory epithelium, or crista, which contains all of the hair cells of the canal (figure 6). The distal ends of the cilia project into a gelatinous structure called the cupula, which extends to the opposite wall of the canal and is otherwise surrounded by the endolymph fluid that fills the canal. During angular acceleration of the head, the endolymph lags behind the wall of the canal because of inertia, exerting a force on the cupula, which bends the cilia (figure 6). If the acceleration ceases and rotation continues at constant velocity, the result will be a transient change in membrane potential since the endolymph and the canal wall will eventually move together and the bending of the cupula will cease. Each labyrinth is equipped with three semicircular canals, the horizontal, superior and posterior, positioned in mutually orthogonal planes. This arrangement provides the ability to detect angular acceleration in any given direction by constructing a vector sum of the deflections that arise in the three canals. Because of the mirror-image symmetry of the two labyrinths, rotation of the head leading to depolarization of hair cells in a given canal will have the opposite effect on the hair cells in the correspondingly oriented canal on the other side of the head.

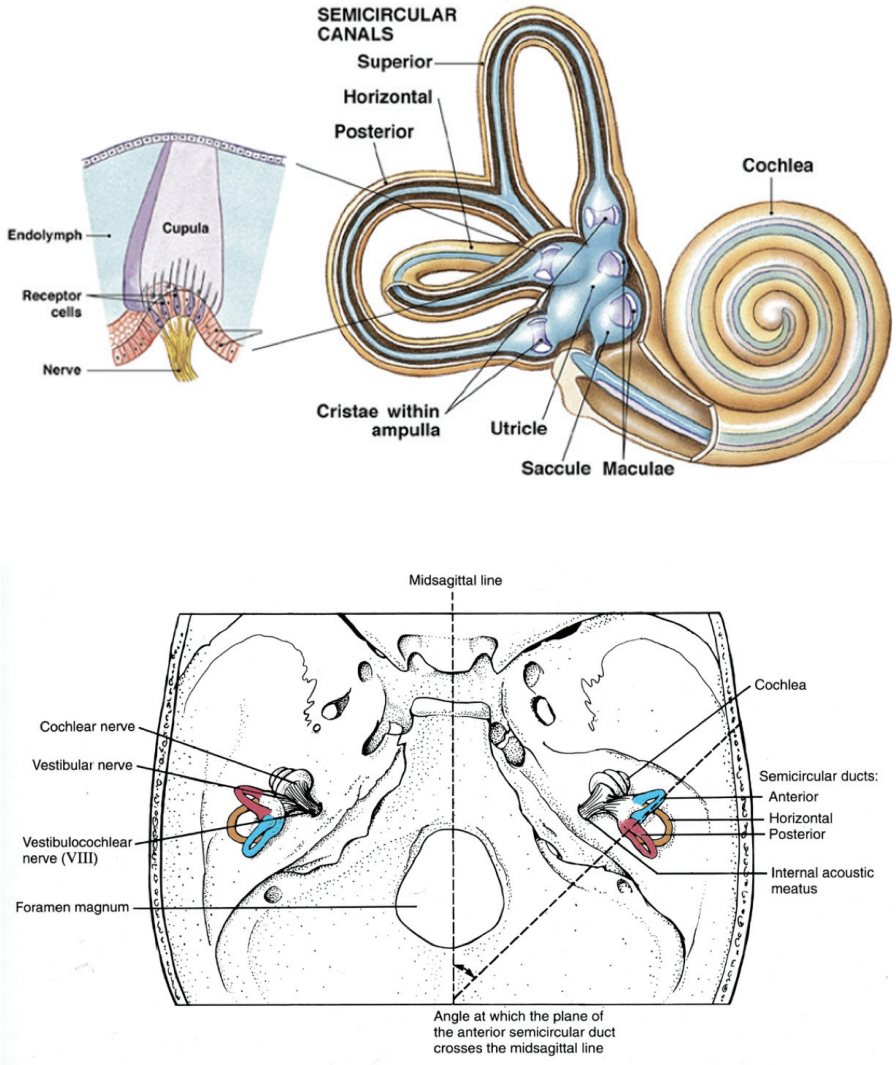

Figure 6. Physiology and anatomy of the semicircular canals.
Top left: Angular rotation of the head produced by pitch, yaw or roll leads to a deflection of the cupula and consequently the cilia of the hair cells because of the inertia of the endolymph. ***Top right:*** Location of the ampullae with their cristae and of the otolith organs and their maculae within the labyrinth. ***Bottom:*** Mutually opposing orientations of semicircular canals on the two sides of the head, indicated by the colored pairs.

2. Primary vestibular afferents

Vestibular sensory afferent fibers from the superior and inferior divisions of Scarpa's ganglion merge to form the vestibular nerve, which together with the cochlear nerve makes up the VIIIth cranial nerve. This nerve enters the brainstem at the level of the lateral vestibular nucleus, caudal to the trigeminal (Vth) nerve. Quantitative studies of the vestibular nerve have shown that the number of vestibular sensory afferent fibers varies greatly between species, from 9 000 in the pigeon to 20 000 in man (Landolt et al 1973; Bergström 1973a). All of the fibers are myelinated, and have diameters in the range of 1-15 microns, with the majority being between 5-7 microns (Bergström et al 1973b).

Upon entering the brainstem, the afferent fibers make glutamatergic synaptic contacts with neurons in the central vestibular nuclei and in the nodulus and uvula of the cerebellum (Büttner-Ennever 1992). As described in chapter one, a characteristic feature of vestibular afferent fibers is their resting discharge, which can be as high as 100 Hz in primates (Goldberg and Fernandez 1971a). There are also differences in the firing patterns that define different fiber types. Some vestibular afferent fibers, in general those having smaller diameters, have resting discharges with very regular interspike intervals. Vestibular afferent fibers with larger diameters fire more irregularly (Goldberg and Fernandez 1971b). There are several other differences between these two classes of fibers, including their sensitivity to electrical stimulation (Goldberg 2000). Regularly discharging fibers tend to have a higher activation threshold and produce smaller responses during galvanic stimulation compared to irregularly discharging fibers (Goldberg et al 1984), a natural consequence of the difference in fiber diameter. Differences in ion channel composition as well as in cell morphology contribute to setting the firing regularity of the afferent fibers (Eatock et al 2008).

3. Vestibular nuclei and their sensory inputs

There are four main cytoarchitecturally defined vestibular nuclei: the superior vestibular nucleus (or nucleus of Bechterew, SVN), the lateral vestibular nucleus (or Deiter's nucleus, LVN), the medial vestibular nucleus (MVN) and the inferior (or descending) vestibular nucleus (IVN or DVN, Highstein and Holstein 2006). These nuclei differ in the size and morphology of their constituent neurons, the pattern of innervation by vestibular afferents (Figure 7), and with respect to their projections to other regions of the CNS.

The SVN extends from the level of the caudal border of the motor trigeminal nucleus to the level just caudal to the abducens nucleus (Brodal and Pompeiano 1957). It is composed of small to medium sized neurons with diameters of 25 – 45 μm in the cat (Mitsacos et al 1983a; Mitsacos et al 1983b). The majority of the neurons receive monosynaptic input from semicircular canal afferents (Abend 1977).

The LVN is situated laterally, between the SVN and DVN, and borders the MVN medially. A characteristic feature of the LVN is the presence of a population of large multipolar neurons with soma diameters between 40 and 70 μm in the cat (Brodal and Pompeiano 1957). Although these large neurons are most numerous, other smaller neurons are also present. The distribution of large and small neurons is heterogeneous within the nucleus, and the large neurons are more numerous in the caudal part of the nucleus (Brodal and Pompeiano 1957). Stimulation of individual branches of the vestibular nerve has shown that neurons within the LVN receive input from utricular, saccular and horizontal and superior semicircular canal afferents (Goldberg and Fernandez 1984).

The MVN is the largest of the vestibular nuclei and extends from the same rostral level as the LVN to the rostral border of the hypoglossal nucleus (Brodal and Pompeiano 1957). It is composed of small and medium sized neurons with some

larger neurons in the mediodorsal part (Brodal and Pompeiano 1957). The MVN receives input predominantly from semicircular canal afferents (Carleton and Carpenter 1984).

The DVN extends from the caudal boarder of the LVN to the caudal border of the MVN (Brodal and Pompeiano 1957). The DVN is innervated by otolith organ as well as semicircular canal afferents (Büttner-Ennever 1992).

In addition to ipsilateral labyrinthine input, the vestibular nuclei receive di- and trisynaptic input from the contralateral labyrinth (Vito et al 1956; Shimazu and Prechts 1966; Mano et al 1968; Kasahara et al 1968). These inputs are predominantly inhibitory in nature (Furuya et al 1976).

Vestibular nuclei also receive synaptic inputs from sources other than the vestibular afferents, including the cerebellum (Andersson and Oscarsson 1978a; 1978b), neck proprioceptor neurons (Boyle and Pompeiano 1981a; 1981b; 1981c; Brink et al 1980), and visceral receptors (Balaban 1997). In this respect the secondary vestibular neurons can be regarded as integration centers for diverse sensory inputs.

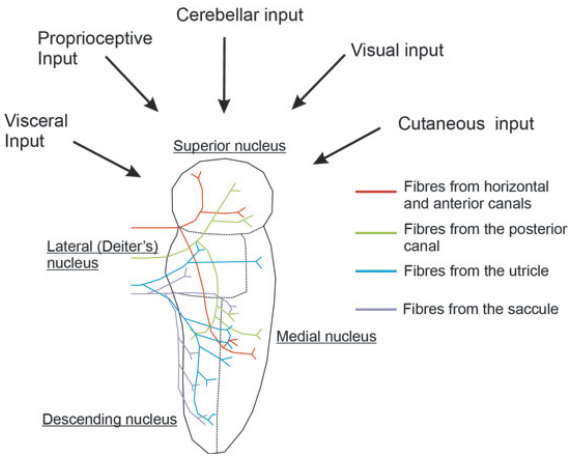

Figure 7. Organization of synaptic inputs to the vestibular nuclei.
Distribution of vestibular sensory afferents from the vestibular end organs onto the vestibular nuclei. The vestibular nuclei also receive inputs from other sources. The innervation pattern of this input is currently not well characterized. *Adapted from Kandel et al 2000 Fig. 40-9 (Original: Gacek and Lyon 1974), and Yates et al 2000, Fig. 7.*

4. Hodological classification of vestibular neurons

The functional organization of the classical vestibular nuclei are difficult to define based on cytological characteristics alone. For this reason, investigators have started to define vestibular neurons groups based on hodology, that is, to distinguish discrete populations within the vestibular nuclear complex each composed of neurons with common projection trajectories. This has been especially well described for vestibulospinal and vestibulo-ocular neurons in birds, amphibians and rodents (mouse: Auclair et al 1999, Pasqueletti et al 2007; chicken: Glover and Petursdottir 1988, Petursdottir 1990, Glover 1994, Diaz et al 1998, 2003; frog: Straka et al 2001, 2002). Vestibulospinal projection neurons are grouped into three hodologically distinct neuron groups. Each group gives rise to a distinct tract that projects to the spinal cord. The neuron groups are named according to the spinal tract to which they give rise. These groups are described in more detail in the next section.

Vestibulo-ocular projection neurons projecting to the oculomotor and trochlear nuclei are divided into four neuron groups, the ipsilateral and contralateral rostral, and ipsilateral and contralateral caudal groups (mouse: Pasqueletti et al 2007; chicken: Glover and Petursdottir 1991; Glover 1996; Glover 2003). Vestibulo-ocular projection neurons projecting to the abducens nucleus have not yet been placed into this hodological scheme.

Several lines of evidence suggest that projection neurons in the vestibular nuclei are specified according to their target neuron projections rather than according to their endorgan-related sensoryinputs (Glover 2003). Another potential example of a target-related specification comes from work on the vestibulosympathetic system. Vestibular projection neurons that give rise to this system seem to be clustered within a small region lying between the inferior nucleus and the medial nucleus (Pan et al 1991; Yates and Miller 1994; Holstein et al 2011). It is however unclear whether these

neurons have a common projection trajectory. Presumably, other vestibular neuron groups with common function and trajectory will eventually emerge from ongoing studies of vestibular hodology.

Neurons within a given hodological group are not found exclusively within the borders of a single cytoarchitectonic nucleus. The anatomical relationship between the hodological vestibulospinal groups and the cytoarchitectonic nuclei is discussed in more detail in the following section. For a review of the vestibulo-occular groups, see Diaz and Glover (2002).

5. The vestibulospinal system

The main function of the vestibulospinal system is to stabilize the position of the head and body in space. This is achieved by the action of the vestibulospinal descending tracts on spinal motor networks controlling neck, back and limb musculature. There are three separate vestibulospinal tracts, the lateral vestibulospinal tract (LVST) and the ipsilateral and contralateral medial vestibulospinal tracts (iMVST and cMVST) (Brodal 1974; Glover & Petursdottir 1988; Diaz et al 2003; Pasqualetti et al. 2007).

LVST

The LVST originates mainly from the lateral (Deiter's) nucleus and projects on the ipsilateral side of the spinal cord. The axons project ventrally within the brain stem and enter the upper cervical part of the spinal cord in the ventral funiculus. As they descend to more caudal segments the axons course just adjacent to the ventral spinal fissure in the lumbar spinal cord (Kuypers 1984). Retrograde labeling studies have shown that these axons as a population innervate all spinal segments extending all the way to the sacral spinal cord (Brodal, 1974). The fibers terminate predominantly in the ipsilateral lamina VIII and medial parts of ipsilateral lamina VII (Nyberg-Hansen

and Mascitti 1964; Erulkar et al 1966). However, a few terminals are also seen contralaterally (Erulkar et al 1966; Kuze et al 1999). Studies in the cat have shown that most LVST fibers are large in caliber (Petras 1967) and have conduction velocities between 20 and 140 meters/second (Wilson et al 1966; Wilson et al 1967). There is evidence of a somatotopic organization. LVST neurons innervating cervical segments are found in the ventral part of the Deiter's nucleus, whereas those innervating the lumbar segments are found in the dorsal part (Pompeiano and Brodal 1957; Wilson et al 1967). However, there is a large overlap between the lumbar- and cervical-projecting cells (Wilson 1967). A study by Abzug et al (1974) showed that about 50 % of the LVST neurons that innervate cervical segments also send collateral branches to the lumbar spinal cord. This would allow for a coordinated action on fore- and hindlimbs. Studies in the cat have shown that stimulation of LVST fibers evokes excitatory postsynaptic potentials (EPSPs) in ipsilateral and contralateral MNs innervating neck, back, forelimb and hindlimb muscles (Lund and Pompeiano 1968; Wilson and Yoshida 1969; Grillner et al 1970; Wilson et al 1970; Hongo et al 1971). Most of the EPSPs recorded in MNs innervating neck and back musculature are monosynaptic in nature (Wilson and Yoshida 1969; Wilson et al 1970). The same is true for EPSPs to some MNs innervating the hindlimbs, in particular those innervating knee and ankle extensors (Wilson and Yoshida 1969; Wilson et al 1970; Grillner et al 1970). However, most of the EPSPs recorded in fore- and hind limb MNs are polysynaptic (Grillner et al 1970; Wilson and Yoshida 1969). Inhibitory postsynaptic potentials (IPSPs) have also been recorded following stimulation of the LVST. These are particularly prevalent in fore- and hind limb flexor-innervating MNs (Wilson and Yoshida 1969). All of the IPSPs recorded are polysynaptic in nature (Wilson and Yoshida 1969), which suggests that they are mediated by the LVST's action on inhibitory spinal INs.

Since the LVST fibers terminate mainly in the ipsilateral spinal cord, with only a few terminals found on the contralateral side (Erulkar et al 1966), their action on contralateral motoneurons can probably be attributed to the activation of CINs. This notion is supported by the findings of Hongo et al (1971), who showed that the LVST has excitatory and inhibitory di- and trisynaptic actions on contralateral hindlimb MNs in the cat. Monosynaptic connections were not present. Furthermore, Krutki et al (2003) showed in the adult cat that spinal CINs receive both mono- and disynaptic input following stimulation of the LVN.

Although we have a fair overview of the LVST's actions on limb MNs, little is known about its actions on MNs innervating axial musculature.

iMVST and cMVST

The MVST originates predominantly from the medial vestibular nucleus, but there are significant contributions from neurons within the lateral and descending nuclei (Akaike 1973a; Rapoport et al 1977; Diaz et al 2003). In the brain stem the fibers as a population project bilaterally in the MLF and enter the spinal cord in the ventral funiculi (Brodal 1974, Nyberg-Hansen 1966a). However, ipsilateral and contralateral fibers derive from distinct neuron groups, the iMVST group and the cMVST group (Glover and Petursdottir 1988; Glover 1994; Pasqualetti et al 2007). Many MVST fibers are observed in the cervical cord, but their number falls dramatically below the mid-cervical segments (Brodal 1974). In the cat the fibers terminate predominantly in the ipsilateral and contralateral laminae VII and VIII of the cervical cord (Nyberg-Hansen 1964), with only a few terminals seen in the rostral parts of the thoracic cord (Akaike 1973a). However, in the rabbit, some MVST fibers reach even caudal segments of the thoracic cord, demonstrating that there might be important differences between species (Akiake and Westerman 1973). The MVST fibers have a

smaller diameter then the LVST fibers (Nyberg-Hansen 1964), and have conduction velocities of 13-76 m/second (Wilson et al 1968; Wilson and Yoshida 1969). The MVST fibers have both inhibitory and excitatory actions on spinal MNs. Most of these are mediated monosynaptically but there are also disynaptic connections (Akiake et al 1973b; Wilson and Yoshida 1969). As for LVST axons, MVST axons are highly branched and a single axon can give off several collaterals to multiple segments (Shinoda et al 2006).

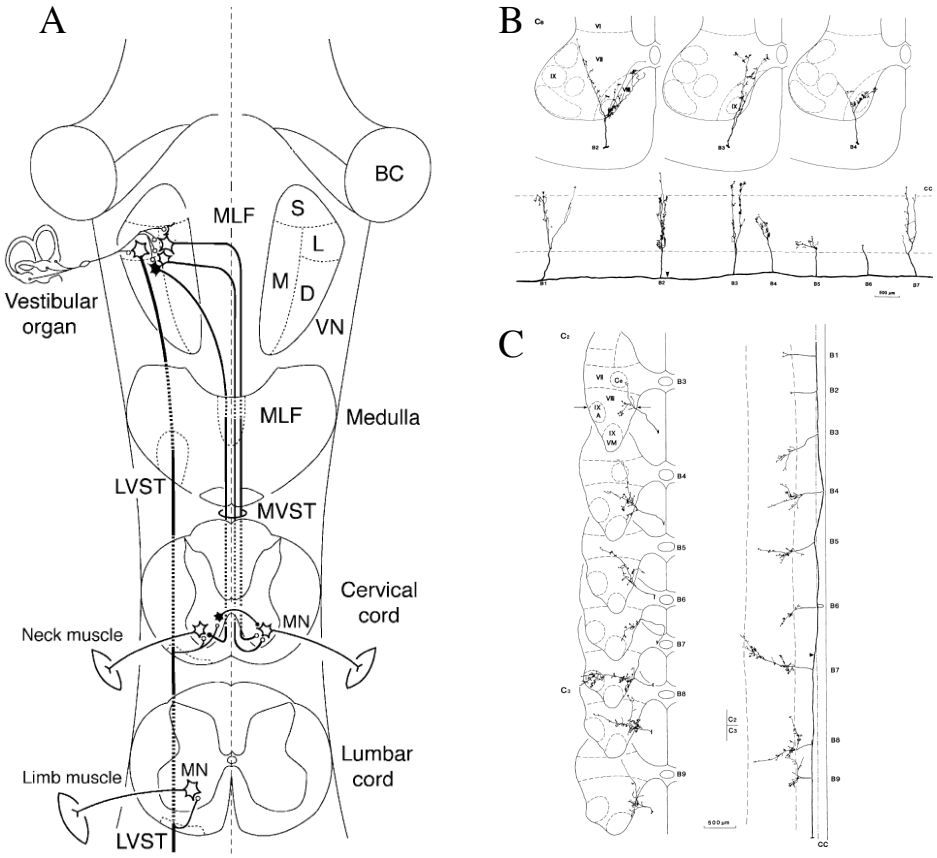

Figure 8. Projection and innervation patterns of vestibulospinal neurons.
A) Nuclear distribution, pathways and synaptic nature of secondary vestibulospinal neurons. LVST neurons project laterally and give excitatory input to ipsilateral MNs in the cervical and lumbar cord. MVST neurons project either ipsilaterally or contralaterally in the MLF and give excitatory and inhibitory input to ipsilateral and contralateral MNs of the cervical cord. S: superior, M: medial, L: lateral and D: descending vestibular nuclei. *Adapted from Shinoda et al 2006.* **B)** Reconstruction of a single axon from the LVST labeled intracellularlly with HRP. *(Adapted from Shinoda et al 1986).* **C)** Reconstruction of a single iMVST axon labeled with HRP. *(Adapted from Shinoda et al 1992).*

6. Development of the vestibulospinal system

The ontogeny of the central vestibular nuclear complex in the rat was addressed with ^{3}H-thymidine radiographic experiments by Altman and Bayer (1980). This study showed that neurons of the vestibular nuclei are generated between embryonic days (E) 11 and E15. Production of neurons in the LVN peaked at E12, in the superior and inferior nuclei at E13 and in the medial nucleus at E14. The growing axons of vestibulospinal neurons reach the cervical spinal cord by E13 (Auclair et al 1993, 1999; Lakke 1997), the lower thoracic cord by E14 (Lakke 1997) and the lumbar cord by postnatal day (P) 2 (Lakke 1997). Presumably the axons reach the lumbar cord already before birth. Stages between E20 and P2 were not analyzed by Lakke (1997).

The origin of the vestibulospinal neurons has been studied using chimeric approaches and more recently transgenic tools in avians (chicken embryo), amphibians (Xenopus) and rodents (mouse). It has been shown that neurons that give rise to the LVST originate primarily from rhombomere (r) 4 of the hindbrain, with some overlap with r3 and r5, especially in the mouse where the rostral boarder stretches into rhombomere 2. (Glover and Petursdottir 1988, 1991; Auclair et al 1999; Pasqualetti et al 2007). Neurons of the iMVST originate from r6, and neurons of the cMVST originate from r5 (Diaz et al 1998; Pasqualetti et al 2007). This pattern of origin seems to be well conserved and is similar in fish, amphibians, avians and rodents (Diaz and Glover 2002; Figure 9).

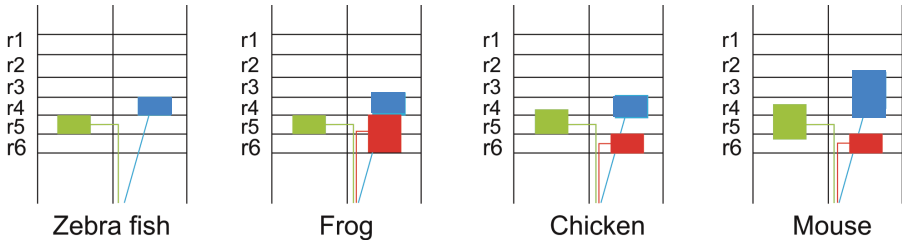

Figure 9. Comparison of the developmental origin of the vestibulospinal neuron groups in zebra fish, frog, chicken and mouse.

Blue: LVST, red: iMVST and green: cMVST. Note that some of the individual groups are not derived exclusively from single rhombomeres. *Adapted and modified from Diaz and Glover 2002 (zebrafish, frog and chicken) and Pasqualetti et al 2007 (mouse).*

7. Function of vestibulospinal reflexes

The general function of the vestibulospinal reflexes is to maintain balance and effective motion and posture in the face of perturbations of head and body position. In particular, effective reflex control of head position is crucial for maintaining uninterrupted and efficient sensory surveillance of the surrounding environment. Vestibulomotor control is achieved by coordinated activation of appropriate neck, trunk and limb muscles. The function of the vestibulospinal reflexes has been well described in the cat.

The vestibulospinal system acts on antigravity limb muscles in such a way as to oppose postural perturbations (Roberts 1968, 1973, 1978). For example, left side-down rotation induces excitatory action on left limb extensors and right limb flexors. Right side-down rotation has the opposite effect. A second mode of action occurs during whole body nose up tilts. In this case there is an activation of extensors in both hindlimbs and activation of flexors in both forelimbs. The reverse activation is seen

during nose-down tilts. These responses ensure maintenance of posture. The ability to maintain posture during such perturbations is greatly compromised in labyrinthectomized animals (Money and Scott 1962). A third mode of action is seen during the air-righting reflex, which ensures that cats, during falls, land on their limbs. In this reflex, extensors of all four limbs are activated in concert. This response is absent in labyrinthectomized animals (Wilson and Jones 1979). Finally, vestibulospinal inputs are important for regulating ongoing motion, both as a corrective measure in the face of unexpected perturbations but also to ensure smooth progression of movement.

8. Role of the reticular formation in vestibulospinal reflexes

Studies in the adult cat have shown that interruption of medial vestibulospinal pathways by lesions of the MLF does not result in marked changes in the vestibular reflexes acting on the neck (i.e. vestibulocolic reflexes). Vestibular reflexes could still be evoked by natural and galvanic stimulation of the labyrinth (Ezure et al 1978; Wilson et al 1979; Bilotto et al 1982), although with somewhat lower gain. The residual response could be mediated by the LVST or other non-vestibular descending systems.

Investigators therefore looked at other potential pathways that could mediate labyrinthine input to the spinal cord. Focus was turned to the interstitiospinal and reticulospinal descending pathways. The former was however quickly dismissed since the interstitiospinal axons project exclusively within the MLF (Nyberg-Hansen 1966b), and are interrupted by the very same lesion.

The reticulospinal neurons are situated in the pons and the medulla, and project to the spinal cord via two major tracts. The medial reticulospinal tract originates from neurons within the nucleus pontis oralis, the nucleus pontis reticularis and the nucleus

reticularis gigantocellularis (Nyberg-Hansen 1966a). The projections to the spinal cord are ipsilateral, and most course within the MLF (Peterson 1979). The lateral reticulospinal tract originates from neurons within the nucleus gigantocellularis and nucleus magnocellularis and projects both ipsilaterally and contralaterally (Nyberg-Hansen 1965; Matsuyama et al 2004a). Reticulospinal axons project to all segments of the spinal cord (Wilson and Peterson 1981; Reviewed in Mori et al 1995), and are thus in a key position to influence motor control.

Anatomical evidence that suggested a vestibulo-reticulospinal connection came from a study by Ladpli and Brodal (1968), who showed that all of the four major vestibular nuclei contain neurons that project to the medial pontomedullary reticular formation.

Physiological studies, using natural stimulation of the labyrinth, showed that neurons within the medial pontomedullary reticular formation (i.e., cells within the nucleus pontis caudalis and nucleus gigantocellularis) could be activated both by semicircular and otolith receptor stimulation (Spyer et al 1974; Fukushima et al 1977; Bolton et al 1992). Furthermore, Peterson et al (1975) showed that neurons within these nuclei could also be activated by electrical stimulation of the vestibular nerve. The measured latencies suggested di- and polysynaptic connections. Although there is convincing evidence for the role of the reticular formation in the function of vestibulospinal reflexes, the details about its specific contribution to the different vestibulospinal reflexes remain elusive.

9. The vestibulosympathetic system

Changes in position from supine to upright present a great challenge to the cardiovascular system. The height of the orthostatic column increases dramatically and greatly decreases the return of venous blood to the heart, leading to orthostatic hypotension. The immediate consequence of orthostatic hypotension is a decrease in cardiac output, leading to poor blood flow into the brain, which often results in syncope. Several mechanisms have evolved that help counter this problem. Contraction of skeletal muscles surrounding the large veins of the legs can help to push blood towards the heart (Ludbrook 1966). Decrease of intrathoracic pressure by contraction of the diaphragm muscle creates a pressure gradient that acts to pull blood towards the heart (Lloyd 1983; Lloyd and Cooper 1983). The most effective way of counteracting orthostatic hypotension, however, is to differentially regulate the sympathetic control of arterioles, thereby channeling the blood flow to the systemic circulation (Gauer and Thron 1965). Baroreceptors within the aortic arch and the carotid arteries have the ability to sense changes in blood pressure and trigger adjustments in sympathetic outflow by a negative feedback mechanism acting through the sympathetic control centers in the brainstem (Stauss 2002; Dampney 1994). However, the baroreceptor reflex is not activated before a sizable drop in blood pressure has occurred and is thus too slow to counteract the early phase of orthostatic hypotension following elevation. Thus, there must be an additional mechanism based on feed-forward input that can rapidly regulate sympathetic outflow. It was hypothesized that the vestibular system, because of its ability to immediately sense changes in posture, might have a role in preventing orthostatic hypotension. The first study that addressed this possibility showed that bilateral transection of the vestibular nerves in the cat greatly compromised the animal's ability to maintain blood pressure

during nose-up body pitch (Doba and Reis 1974). Several studies have also shown that electrical stimulation of the vestibular nerve evokes changes in sympathetic nerve activity (Yates 1992; Kerman et al 2000). This has also been shown with natural stimulation of the vestibular afferents (Yates and Miller 1994). Supporting results have also been found in human studies. Galvanic stimulation of the vestibule leads to increased activity in muscle sympathetic nerves (Bent et al 2006; Voustianiouk et al 2006). Several studies by Ray have shown that natural stimulation of the vestibular afferents in humans by head-down pitch also gives an increase in muscle sympathetic nerve activity (Ray and Carter 2003; Shortt and Ray 1997). Furthermore there is some evidence that links the higher prevalence of orthostatic hypotension in the elderly to attenuation of the vestibulosympathetic reflex (Ray and Monahan 2002; Monahan and Ray 2002).

Several studies have begun to define the peripheral and central substrates of the vestibulosympathetic reflex. In both cats and humans it has been shown that the most effective stimulation of the sympathetic nerves is achieved by activation of otolith receptors (Yates and Miller 1994; Costa et al 1995; Ray et al 1998). More specifically, vestibulosympathetic responses could be attributed to a group of otolith receptors that are sensitive to pitch movements, which are predominantly found in the saccule.

By making chemical lesions in the brain stem of the cat, Yates and colleagues have shown that a region within the inferior and the medial vestibular nuclei is necessary for the generation of vestibulosympathetic responses (Yates et al 1993; Yates and Miller 1994). Lesions in other parts of the vestibular complex did not affect the activation of sympathetic nerves. These findings support the results of a similar study using electrolytic lesions (Pan et al 1991). The importance of this region of the vestibular complex for the vestibulosympathetic reflex fits well with findings that this

region receives predominantly input from otolith afferents (Kasper et al 1988; Wilson et al 1990). Anatomical studies have shown that there are indirect projections from the inferior and medial vestibular nuclei to the rostral ventrolateral medulla (RVLM), a principal center involved in cardiovascular control (Porter and Balaban 1997; Holstein et al 2011). Physiological studies show that neurons within the RVLM respond to stimulation of the vestibular nerve (Yates et al 1992, 1995). Furthermore, lesions of the RVLM abolish vestibulosympathetic responses (Yates et al 1995). It is thus likely that the vestibulosympathetic responses recorded in sympathetic nerves are mediated by projections from the inferior and medial vestibular nuclei via the RVLM to the preganglionic sympathetic neurons in the spinal cord.

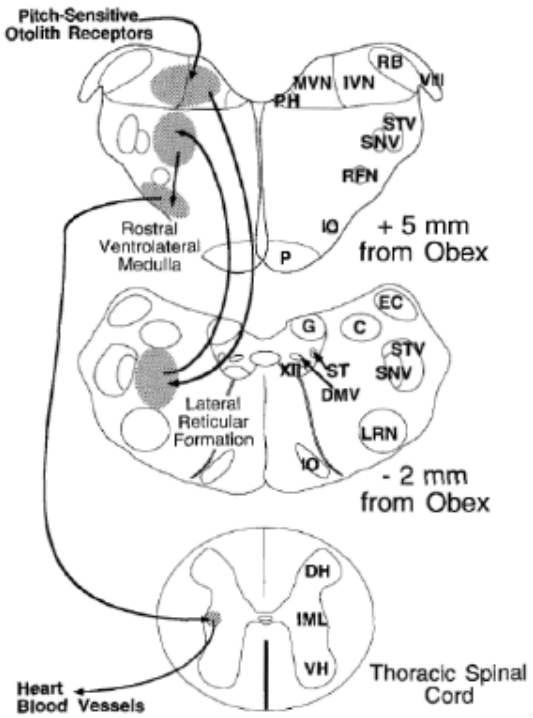

Figure 10.

Organization of the central vestibulosympathetic pathway in the cat.

Pitch-sensitive otolith organ receptors activate secondary vestibular neurons within the inferior and medial vestibular nuclei. These neurons project to the caudal ventrolateral medulla which projects indirectly to the RVLM. The RVLM neurons send long descending axons to the thoracic spinal cord that make synaptic contacts with sympathetic preganglionic neurons in the intermediolateral column. *Adapted from Yates 1996.*

10. Other vestibular projections

The vestibular nuclei project to several other targets that will only be mentioned briefly here as they do not pertain directly to my thesis research. Vestibulo-ocular projections make up the sensory basis of the vestibulo-ocular reflex, which generates compensatory eye movements in response to head movements such that the direction of gaze is maintained. Much like the vestibulospinal neurons, vestibulo-ocular neurons are organized into discrete hodological groups that have specific patterns of functional connections (reviewed in Glover 2003). A second well-described vestibular projection is the vestibulocerebellar projection. This projection originates from the caudal part of the MVN and terminates in the anterior and posterior vermis, the uvula-nodulus and flocculus (reviewed in Barmack 2003). It is thought that the vestibulo-cerebellar projection contributes to fine-tuning of vestibular-related reflexes (reviewed in Barmack 2003). Finally, vestibular neurons project to the thalamus to influence several parts of the cerebral cortex, most notably the parietal cortex and the somatosensory cortex, to provide conscious surveillance of vestibular inputs. Several thalamic nuclei are involved in this pathway (reviewed in Fukushima 1997). Vestibulo-thalamic projections originate from at least three vestibular nuclei, the medial, descending and superior (Kotchabakdi et al 1980). The necessity of these connections has been shown in patients with various forms of labyrinthine defects. These patients show significant problems with self-movement perception, spatial perception and memory (reviewed in Fukushima 1997).

METHODS

1. Brainstem–spinal cord preparation

In all papers included in my thesis I have used the brainstem-spinal cord preparation of the newborn mouse (Szokol et al. 2008, Szokol and Perreault 2009). This preparation was originally developed to study connections between medullary reticulospinal neurons and spinal motoneurons and interneurons (Szokol et al. 2008, Szokol and Perreault 2009, Szokol et al. 2011). With few modifications, I have used this preparation to study the connections between vestibulospinal neurons and spinal motoneurons (Paper I), sympathetic preganglionic neurons (Paper II) and spinal commissural interneurons with descending axons (Paper III). In all papers included in my thesis I performed the majority of the experiments on mice of the ICR strain aged postnatal day (P) 0–5. To test the generality of my findings, I also performed experiments (in paper I) on neonatal mice of other strains that were available to me during the study (BalbC; NZEG, obtained from Martyn Goulding, Salk Institute; and Nkx 6.2lacZ, obtained from Johan Ericson, Karolinska Institute).

I used the following dissection procedure.

The mice were deeply anaesthetized with isoflurane (Abbott, Scandinavia AB). The skull was opened dorsally, and the animal was decerebrated with a transection (using a spatula) just rostral to the superior colliculus. We chose this level of decerebration because it has been shown in cats and rabbits to preserve the ability to maintain balance and walk (when supported on a treadmill) (cat: Whelan 1996; rabbit: Musienko 2008). The mice were then placed in ice-cold glycerol-based dissecting solution (containing (in mM): glycerol 250, KCl 2, D-glucose 11, $CaCl_2$ 0.15, $MgSO_4$ 2, NaH_2PO_4 1.2, Hepes 5 and $NaHCO_3$ 25) which reduces swelling and increases the quality of the preparation (Ye et al. 2006; Tanaka et al. 2008). Within 30 minutes, the

brainstem and spinal cord were carefully dissected out along with ventral and dorsal roots and selected cranial nerves. After dissection, the solution was immediately replaced by room temperatured (22 – 24 °C) artificial cerebrospinal fluid (aCSF) containing (in mM): NaCl 128,KCl 3, D-glucose 11,$CaCl_2$ 2.5, $MgSO_4$ 1, NaH_2PO_4 1.2, Hepes 5 and $NaHCO_3$25.

2. Retrograde labeling of spinal cord and brainstem neurons

I labeled target neurons retrogradely with conjugated dextran-amines using the technique of Glover (Glover et al 1986; Glover 1995). This or similar methods have been used to label specific neuron populations in various species including chicken, mouse, rat, turtle and lamprey (Glover and Petursdottir 1988; O'Donovan et al 1993; Bonnot et al 2002; Stokke et al 2002; Nissen et al 2008; McClellan et al 1994). To label spinal cord motoneurons (MNs) and sympathetic preganglionic neurons (SPNs) (Paper I, II and III), I applied crystals of Calcium Green-conjugated dextran amine (CGDA, 3000 MW, Molecular Probes) or rhodamine conjugated dextran amine (RDA3000 MW, Molecular Probes) to the freshly transected ventral root of the segment of choice. During crystal application, I removed surplus CGDA or RDA by mouth suction through a micropipette to avoid contamination of nearby roots or the spinal cord itself. Retrograde labeling was allowed to continue in aCSF at room temperature in the dark for 3 h, at which time CGDA or RDA fluorescence was readily visible in the MN and SPN somata. To label spinal cord descending commissural inter neurons (dCINs) (Paper II) I applied the crystals to the freshly cut contralateral ventral and ventrolateral funiculi (see Figure 11). Fluorescence was readily visible in the dCIN somata after 4 hours of incubation at room temperature. Finally, to label vestibulospinal neurons (Paper I), I applied crystals to the ipsilateral ventral and ventrolateral funiculi at the level of C1. Fluorescence was readily visible

in the vestibulospinal neuron somata after 8-10 hours of incubation at room temperature.

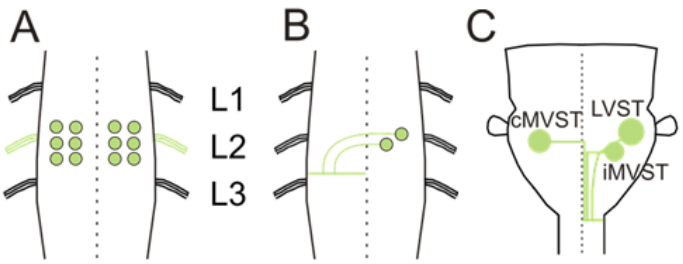

Figure 11. Labeling protocols for brainstem and spinal cord neurons.

A) Vestibulospinal neuron groups (LVST, iMVST and cMVST) labeled by application of CGDA crystals to VF and VLF at the level of C1. **B)** Labeling of spinal motoneurons and sympathetic preganglionic neurons by application of CGDA crystals to cut ventral roots. **C)** Labling of spinal descending commisural interneurons by application of CGDA to the contralateral VF and VLF.

3. Optical recording of calcium responses

After the retrograde labeling was complete I transferred the preparations containing labeled MNs, dCINs or vestibulospinal neurons to a Sylgard-coated chamber where I pinned down ventral side up (dorsal side up in the case of vestibulospinal neurons) using stainless-steel (Minuten) pins. The chamber was perfused with oxygenated aCSF at a rate of 3.6 ml/min, giving a total volume exchange every 3 min. I visualized the labeled MNs and SPNs through the ventral white matter with a 40× water immersion objective (LUMPlanFl, 0.8 NA, Olympus, Norway) using an epi-fluorescence microscope (Axioskop FS2, Carl Zeiss, Oberkochen, Germany) equipped with a 100W halogen lamp driven by a DC power supply (PAN35-20A, Kikusui Electronics Corporation, Japan) and excitation and emission filters (BP 450–490 nm and LP 515 nm, respectively). I visualized the labeled dCINs through the obliquely cut transverse surface (as described by Szokol and Perreault 2009). Finally, I visualized vestibulospinal descending neurons through the dorsal brainstem white mater. Fluorescence changes associated with neuronal activity, which I refer to as 'Ca2+ transients' or 'responses', were registered using a cooled CCD camera (Cascade 650, Photometrics, Texas Instruments, USA) mounted on a video zoom adaptor (44 C 1/3" (3CCD) 0.33x to 1.6x, Zeiss). As higher frame rates with reduced exposure times require stronger illumination and lead to rapid bleaching, I routinely acquired image series at 4 frames per second using the image-processing software Metamorph 5.0 (Universal Imaging Corporation, Molecular Devices) with the exception of a subgroup of experiments described in Paper I (Fig. 3), paper II (Fig. 4) and III (Fig. 2 and Fig. 5) where I recorded at 100 frames per second to more accurately measure the onset latencies of the responses.

4. Ventral root recording

In Paper I, I performed ventral root recordings from the axons of MNs simultaneously as I recorded calcium responses (Fig. 3, Paper I). I recorded from labeled ventral roots by positioning them at the mouth of fire-polished borosilicate glass suction electrodes filled with the same aCSF as in the recording chamber, and then sucking them into an omega configuration. The recorded electrical activities were fed to a differential amplifier (DPA-2FS, NPI electronic, Germany), band-pass filtered at 30 Hz–10 k Hz and digitized at 5 kHz. Waveform recording traces were analyzed off-line in Clampfit 9.0 (Axon Laboratory).

5. Electrical stimulation of the VIIIth nerve

To activate vestibule-spinal neurons I stimulated the VIIIth cranial nerve with a fire-polished borosilicate glass(Harvard Apparatus, UK) suction electrode coupled to a digital stimulator (DS 8000, WPI, UK). I regularly verified the electrode position and suction during the experiment. Data acquired after eventual electrode repositioning were analyzed separately from previous data. Detailed descriptions of the different stimulation protocols are given in the Methods section of the individual papers.

6. Pharmacological experiments

I used the following chemicals and procedures for pharmacological experiments in all three papers included in my thesis.

$GABA_A$ receptors were blocked with biccuculline (20 μM, Tocris) or picrotoxin (PTX, 40 μM, Sigma) and and glycine receptors were blocked with strychnine (0.2 μM, Sigma). To reduce activity in polysynaptic pathways I used mephenesin (1mM,

Sigma) (Kaada, 1950; Ziskind-Conhaim, 1990; Lev-Tov & Pinco, 1992). For selective application of drugs to the spinal cord I placed a Vaseline barrier at the C1 segment and bath-applied the drugs only to the compartment below this.

7. Data analysis

I used the following protocol for analysis of the acquired calcium imaging data. Much of the protocol is based on the procedure used by Szokol et al 2008.

Circular digital apertures of identical size and shape, termed regions of interest (ROIs) in the MetaMorph software, were placed manually over individual neuron somata that were clearly visible in one focal plane. I routinely analyzed six MNs per motor column in each recording. In recordings of dCINs I analyzed all recorded neurons. The Ca^{2+} transients in each ROI were quantified as changes in fluorescence (ΔF) divided by the baseline fluorescence F_0 before the stimulation ($\Delta F/F_0 = (F–F_0)/F_0$) to compensate for variability in the CGDA labeling intensity among MNs. The data were converted to text files using a custom-made program ("File Convert" written by Bruce Piercey) then imported into Clampfit 9.0 where they could be expressed as waveforms. A detectable response was defined as a continuous positive deflection exceeding a detection limit of two standard deviations above the mean of the baseline. Response magnitude was defined as the area under the waveform above the detection limit. See Methods section of the individual papers for a more detailed description of the analysis protocol.

8. Histology

To investigate the extent of lesions (Papers I, II and III) or the locations of stimulation sites (Paper III), at the end of each experiment I fixed the preparations in cold 4 % paraformaldehyde over night. The tissue was subsequently cryoprotected by

incubation in 20 % sucrose (in PBS w/v), and embedded in Optimum Cutting Temperature (OCT) formulation, frozen and sectioned at 30 – 100 μm in the transverse, parasagittal or frontal plane using a cryostat (Leica, CM 3050S). I collected the sections onto Super Frost® slides (Menzel GmbH & Co KG, Braunschweig, Germany) and dried them overnight. I stained the sections with haematoxyin (Papers I, II and III) or methylene blue (Paper II) using conventional procedures (5% w/v Harris haematoxylin, 3% w/v Methylene blue, both Sigma). I acquired images with a ProgRes C14 CCD camera mounted on an Olympus AX70 microscope, or a Hamamatsu C4880 CCD camera mounted on a Leica DMRXA microscope

9. Data presentation and statistics

Calcium responses

In all papers I present calcium responses both as pseudocolor images and fluorescence intensity waveforms. The pseudocolour representations were made by filtering the complete image series of the recording session in Metamorph with a low pass 3 × 3 filter and then converting grey scale values to colors using a rainbow index, with transition from blue to red to white representing increasing response size. Images presented are from single frames taken before, during or after stimulation. The waveform representations of calcium responses are either from single neurons or an average of 6 neurons (see papers for details). Both waveforms and the pseudocolor images were imported into Corel Draw Graphics Suite X4 (Corel Corporation, Canada), which was the main software for the production of figures.

Statistics

Groups of data were compared using either the Student's t-test (for data that was normally distributed), or the non-parametric Mann-Whitney U test (for data that was not normally distributed or had too low a sample size to be tested for normal distribution). Values are presented as mean ± standard deviation or mean ± standard error of the mean; see individual papers for details.

10. The advantages and limitations of calcium imaging as a tool to study neuronal circuits

Calcium-sensitive indicators have been used for decades to reveal cellular calcium dynamics. Fluorescence-based calcium measurement was initially based on calcium-sensitive proteins (aequorin being the first to gain general use) isolated from marine animals. Later, a series of fluorescent calcium indicators were developed in the laboratory of Roger Tsien in the late 1970's, based on the molecule 1,2-bis(o-aminophenoxy)ethane-N,N,N',N'-tetraacetic acid (BAPTA) (Tsien 1992). A whole variety of indicators now exists, with very different properties. Binding of calcium to an indicator leads to changes in fluorescence by one of three mechanisms (Adams 2005). Binding of calcium can lead to a shift in excitation and emission peaks. This mechanism is employed by the so-called "ratiometric" calcium indicators, such as quin-2, fura-2, indo-1 and ratiometric pericam (Tsien 1980; Grynkiewicz et al 1985). Binding of calcium can alternatively lead to changes in fluorescence intensity, with no shift in emission and excitation wavelength. This mechanism is employed by Calcium Green dyes, fluo-3 and rhod-2 (Minta et al 1989). Finally, binding of calcium can result in fluorescence resonance energy transfer (FRET) such as in the genetically encoded indicators of the cameleon family (Miyawaki et al 1997).

Since their discovery, calcium indicators have played an important role in investigations of neuronal circuits and are considered to be reliable indicators of postsynaptic neuronal activity (O'Donovan 2008). Neurons in living preparations can be loaded with calcium indicators in several different ways. The simplest method is applying the indicator, in a membrane prermeant form, directly to the bath containing the preparation (Grynkiewicz et al 1985; Brustein et al 2003; Stosiek et al 2003; Wilson et al 2007). This is an effective but non-selective method of loading. Neurons can also be labeled retrogradely with calcium indicators conjugated to dextran amines (O'Donovan et al 1993, Glover et al 1986). This offers a way of labeling specific groups of neurons in a preparation. Finally, cells can be labeled by electroporation (Bonnot et al 2005). This offers a somewhat less selective labeling protocol then the retrograde approach, but is considerably faster, and might be more preferable in preparations with poor long-term viability.

The biggest advantage of calcium imaging relative to classical electrical recording is that it provides the ability to simultaneously record from a large number of neurons at single cell resolution. Over the last two decades this has given us important insights into the neuronal circuitry of the mouse, rat and chicken spinal cord (Lev-Tov and O'Donovan 1995; Bonnot et al 2002; O'Donovan et al 2005; Wilson et al 2007). More recently calcium imaging has been employed to study the connectivity between descending neurons of the brain stem and spinal motoneurons and interneurons (Szokol et al 2008, 2009, 2011; Kasumacic et al 2010). However, calcium imaging is not without limitations. Because of the poor temporal resolution (compared to electrical recordings), it cannot be used as a definitive tool to distinguish between mono- and polysynaptic connections. Furthermore, since calcium influx is only associated with activation of voltage-sensitive calcium channels and thus excitatory postsynaptic events (although it can also be released from intracellular stores),

inhibitory connections cannot be visualized directly. Moreover, it is difficult to distinguish postsynaptic potentials and action potentials, both of which can give detectable calcium signals. Lastly, because neuronal circuits have a 3-dimensional organization, it can be difficult to visualize calcium signals in neurons that lie deep within the brain stem or spinal cord due to the optics of the tissue. One way to address this issue has been to generate semi-intact preparations in which slices are made into the spinal cord to provide optical access to deeper structures (Szokol and Perreault, 2009). As long as this does not interrupt any of the circuit connections it can provide clearer views of neuronal activity that are difficult to achieve otherwise.

AIMS OF THIS THESIS

1. Establish a preparation for functional studies of the vestibulospinal system in the newborn mouse.

2. Characterize vestibulospinal connections in the newborn mouse and compare to current knowledge about these connections in adult mammals.

3. Investigate vestibulosympathetic connections in the newborn mouse.

SUMMARIES OF INDIVIDUAL PAPERS

Paper I

Segmental patterns of vestibular-mediated synaptic inputs to axial and limb motoneurons in the neonatal mouse assessed by optical recording.

Nedim Kasumacic, Joel C. Glover and Marie-Claude Perreault

Journal of Physiology (2010) 588:4905-4925

In this paper we used calcium imaging to study the connections between vestibulospinal neurons and spinal motoneurons in the neonatal mouse. The main aims of this study were to 1) investigate whether synaptic connections between vestibulospinal neurons and motoneurons are present and functional in the newborn mouse, and 2) characterize the relative contributions of the three vestibulospinal tracts (LVST, iMVST and cMVST) to the activation of MNs at different segmental levels of the spinal cord.

Stimulation of the vestibular nerve evoked calcium responses in MNs in both the medial and lateral motor columns (MMC and LMC) of all the segments studied, both on the ipsilateral and contralateral sides, with the exception of the ipsilateral MMC in L2 and L5. By selectively interrupting the three vestibulospinal tracts with brainstem or spinal cord lesions we were able to characterize the specific contribution of each tract to the vestibulospinal input to MNs in the different spinal segments. Based on the results in this paper we propose an innervation pattern in which the MVSTs provide input primarily to neck- and forelimb-innervating MNs, whereas the LVST provides input primarily to forelimb, trunk and hindlimb MNs. The innervation

pattern proposed in this paper (Figure 10) is similar to that described in adult cats and rabbits where it has been shown that ipsilateral axial MNs in the cervical cord receive inputs from both the LVST and MVST, whereas ipsilateral forelimb MNs receive input from the LVST alone. Contralateral neck and forelimb MNs receive inputs from the cMVST (cf. Wilson et al 1995; Shinoda et al 2006; Akaike et al 1973). From this study, we conclude that the connections between vestibulospinal neurons and spinal motoneurons are synaptically functional at birth with a segment- and tract-specific organization similar to that in adult mammals. In addition, we obtained information about the vestibulospinal connections to axial motoneurons in the lumbar cord that had not been investigated previously in adult mammals. Here, we found an interesting asymmetry in which contralateral but not ipsilateral axial motoneurons were activated by the LVST. Lastly, we observed interesting temporal differences in the activation of hindlimb motoneurons in the L2 (primarily flexor-innervating) and L5 (primarily extensor-innervating) segments. L2 motoneurons gave an "OFF" response, whereas L5 motoneurons gave an "ON" response, indicating a functional interaction that minimizes co-activation of these two hindblimb motoneuron populations.

Paper II

Vestibular synaptic inputs and pathways to sympathetic preganglionic neurons in the neonatal mouse.

Nedim Kasumacic, Joel C. Glover and Marie-Claude Perreault

Submitted to

Studies from cats and humans have shown that the vestibular system has a key role in counteracting orthostatic hypotension. In this paper, using calcium imaging, we have investigated the pathways and synaptic connections between vestibular neurons and sympathetic preganglionic neurons (SPNs) in the thoracic cord.

We labeled SPNs in spinal segments T2, T4, T6, T8, T10 and T12 by applying Calcium Green Dextran Amine to the ventral roots. We imaged the SPNs through the obliquely cut transverse surface of the spinal cord during electrical stimulation of the vestibular nerve.

Stimulation of the vestibular nerve evoked responses in SPNs on ipsilateral and contralateral sides of all the thoracic segments that we studied. We focused on segment T10 and performed additional experiments to investigate the synaptic connectivity in more detail. Response latencies that we recorded suggest a polysynaptic pathway. This is supported by application of mephenesin, which selectively blocks polysynaptic pathways, selectively to the spinal cord. This abolishes the responses completely. Blockade of GABA-A receptor-mediated transmission in the spinal cord leads to an increase in the responses recorded, which suggests a dual excitatory and inhibitory connection. Finally, by making selective lesions in the brain stem or spinal cord we were able to map out some of the main

features of the connectivity of the vestibulosympathetic system. We found little evidence to support direct connections mediated by vestibulospinal tracts, but rather evidence for an indirect pathway that is dependent on neuron populations in the caudal and rostral ventrolateral medulla. We conclude that synaptic connections within the vestibulosympathetic system are functional at birth and involve a polysynaptic circuit within the brain stem similar to that described in adult mammals.

Paper III

Vestibular inputs to descending commissural interneurons in the thoracic and lumbar spinal cord of the neonatal mouse investigated with calcium imaging

Nedim Kasumacic, Joel C. Glover and Marie-Claude Perreault.

Manuscript

In paper I we showed that vestibulospinal inputs to contralateral thoracolumbar motoneurons (MNs) in the neonatal mouse are mediated exclusively via axons descending in the lateral vestibulospinal tract (LVST). According to the literature on adult mammals and our own experiments in neonatal mice, in which contralateral hemisection at the C1 level has no impact on responses in thoracolumber spinal MNs, LVST axons enter the spinal cord only ipsilaterally. This together with the fact that local lesions of the midline eliminate LVST-mediated responses in contralateral MNs, suggests a likely contribution from commissural interneurons (CINs) to responses in contralateral MNs. In this paper, we test directly for the presence of LVST inputs to thoracolumbar descending CINs (dCINs). Using calcium imaging in the neonatal mouse brainstem-spinal cord preparation, we recorded responses evoked by electrical stimulation of the vestibular nerve in more than 250 individual dCINs in the T7, L2 and L5 segments. We found that 95 % of the T7 dCINs, 36 % of the L2 dCINs and 93 % of the L5 dCINs examined responded to vestibular nerve stimulation. The onset latencies of the responses ranged between 29-105 ms (mean of 68 ms, 76 ms and 84 ms for T7 and L2 dCINs, respectively). The responsive dCINs in L2 were the most ventral of the labeled dCIN population; virtually no responsive dCINs were located dorsal to the central canal in this segment. These results support the existence of dCIN-mediated LVST pathways to contralateral MNs of the thoracolumbar cord. The

ranges of response latencies suggest the presence of both mono- and polysynaptic connections between LVST neurons and dCINs and therefore other groups of spinal interneurons are likely to be involved in mediating the LVST inputs to contralateral MNs. The potential contribution of commissural LVST axon collaterals to contralateral MNs remains to be examined. The data also suggest the existence of a topographical organization according to which LVST neurons target preferentially the most ventrally located dCINs in L2 but a more widespread population in T7 and L5. This may be functionally linked to the marked stimulus-related difference ("OFF" versus "ON", respectively) in the responses of T2 and T5 hindlimb-innervating MNs observed in Paper 1.

LIST OF REFERENCES

Abend WK. Functional organization of the superior vestibular nucleus of the squirrel monkey.

Brain Res. 1977 132:65-84.

Abzug C., Maeda M., Peterson BW.and Wilson VJ. Cervical branching of lumbar vestibulospinal axons.

J Physiol. 1974 243:499-522.

Adams SA. How calcium indicators work.

In Imaging in Neuroscience and Development: A Laboratory Manual, 2005 ed. Yuste R and Konnerth A.CSHL Press

Akaike T., Fanardjian VV., Ito M., Kumada M. and Nakajima H. Electrophysiological analysis of the vestibulospinal reflex pathway of rabbit. I. Classification of tract cells.

Exp Brain Res. 1973a 17:477-96.

Akaike T., Fanardjian VV., Ito M. and Ono T. Electrophysiological analysis of thevestibulospinal reflex pathway of rabbit. II. Synaptic actions upon spinal neurones.

Exp Brain Res. 1973b 17:497-515.

Akaike T. and Westerman RA. Spinal semental levels innervated by different types of vestibulo-spinal tract neurones in rabbit.

Exp Brain Res. 1973 17:443-6

Altman J. and Bayer SA. Development of the brain stem in the rat. III. Thymidine-radiographic study of the time of origin of neurons of the vestibular and auditory nuclei of the upper medulla.

J Comp Neurol. 1980 194:877-904.

Andersson G. and Oscarsson O. Projections to lateral vestibular nucleus from cerebellar climbing fiber zones.

Exp Brain Res. 1978a 32:549-64.

Andersson G. and Oscarsson O. Climbing fiber microzones in cerebellar vermis and their projection to different groups of cells in the lateral vestibular nucleus.

Exp Brain Res. 1978 32:565-79.

Auclair F., Bélanger MC. and Marchand R. Ontogenetic study of early brain stem projections to the spinal cord in the rat.

Brain Res Bull. 1993;30(3-4):281-9.

Auclair F., Marchand R. and Glover JC. Regional patterning of reticulospinal and vestibulospinal neurons in the hindbrain of mouse and rat embryos.

J Comp Neurol. 1999 411:288-300.

Balaban CD. Projections from the parabrachial nucleus to the vestibular nuclei in rabbits: A visceral relay to vestibular circuits

Assoc. Res. Otolaryngol. Abstr. 20:1997, p. 68.

Barmack NH. Central vestibular system: vestibular nuclei and posterior cerebellum.

Brain Res Bull 2003 60: 511 - 541

Benson AJ. The vestibular sensory system.

In The Senses Chapter 16, ed. Barlow HB. And Mollon JD., Cambridge unversity press 1982

Bent LR., Bolton PS. and Macefield VG. Modulation of muscle sympathetic bursts by sinusoidal galvanic vestibular stimulation in human subjects.

Exp Brain Res. 2006 174:701-11.

Bergström B. Morphology of the vestibular nerve. II. The number of myelinated vestibular nerve fibers in man at various ages.

Acta Otolaryngol. 1973 76:173-9.

Bergström B. Morphology of the vestibular nerve. III.Analysis of the calibers of the myelinated vestibular nerve fibers in man at various ages.

Acta Otolaryngol. 1973 Nov;76(5):331-8.

Bilotto G., Goldberg J., Peterson BW. and Wilson VJ. Dynamic properties of vestibular reflexes in the decerebrate cat.

Exp Brain Res. 198247:343-52.

Bolton PS., Goto T., Schor RH., Wilson VJ., Yamagata Y. and Yates BJ. Response of pontomedullary reticulospinal neurons to vestibular stimuli in vertical planes.Role in vertical vestibulospinal reflexes of the decerebrate cat.

J Neurophysiol. 1992 67:639-47.

Bonnot A., Mentis GZ., Skoch J. and O'Donovan MJ. Electroporation loading of calcium-sensitive dyes into the CNS.

J Neurophysiol. 2005 93:1793-808.

Bonnot A., Whelan PJ., Mentis GZ. and O'Donovan MJ. Spatiotemporal pattern of motoneuron activation in the rostral lumbar and the sacral segments during locomotor-like activity in the neonatal mouse spinal cord.

J Neurosci. 2002 22:RC203.

Boyle R. and Pompeiano O. Responses of vestibulospinal neurons to neck and macular vestibular inputs in the presence or absence of the paleocerebellum.

Ann N Y Acad Sci. 1981a 374:373-94.

Boyle R. and Pompeiano O. Convergence and interaction of neck and macular vestibular inputs on vestibulospinal neurons.

J Neurophysiol. 1981b 45:852-68.

Boyle R. and Pompeiano O. Relation between cell size and response characteristics of vestibulospinal neurons to labyrinth and neck inputs.

J Neurosci. 1981 1:1052-66.

Brink EE., Hirai N. and Wilson VJ. Influence of neck afferents on vestibulospinal neurons.

Exp Brain Res. 1980 38:285-92.

Brodal A. Anatomy of the vestibular nuclei and their connections.

In Handbook of Sensory Physiology, Vol. VI/1:Vestibular system (H.H. Kornhuber,ed)1974

Brodal A. and Pompeiano O. The vestibular nuclei in the cat

J Anat. 1957 91:438-54.

Brustein E., Marandi N., Kovalchuk Y., Drapeau P. and Konnerth A. "In vivo" monitoring of neuronal network activity in zebrafish by two-photon Ca(2+) imaging.

Pflugers Arch. 2003 446:766-73.

Büttner-Ennever JA. Patterns of connectivity in the vestibular nuclei.

Ann N Y Acad Sci. 1992 656:363-78.

Cabaj A., Stecina K. and Jankowska E. Same spinal interneurons mediate reflex actions of group Ib and group II afferents and crossed reticulospinal actions.

J Neurophysiol. 2006 95:3911-22.

Carleton SC. and Carpenter MB. Distribution of primary vestibular fibers in the brainstem and cerebellum of the monkey.

Brain Res. 1984 294:281-98.

Costa F., Lavin P., Robertson D. and Biaggioni I. Effect of neurovestibular stimulation on autonomic regulation.

Clin Auton Res. 1995 5:289-93.

Dampney RA. Functional organization of central pathways regulating the cardiovascular system.

Physiol Rev. 1994 74:323-64.

Dasen JS. and Jessell TM. Hox networks and the origins of motor neuron diversity.

Curr Top Dev Biol. 2009 88:169-200.

Davies HE. and Edgley SA. Inputs to group II-activated midlumbar interneurones from descending motor pathways in the cat.

J Physiol. 1994 479: 463-73.

Diaz C. and Glover JC. Comparative aspects of the hodological organization of the vestibular nuclear complex and related neuron populations.

Brain Res Bull. 2002 57:307-12.

Díaz C., Puelles L., Marín F. and Glover JC. The relationship between rhombomeres and vestibular neuron populations as assessed in quail-chicken chimeras.

Dev Biol. 1998 202:14-28.

Doba N. and Reis DJ. Role of the cerebellum and the vestibular apparatus in regulation of orthostatic reflexes in the cat.

Circ Res. 1974 40:9-18.

Dougherty KJ. and Kiehn O. Functional organization of V2a-related locomotor circuits in the rodent spinal cord.

Ann N Y Acad Sci. 2010 1198:85-93.

Eatock RA., Xue J. and Kalluri R. Ion channels in mammalian vestibular afferents may set regularity of firing.

J Exp Biol. 2008 211:1764-74.

Eide AL., Glover JC., Kjaerulff O. and Kiehn O. Characterization of commissural interneurons in the lumbar region of the neonatal rat spinal cord.

J Comp Neurol. 1999 403:332-45.

Erulkar SD., Sprague JM., Whitsel BL., Dogan S. and Jannetta PJ. Organization of the vestibular projection to the spinal cord of the cat.

J Neurophysiol. 1966 29:626-64.

Ezure K., Sasaki S., Uchino Y. and Wilson VJ. Frequency-response analysis of vestibular-induced neck reflex in cat. II. Functional significance of cervical afferents and polysynaptic descending pathways.

J Neurophysiol. 1978 41:459-71.

Fukushima K. Corticovestibular interactions: anatomy, electrophysiology, and functional considerations.

Exp Brain Res. 1997 117:1-16

Fukushima Y., Igusa Y. and Yoshida K. Characteristics of responses of medial brain stem neurons to horizontal head angular acceleration and electrical stimulation of the labyrinth in the cat.

Brain Res. 1977 120:564-70.

Furuya N., Kawano K. and Shimazu H. Transcerebellar inhibitory interaction between the bilateral vestibular nuclei and its modulation by cerebellocortical activity.

Exp Brain Res. 1976 25:447-63.

Gacek RR. and Lyon M. The localization of vestibular efferent neurons in the kitten with horseradish peroxidase.

Acta Otolaryngol. 1974 77:92-101.

Gauer, OH. and Thron, H. L. Postural changes in the circulation.

Handbook ofPhysiology, Sec. 2, Circulation III, pp. 2409--2439, Amer. Physiol. See., 1965

Glover JC. The organization of vestibulo-ocular and vestibulospinal projections in the chicken embryo.

Eur J Morphol. 1994 32:193-200.

Glover JC. Retrograde and anterograde axonal tracing with fluorescent dextran-amines in the embryonic nervous system.

Neurosci Prot 1995 30, 1–13.

Glover JC. Development of second-order vestibular projections in the chicken embryo.

Ann N Y Acad Sci. 1996 781:13-20.

Glover JC. Development of vestibule-ocular circuitry in the chicken embryo.

J Physiol 2003 97:17-25

Glover JC. and Petursdottir G. Pathway specificity of reticulospinal and vestibulospinal projections in the 11-day chicken embryo.

J Comp Neurol. 1988 270:25-38

Glover JC. and Petursdottir G. Regional specificity of developing reticulospinal, vestibulospinal, and vestibulo-ocular projections in the chicken embryo.

J Neurobiol. 1991 22:353-76.

Glover JC., Petursdottir G. and Jansen JK. Fluorescent dextran-amines used as axonal tracers in the nervous system of the chicken embryo.

J Neurosci Methods.1986 18:243-54.

Goldberg JM. Afferent diversity and the organization of central vestibular pathways.

Exp Brain Res. 2000 130:277-97.

Goldberg JM. and Fernandez C. Physiology of peripheral neurons innervating semicircular canals of the squirrel monkey. I. Resting discharge and response to constant angular accelerations.

J Neurophysiol. 1971a 34:635-60.

Goldberg JM. and Fernandez C. Physiology of peripheral neurons innervating semicircular canals of the squirrel monkey. III. Variations among units in their discharge properties.

J Neurophysiol. 1971b 34: 676-84.

Goldberg JM. and Fernandez C. The vestibular system

American Physiological Society, Handbook of Physiology 1984, The nervous system, volume III Chapter 21: 977-1022

Goldberg JM., Smith CE. and Fernández C. Relation between discharge regularity and responses to externally applied galvanic currents in vestibular nerve afferents of the squirrel monkey.

J Neurophysiol. 1984 51: 1236-56.

Grillner S., Hongo T. and Lund S. The vestibulospinal tract.Effects on alpha-motoneurones in the lumbosacral spinal cord in the cat.

Exp Brain Res. 197010:94-120.

Grynkiewicz G., Poenie M. and Tsien RY.A new generation of Ca2+ indicators with greatly improved fluorescence properties.

J Biol Chem. 1985 260:3440-50.

Highstein SM. and Holstein GR. The anatomy of the vestibular nuclei.

Prog Brain Res. 2006 151:157-203.

Hollyday M. Organization of motor pools in the chick lumbar lateral motor column

J Comp Neurol. 1980 194:143-70.

Holstein GR., Martinelli GP.and Friedrich VL. Anatomical observations of the caudal vestibulo-sympathetic pathway.

J Vestib Res. 201121:49-62.

Hongo T., Kudo N. and Tanaka R. Effects from the vestibulospinal tract on the contralateral hindlimb motoneurones in the cat.

Brain Res. 1971 31:220-3.

Hudspeth AJ. The cellular basis of hearing: the biophysics of hair cells.

Science. 1985 230:745-52.

Kaada BR. Site of action of myanesin in the central nervous system.

J Neurophysiol. 1950 13:89-104.

Kandel E., Schwartz J. and Jessell TM. Principles of Neural Science *McGraw-Hill Medical 4th edition 2000.*

Kasahara M., Mano N., Oshima T., Ozawa S. and Shimazu H. Contralateral short latency inhibition of central vestibular neurons in the horizontal canal system.

Brain Res. 1968 8:376-8.

Kasper J., Schor RH. and Wilson VJ. Response of vestibular neurons to head rotations in vertical planes. I. Response to vestibular stimulation.

J Neurophysiol. 1988 60:1753-64.

Kerman IA., McAllen RM. and Yates BJ. Patterning of sympathetic nerve activity in response to vestibular stimulation.

Brain Res Bull. 2000 53:11-6.

Kiehn O. and Butt SJ. Physiological, anatomical and genetic identification of CPG neurons in the developing mammalian spinal cord.

Prog Neurobiol. 2003 4:347-61.

Kotchabakdi N, Rinvik E, Walberg F, Yingchareon K. The vestibulothalamic projections in the cat studied by retrograde axonal transport of horseradish peroxidase.

Exp Brain Res 1980 40: 405- 418

Krutki P., Jankowska E. and Edgley SA. Are crossed actions of reticulospinal and vestibulospinal neurons on feline motoneurons mediated by the same or separate commissural neurons?

J Neurosci. 2003 23:8041-50.

Kuypers HGJM. Anatomy of descending pathways

In Handbook of physiology, chapter 13. 1984

Ladpli R. and Brodal A. Experimental studies of commissural and reticular formation projections from the vestibular nuclei in the cat.

Brain Res. 1968 8:65-96.

Lakke EA. The projections to the spinal cord of the rat during development: a timetable of descent.

Adv Anat Embryol Cell Biol. 1997;135:I-XIV, 1-143.

Landmesser L. The distribution of motoneurones supplying chick hind limb muscles.

J Physiol. 1978 284:371-89.

Landolt JP, Topliff ED, Silverberg JD. Size distribution analysis of myelinated fibers in the vestibular nerve of the pigeon.

Brain Res. 1973 54:31-42.

Lev-Tov A. and Pinco M. In vitro studies of prolonged synaptic depression in the neonatal rat spinal cord.

J Physiol. 1992 447:149-69.

Lev-Tov A. and O'Donovan MJ. Calcium imaging of motoneuron activity in the en-bloc spinal cord preparation of the neonatal rat.

J Neurophysiol. 1995 74:1324-34.

Lloyd TC Jr. Effect of inspiration on inferior vena caval blood flow in dogs.

J Appl Physiol. 1983 55:1701-8.

Lloyd TC Jr. and Cooper JA. Effect of diaphragm contraction on canine heart and pericardium.

J Appl Physiol. 1983 54:1261-8.

Ludbrook J. The musculovenous pumps in the human lower limb.

Am Heart J. 1966 71:635-41.

Lund S. and Pompeiano O. Monosynaptic excitation of alpha motoneurones from supraspinal structures in the cat.

Acta Physiol Scand. 1968 73:1-21.

Mano N., Oshima T. and Shimazu H. Inhibitory commissural fibers interconnecting the bilateral vestibular nuclei.

Brain Res. 1968 8:378-82.

Matsuyama K., Mori F., Nakajima K., Drew T., Aoki M. and Mori S. Locomotor role of the corticoreticular-reticulospinal-spinal interneuronal system.

Prog Brain Res. 2004143:239-49.

McClellan AD., McPherson D. and O'Donovan MJ. Combined retrograde labeling and calcium imaging in spinal cord and brainstem neurons of the lamprey.

Brain Res. 1994 663:61-8.

McCrea DA. And Rybak IA. Organization of mammalian locomotor rhythm and pattern generation.

Brain Res Rev. 2008 1:134-46

Minta A., Kao JP. and Tsien RY. Fluorescent indicators for cytosolic calcium based on rhodamine and fluorescein chromophores.

J Biol Chem. 1989 264:8171-8.

Mitsacos A., Reisine H. and Highstein SM. The superior vestibular nucleus: an intracellular HRP study in the cat. II. Non-vestibulo-ocular neurons.

J Comp Neurol. 1983 215:78-91.

Mitsacos A., Reisine H. and Highstein SM. The superior vestibular nucleus: an intracellular HRP study in the cat. I. Vestibulo-ocular neurons.

J Comp Neurol. 1983 215:92-107.

Miyawaki A., Llopis J., Heim R., McCaffery JM., Adams JA., Ikura M. and Tsien RY. Fluorescent indicators for Ca2+ based on green fluorescent proteins and calmodulin.

Nature. 1997 388:882-7.

Monahan KD. and Ray CA. Vestibulosympathetic reflex during orthostatic challenge in aging humans.

Am J Physiol Regul Integr Comp Physiol. 2002 283:R1027-32.

Money KE. And Scott JW. Function of separate sensory receptors of non-auditory labyrinth of the cat.

Am. J. Physiol. 1962 202:1211-120

Musienko PE., Zelenin PV., Lyalka VF., Orlovsky GN. and Deliagina TG. Postural performance in decerebrated rabbit.

Behav Brain Res. 2008 190:124-34.

Nyberg-Hansen R. Sites and mode of termination of reticulo-spinal fibers in the cat. An experimental study with silver impregnation methods.

J Comp Neuronl. 1965 124:71-99

Nissen UV., Moldovan M., Hounsgaard J. and Glover JC. Organization of projection-specific interneurons in the spinal cord of the red-eared turtle.

Brain Behav Evol. 2008 72:179-91.

Nyberg-Hansen R. Origin and termination of fibers from the vestibular nuclei descending in the medial longitudinal fasciculus. An experimental study with silver impergnation methods in the cat.

J Comp Neurol. 1964 122:355-67

Nyberg-Hansen R. Functional organization of descending supraspinal fibre systems to the spinalcord.Anatomical observations and physiological correlations.

Ergeb Anat Entwicklungsgesch. 1966a 39:3-48.

Nyberg-Hansen R. Sites of termination of interstitiospinal fibers in the cat. An experimental study with silver impregnation methods.

Arch Ital Biol. 1966b 104:98-111.

Nyberg-Hansen R. and Mascitti TA. Site and mode of termination of fibers of the vestibulospinal tract in the cat.An experimental study with silver impregnation methods.

J Comp Neurol. 1964 122:369-83.

O'Donovan MJ., Bonnot A., Mentis GZ., Arai Y., Chub N., Shneider NA. and Wenner P. Imaging the spatiotemporal organization of neural activity in the developing spinal cord.

Dev Neurobiol. 2008 68:788-803.

O'Donovan MJ., Bonnot A., Wenner P. and Mentis GZ. Calcium imaging of network function in the developing spinal cord.

Cell Calcium. 2005 37:443-50.

O'Donovan MJ., Ho S., Sholomenko G. and Yee W. Real-time imaging of neurons retrogradely and anterogradely labelled with calcium-sensitive dyes.

J Neurosci Methods.1993 46:91-106.

Pan PS., Zhang YS. and Chen YZ. Role of the nucleus vestibularis medialis in vestibulo-sympathetic response in rats.

Sheng Li Xue Bao. 1991 43:184-8.

Pasqualetti M., Díaz C., Renaud JS., Rijli FM. and Glover JC. Fate-mapping the mammalian hindbrain: segmental origins of vestibular projection neurons assessed using rhombomere-specific Hoxa2 enhancer elements in the mouse embryo.

J Neurosci. 2007 27:9670-81.

Peterson BW. Reticulospinal projections to spinal motor nuclei.

Annu Rev Physiol. 197941:127-40.

Peterson BW., Filion M., Felpel LP. And Abzug C. Responses of medial reticular neurons to stimulation of the vestibular nerve.

Exp Brain Res 1975 22:335-350

Petras JM. Cortical, tectal and tegmental fiber connections in the spinal cord of the cat.

Brain Res. 1967 6:275-324.

Petursdottir G. Vestibulo-ocular projections in the 11-day chicken embryo: pathway specificity.

J Comp Neurol. 1990 297:283-97.

Pompeiano O. and Brodal A. The origin of vestibulospinal fibres in the cat.An experimental-anatomical study, with comments on the descending medial ongitudunal fasciculus.

Arch. Ital. Biol. 1957, 95:166-198

Porter JD. and Balaban CD. Connections between the vestibular nuclei and brain stem regions that mediate autonomic function in the rat.

J Vestib Res. 1997 7:63-76.

Purves D. Neuroscience

Sinauer Associates, Inc. 4th edition 2007

Rapoport S., Susswein A., Uchino Y. and Wilson VJ. Properties of vestibular neurones projecting to neck segments of the cat spinal cord.

J Physiol. 1977 268:493-510.

Ray CA. and Carter JR. Vestibular activation of sympathetic nerve activity.

Acta Physiol Scand. 2003 177:313-9.

Ray CA., Hume KM. and Steele SL. Sympathetic nerve activity during natural stimulation of horizontal semicircular canals in humans.

Am J Physiol. 1998 275:R1274-8.

Ray CA. and Monahan KD. Aging attenuates the vestibulosympathetic reflex in humans.

Circulation. 2002 105:956-61.

Raymond J., Dememes D. and Nieoullon A. Neurotransmitters in vestibular pathways.

Prog Brain Res. 1988 z76:29-43.

Roberts TDM. Labyrinthine control of postural muscles.

In 3d symposium on the role of the vestibular organs in space exploration, 1968,NASA SP-152:149-168

Roberts TDM. Reflex balance

Nature 1973, 244:156-158

Roberts TDM. Neurophysiology of postural mechanisms

2nd Ed. London Butterworths 1978

Romanes GJ. The motor cell columns of the lumbo-sacral spinal cord of the cat.

J Comp Neurol. 1951 2:313-63.

Romanes GJ. The development and significance of the cell columns in the ventral horn of the cervical and upper thoracic spinal cord of the rabbit.

J Anat. 1941 76:112-130.5.

Romanes GJ. The motor pools of the spinal cord.

Prog Brain Res. 1964 11:93-119.

Routal RV. andPal GP.A study of motoneuron groups and motor columns of the human spinal cord.

J Anat. 1999 195:211-24.

Shimazu H. and Precht W. Inhibition of central vestibular neurons from the contralateral labyrinth and its mediating pathway.

J Neurophysiol. 1966 29:467-92.

Shinoda Y., Ohgaki T. and Futami T. The morphology of single lateral vestibulospinal tract axons in the lower cervical spinal cord of the cat.

J Comp Neurol. 1986 249:226-41.

Shinoda Y., Ohgaki T., Futami T. and Sugiuchi Y. Vestibular projections to the spinal cord: the morphology of single vestibulospinal axons.

Prog Brain Res. 198876:17-27.

Shinoda Y., Ohgaki T., Sugiuchi Y. and Futami T. Morphology of single medial vestibulospinal tract axons in the upper cervical spinal cord of the cat.

J Comp Neurol. 1992316:151-72.

Shortt TL. and Ray CA. Sympathetic and vascular responses to head-down neck flexion in humans.

Am J Physiol. 1997 272:H1780-4.

Spyer KM., Ghelarducci B. and Pompeiano O. Gravity responses of neurons in main reticular formation.

J Neurophysiol. 1974 37:705-21.

Stauss HM. Baroreceptor reflex function.

Am J Physiol Regul Integr Comp Physiol. 2002 283:R284-6.

Stosiek C., Garaschuk O., Holthoff K. and Konnerth A. In vivo two-photon calcium imaging of neuronal networks.

Proc Natl Acad Sci U S A. 2003 100:7319-24.

Straka H., Baker R. and Gilland E. Rhombomeric organization of vestibular pathways in larval frogs.

J Comp Neurol. 2001 437:42-55.

Straka H, Holler S, Goto F. Patterns of canal and otolith afferent input convergence in frog second-order vestibular neurons.

J Neurophysiol. 2002 88:2287-301.

Szokol K., Glover JC. and Perreault MC. Differential origin of reticulospinal drive to motoneurons innervating trunk and hindlimb muscles in the mouse revealed by optical recording.

J Physiol. 2008 586:5259-76.

Szokol K., Glover JC. and Perreault MC. Organization of functional synaptic connections between medullary reticulospinal neurons and lumbar descending commissural interneurons in the neonatal mouse.

J Neurosci. 2011 31:4731-42.

Szokol K. and Perreault MC. Imaging synaptically mediated responses produced by brainstem inputs onto identified spinal neurons in the neonatal mouse.

J Neurosci Methods.2009 180:1-8.

Takakusaki K., Kohyama J., Matsuyama K. and Mori S. Medullary reticulospinal tract mediating the generalized motor inhibition in cats: parallel inhibitory mechanisms acting on motoneurons and on interneuronal transmission in reflex pathways.

Neuroscience. 2001 103:511-27.

Tanaka Y., Tanaka Y., Furuta T., Yanagawa Y.and Kaneko T. The effects of cutting solutions on the viability of GABAergic interneurons in cerebral cortical slices of adult mice.

J Neurosci Methods 2008 171, 118–125.

Tosney KW and Landmesser L. Specificity of early motoneuron growth cone outgrowth in the chick embryo.

J Neurosci. 1985 9:2336-44.

Tsien RY. New calcium indicators and buffers with high selectivity against magnesium and protons: design, synthesis, and properties of prototype structures.

Biochemistry. 1980 19:2396-404.

Tsien RY. Intracellular signal transduction in four dimensions: from molecular design to physiology.

Am J Physiol. 1992 263:C723-8.

Vito RV., DeBrusa A. and Arudini A. Cerebellar and vestibular influences on Deitersian units.

Jour. Neurophysiol 1956, 19:241

Voustianiouk A., Kaufmann H., Diedrich A., Raphan T., Biaggioni I., Macdougall H., Ogorodnikov D. and Cohen B. Electrical activation of the human vestibulo-sympathetic reflex.

Exp Brain Res. 2006 171:251-61.

Whelan PJ. Control of locomotion in the decerebrate cat.

Prog Neurobiol. 1996 49:481-515.

Wilson JM., Dombeck DA., Díaz-Ríos M., Harris-Warrick RM. and Brownstone RM. Two-photon calcium imaging of network activity in XFP-expressing neurons in the mouse.

J Neurophysiol. 2007 97:3118-25.

Wilson VJ. and Melvill-Jones G. Mammalian vestibular physiology.

Plenum Press, New York 1979

Wilson VJ., Kato M., Peterson BW. and Wylie RM.A single-unit analysis of the organization of Deiters' nucleus.

J Neurophysiol. 1967 30:603-19.

Wilson VJ., Kato M., Thomas RC. and Peterson BW. Excitation of lateral vestibular neurons by peripheral afferent fibers.

J Neurophysiol. 1966 29:508-29.

Wilson VJ. and Peterson BW. Vestibulospinal and reticulospinal systems

American Physiological Society, Handbook of Physiology 1981, Chapter 14: 667-701

Wilson VJ., Peterson BW., Fukushima K., Hirai N. and Uchino Y. Analysis of vestibulocollic reflexes by sinusoidal polarization of vestibular afferent fibers.

J Neurophysiol. 1979 42:331-46.

Wilson VJ., Wylie RM. and Marco LA. Organization of the medial vestibular nucleus.

J Neurophysiol. 1968 31:166-75.

Wilson VJ., Yamagata Y., Yates BJ., Schor RH. and Nonaka S. Response of vestibular neurons to head rotations in vertical planes. III. Response of vestibulocollic neurons to vestibular and neck stimulation.

J Neurophysiol. 1990 64:1695-703.

Wilson VJ. and Yoshida M. Comparison of effects of stimulation of Deiters' nucleus and medial longitudinal fasciculus on neck, forelimb, and hindlimb motoneurons.

J Neurophysiol. 1969 32:743-58.

Wilson VJ., Yoshida M. and Schor RH. Supraspinal monosynaptic excitation and inhibition of thoracic back montoneurons.

Exp Brain Res. 197011:282-95.

Yates BJ. Vestibular influences on the sympathetic nervous system.

Brain Res Brain Res Rev. 1992 17:51-9.

Yates BJ. Vestibular influences on the autonomic nervous system.

Ann N Y Acad Sci. 1996 781:458-73.

Yates BJ., Goto T. and Bolton PS. Responses of neurons in the caudal medullary raphe nuclei of the cat to stimulation of the vestibular nerve.

Exp Brain Res. 199289:323-32.

Yates BJ., Holmes MJ. and Jian BJ. Adaptive plasticity in vestibular influences on cardiovascular control.

Brain Res Bull. 2000 53:3-9.

Yates BJ. and Miller AD. Properties of sympathetic reflexes elicited by natural vestibular stimulation: implications for cardiovascular control.

J Neurophysiol. 1994 71:2087-92.

Yates BJ., Jakus J. and Miller AD. Vestibular effects on respiratory outflow in the decerebrate cat.

Brain Res. 1993 629:209-17.

Yates BJ., Siniaia MS. and Miller AD. Descending pathways necessary for vestibular influences on sympathetic and inspiratory outflow.

Am J Physiol. 1995 268:R1381-5.

Ye JH., Zhang J., Xiao C. and Kong JQ. Patch-clamp studies in the CNS illustrate a simple new method for obtaining viable neurons in rat brain slices: glycerol replacement of NaCl protects CNS neurons.

J Neurosci Methods 2006 158, 251–259.

Ziskind-Conhaim L.NMDA receptors mediate poly- and monosynaptic potentials in motoneurons of rat embryos.

J Neurosci. 1990 10:125-35.

I

II

Vestibular-mediated synaptic inputs and pathways to sympathetic preganglionic neurons in the neonatal mouse

Nedim Kasumacic, Joel C. Glover* and Marie-Claude Perreault*

Laboratory of Neural Development and Optical Recording (NDEVOR), Department of Physiology, Institute of Basic Medical Sciences, University of Oslo, N-0317 Oslo, Norway

Running head: Imaging vestibular inputs to sympathetic preganglionic neurons

Number of Figures: 9

Keywords: Calcium imaging, vestibulospinal, thoracic, spinal cord, motoneuron, medullary reticulospinal

*** Co-contributing authors, to whom correspondence should be addressed:**

Dr. Joel C. Glover

Department of Physiology, Institute of Basic Medical Sciences, University of Oslo,

PB 1103 Blindern, N-0317, Oslo, Norway

Email: joel.glover@medisin.uio.no

Dr. Marie-Claude Perreault

Current address: Department of Physiology, Emory University School of Medicine,

Whitehead Biomedical Research Building, 615 Michael Street, Atlanta, GA, 0322, USA.

Email: m-c.perreault@emory.edu

Acknowledgments

We are grateful to Kobra Sultani and Marian Berge Andersen for technical assistance, Magne Sand Sivertsen for help with graphics and videos, and Bruce Piercey for writing the FileConvert program. This work was supported by grants from the Medical Faculty of University of Oslo and the Norwegian Research Council to M-C.P. and J.C.G.

Author contributions

NK, JCG and MCP designed and planned experiments. NK and JCG carried out experiments. NK, JCG and MCP analyzed data, wrote the manuscript and approved the final version of the manuscript.

ABSTRACT *(241 words)*

To assess how early vestibulosympathetic projections become functional postnatally, and to establish a preparation in which vestibulosympathetic circuitry can be characterized more precisely, we used an optical approach to record vestibular nerve-evoked synaptic inputs to thoracic sympathetic preganglionic neurons (SPNs) in newborn mice. Stimulation of the vestibular nerve was performed in an isolated brainstem-spinal cord preparation after retrogradely labeling with the fluorescent calcium indicator Calcium Green Dextran Amine (CGDA) the SPNs and the somatic motoneurons (MNs) in the thoracic (T) segments T2, 4, 6, 8, 10 and 12. Synaptically mediated calcium responses could be visualized and recorded in individual SPNs and MNs, and analyzed with respect to latency, temporal pattern, magnitude and synaptic pharmacology. Vestibular nerve stimulation evoked responses in all SPNs and MNs investigated. The SPN responses had onset latencies from 90-200 msec, compared to much shorter latencies in MNs, and were completely abolished by mephenesin, a drug that preferentially reduces polysynaptic over monosynaptic transmission. Bicuculline and picrotoxin but not strychnine increased the magnitudes of the SPN responses without changing the onset latencies, suggesting a convergence of concomitant excitatory and inhibitory synaptic inputs. Lesions strategically placed to test the involvement of direct vestibulospinal pathways versus indirect pathways within the brain stem showed that vestibulosympathetic inputs in the neonate are mediated predominantly, if not exclusively, by the latter. Thus, already at birth, synaptic connections in the vestibulosympathetic reflex are functional and require the involvement of the ventrolateral medulla as in adult mammals.

INTRODUCTION

When the body is tilted from horizontal to vertical, blood tends to accumulate in the legs and blood pressure may fall in the upper body, a phenomenon known as orthostatic hypotension. Normally, compensatory mechanisms including the baroreceptor reflex, contraction of leg muscles and the negative thoracic pressure created by inspiration work in synergy to counteract orthostatic hypotension. However, the earliest phase of compensation occurs too quickly to be explained by these mechanisms, indicating an anticipatory mechanism that reads body tilt more rapidly. It is now well established that the vestibular system has influence over the sympathetic nervous system and cardiovascular control (reviewed in Yates 1996; Yates and Bronstein 2005; Wilson et al 2006). Thus, vestibulosympathetic reflexes triggered by stimulation of vestibular afferents are now considered to constitute the rapid compensatory component that counteracts orthostatic hypotension.

In the first study that proposed a connection between the vestibular system and the sympathetic nervous system it was shown that bilateral transection of the vestibular nerves in cats greatly compromised their ability to compensate for orthostatic hypotension (Doba and Reis 1974). More recently this effect has been shown to have a regional character (reviewed in Kerman et al 2000), with compensation in hindlimb vasculature much more dependent on intact vestibular afferents than compensation in forelimb vasculature (Kerman et al 2000; Wilson et al 2006). Studies in rodents and humans have indicated that attenuation of vestibular afferent signals in the elderly and in post-flight astronauts may be responsible for the orthostatic intolerance that these subjects experience (Buckey et al 1996; Ray and Monahan 2002; Etard et al 2004). Several studies in cats have shown that electrical or natural stimulation of vestibular afferents influences the firing rate of sympathetic nerves (sympathetic chain, muscle sympathetic efferents, cervical, splanchnic and renal nerves)

through combined excitatory and inhibitory synaptic inputs (reviewed in Yates 1992; Kerman et al 2000a). Similar results (using electrical, caloric or natural stimulation) have been obtained in human studies (reviewed in Ray and Carter 2003; Carter and Ray 2008).

While there is ample evidence that vestibular inputs influence the sympathetic nervous system, the underlying neural pathways that mediate this are not completely understood. Lesion studies in the cat have identified a region within the vestibular nuclear complex situated partly in the medial nucleus and partly in the inferior nucleus that is necessary for vestibulosympathetic control (Yates et al 1993; Yates and Miller 1994). However, there is currently no evidence suggesting a direct monosynaptic connection between vestibular neurons and sympathetic preganglionic neurons. A model has been proposed based on anatomical and electrophysiological evidence in which vestibulosympathetic influence is mediated by vestibular neurons that project onto a network of neurons in the rostral and caudal ventrolateral medulla (RVLM and CVLM) as well as the nucleus of the tractus solitarius (NTS) (reviewed in Yates 1996, Balaban and Porter 1998; Yates and Bronstein 2005; Holstein et al 2011). Neurons in the RVLM appear to be the principal source of the descending axons that mediate the vestibulosympathetic responses (Lee et al 2007), and have been shown to make monosynaptic and polysynaptic excitatory (glutamatergic) and inhibitory (GABAergic) connections onto sympathetic preganglionic neurons (SPNs; Deuchars et al 1995,1997). Another potential pathway involved is a vestibulo-raphespinal projection that has been demonstrated anatomically and electrophysiologically (Bacon et al 1990; Yates et al 1993; Porter and Balaban 1997; see however Iiagawa et al 2007).

Although these studies have provided a description of neural substrates sufficient and in some cases necessary to mediate the vestibulosympathetic reflex in the cat, less is known about the

organization of this reflex in other mammalian species. A few studies have begun to investigate the vestibulosympathetic reflex in the rat, demonstrating its contribution to the maintenance of blood pressure during gravitational stress (Gotoh et al 2003; Tanaka et al 2006; Abe et al 2008). Other studies have shown that some neurons in the descending vestibular nucleus and caudal half of the medial vestibular nucleus of the rat contain imidazoleacetic acid-ribotide, a putative neurotransmitter for blood pressure regulation (Friedrich et al 2007; Martinelli et al 2007) and begun to characterize the sympathetic effects of neurochemically-defined subpopulations of RVLM neurons (Burke et al 2011). An important advance would be to characterize vestibulosympathetic circuitry in the mouse because of the opportunities for transgenic manipulation including optogenetic recording and stimulation approaches (reviewed in Zhang et al 2007).

An additional issue that has not yet been addressed is the ontogeny of the vestibulo-sympathetic reflex and its underlying circuitry. This can also be characterized in the mouse, which lends itself well to both anatomical and physiological studies of bulbospinal projections in embryos and neonates (Auclair et al 1999; Pasqualetti et al 2007; Szokol et al 2008; Szokol and Perreault 2009, and see below).

Here, we begin to investigate the functional organization of the murine vestibulosympathetic connections using an *ex vivo* preparation of the brain stem and spinal cord of the neonatal mouse that permits high throughput optical recording of synaptically evoked calcium responses in spinal neurons (Szokol et al 2008; Szokol and Perreault 2009; Kasumacic et al 2010, Szokol et al 2011). We have found that electrical stimulation of the vestibular nerve evokes calcium responses in SPNs throughout the thoracic cord. A variety of lesions within the brain stem and upper cervical cord indicate the involvement of an indirect descending

pathway with a relay within the ventrolateral medulla, as has been proposed in adult mammals. The inability to induce the same responses by direct stimulation of the LVST supports this conclusion. Long response latencies similar to those demonstrated in the adult cat (Yates et al 1995), together with pharmacological experiments using selective application of mephenesin to the spinal cord, suggest that the spinal component of the indirect pathway is also polysynaptic. An increase in response magnitude during pharmacological blockade of GABA receptors within the spinal cord indicates the presence of both inhibitory and excitatory components. A preliminary account of this work has been reported elsewhere (Kasumacic et al 2009, 2010).

MATERIALS AND METHODS

Animals and brainstem-spinal cord preparation

Experiments were performed on newborn mice of the ICR strain (n = 70), at postnatal days (P) 0 - 5. Mice were deeply anesthetized with isoflurane (Abbott, Scandinavia AB) and decerebrated at the level of the superior colliculus. Decerebration was followed by rapid dissection of the brain stem and spinal cord using the same procedure as described in Kasumacic et al (2010). All efforts were made to minimize the number of animals used in accordance with the European Communities Council directive 86/609/EEC and the National Institutes of Health guidelines for the care and use of animals. All procedures were approved by the National Animal Research Authority in Norway (Forsøksdyrutvalget).

Retrograde labeling of SPNs and somatic MNs with fluorescent calcium indicator

After dissection the preparation was placed in oxygenated artificial cerebrospinal fluid (aCSF) containing in mM: NaCl 128, KCl 3, D-glucose11 $CaCl_2$ 2.5, $MgSO_4$ 1, NaH_2PO_4 1.2, Hepes 5, and $NaHCO_3$ 25. Sympathetic preganglionic neurons (SPNs) and somatic motoneurons (MNs) in the thoracic cord (T2, T4, T6, T8, T10 and/or T12 segments) were labeled retrogradely by applying crystals of Calcium Green 1-conjugated dextran amine (CGDA, 3000 MW, Molecular Probes) to the cut ventral roots. Retrograde labelling continued in the dark at room temperature (23–25 ◦C) for 3 h.

Optical recording of calcium responses

Brainstem-spinal cord preparations were transferred to a sylgard-coated chamber and pinned ventral side up with stainless steel (Minuten) pins inserted through the peeled dura mater. Prior to transferring to the recording chamber, an oblique transection (about 45 degrees from the horizontal) was performed at the level of the segment containing the CGDA-labeled

neurons (see Szokol and Perreault 2009 and Szokol et al. 2011 for more details). The transected end was slightly bent and positioned on a trapezoidal block of sylgard glued to the bottom of the chamber so that the obliquely cut surface lay horizontally under the objective (Fig. 1A). In some preparations, SPNs and somatic MNs were labeled in three different thoracic segments (n = 9). In these preparations, oblique cuts were made sequentially starting first with the most caudal segment. Subsequent oblique cuts were performed only after completing optical recording from the caudalmost segments. During recording, labeled neurons were imaged using a 40x water immersion objective (LUMPlanFl, 0.8 NA, Olympus, Norway) on an upright epi-fluorescence microscope (Axioskop FS 2, Carl Zeiss, Oberkochen, Germany) equipped with a 100 W halogen lamp and excitation (BP 450-490 nm) and emission (LP 515 nm) filters and the preparation was perfused continuously with oxygenated aCSF at a rate of 7.5 ml/min (total volume exchange every 2 minutes). Fluorescence intensity changes elicited by stimulation (Ca2+ responses) were registered using a cooled CCD camera (Cascade 650, Photometrics, Texas Instruments, USA) mounted on a video zoom adaptor, using the image-processing software Metamorph 7.7 (Universal Imaging Corporation, Molecular Devices, USA). Image series were routinely acquired at 4 frames/sec and a binning of 3x3. However, in some experiments (n = 10), we used a higher frame rate (100 frames/sec) and higher binning (6x6) to record latencies of the responses at higher temporal resolution. High frame rate recordings could not be performed for long periods because they require higher intensity illumination which rapidly photobleaches the CGDA.

Electrical stimulation

The entire eighth (VIIIth) cranial nerve was stimulated electrically with a suction electrode made from borosilicate glass (Harvard Apparatus, Cat. #: 30-0056). Nerve stimulation consisted of 5 s trains (200 μs pulse duration) at 5 Hz, with a current strength between 60 -

250 μA. In an additional series of experiments (n = 18), we stimulated the lateral vestibular tract (LVST) group, which is the source of the LVST, lying principally within the LVN (Díaz et al 2003, Pasqualetti et al 2007 and references therein) using a monopolar tungsten microelectrode (Parylene-coated, shaft diameter 0.254 mm, tip diameter 1–2 μm, impedance 0.1MΩ at 1 kHz; WPI, USA). To gain access to the LVN we first carefully removed the cerebellum and the dura mater on the dorsal surface of the brain stem. For LVST group stimulation, we used the same parameters as for VIIIth nerve stimulation except that current strengths were lower (50 – 200 μA). The locations of stimulation sites in the LVN were confirmed histologically after making electrolytic lesions (see Szokol and Perreault 2009 for details). In some of these preparations (n = 4), we compared directly the location of the electrolytic lesion to the location of the LVST neurons by labeling these retrogradely on the side opposite to the stimulation by applying crystals of rhodamine dextran amine (RDA 3kD, Invitrogen) to their transected axons in the ventral and ventrolateral funiculi at C1 immediately after making the electrolytic lesion. In 3 of 18 preparations we also blocked glutamatergic synapses selectively in the brain stem using kynurenic acid (see below).

Pharmacological experiments

After isolating the brain stem and the spinal cord with a Vaseline barrier made at the C1 level, bicuculline (20μM, Tocris), picrotoxin (40μM, Sigma), strychnine (0.2μM, Sigma) or mephenesin (1mM, Sigma) were superfused into the compartment containing the spinal cord, or kynurenic acid (5mM, Sigma) was superfused into the compartment containing the brain stem. The tightness of the barrier was verified by adding the dyes Phenol Red or Fast Green to one of the compartments at the end of the experiment. Recordings were started 10 minutes after drug application.

Spinal cord, MLF, and medullary lesions

Spinal cord hemisections (Figure 2A) were made just rostral to the C1 ventral root and longitudinal lesions of the midline spanned rostrocadually across two segments (T9 and T10). Lesions of the medial longitudinal fasciculus (MLF) were made from the dorsal surface of the brainstem by transecting the fasciculus bilaterally at about 200 μm rostral to the obex. The MLF lesion extended about 150 μm from each side of the midline, encompassing the entire mediolateral extent of the MLF in neonatal mice (Paxinos *et al.* 2007 and our own anatomical observations). The MLF lesions effectively eliminate medial vestibulospinal tract (MVST) projections as well as many reticulospinal projections originating rostral to the lesion. Medullary lesions were designed to ablate the regions containing the ipsilateral and contralateral CVLMs and RVLMs, all contralateral vestibulospinal tracts, while sparing the ipsilateral lateral vestibulospinal tract (LVST). This was done by first removing nearly the entire contralateral medulla down to C1, thus eliminating the CVLM, RVLM and all vestibulospinal tracts on that side. Then, a large portion of the lateral ipsilateral medulla was removed spanning from below the LVST group (whose location we are very familiar with through anatomical mapping in several previous studies in addition to this one) caudally to the C2/C3 boundary, sparing medially the LVST and the MLF (Figure 2B). Optical recordings of calcium responses in SPNs and somatic MNs (see below) was always performed both before and after each of these two lesions. The various lesions were made using either fine iridectomy scissors (spinal cord hemisections, midline lesions, medullary lesions) or a custom made wedged blade (midline lesions, MLF lesions) and their locations and spatial extents were confirmed histologically.

Histology

Preparations were fixed overnight in 4 % paraformaldehyde, cryoprotected in 20 % sucrose, embedded in OCT (Tissue-Tek) and frozen. Serial cryostat (Leica, CM3050S) sections (50 μm) made in the transverse, sagittal or frontal plane were stained with Harris haematoxylin (5 % w/v Harris Haematoxylin, Sigma) and mounted on Super Frost glass slides with a gelatin–glycerol medium.

Data analysis

The timing markers for the VIIIth nerve stimulation and the gating pulse from the CCD camera were recorded at 5 kHz (Digidata1320A; Molecular Devices). To synchronize the electrical and the optical recordings, a digital pulse from the Digidata unit was sent to the CCD camera. Using the MetaMorph software, circular digital apertures of identical size and shape (regions of interest or ROIs) were placed manually over all the individual neuron somata that were clearly in focus. To compensate for variability in the CGDA labeling intensity between the different neurons, the change in fluorescence (ΔF) in each ROI was normalized to the baseline fluorescence F0 before the stimulation (ΔF/F0 = (F-F0)/F0). The video files were converted to text files using a custom-made program (FileConvert) and imported into Clampfit 9.2 (Molecular Devices) where the data were expressed as waveforms. The magnitudes of the responses were measured by calculating the areas under the waveforms that exceeded the mean value of the pre-stimulus baseline by 2 SD. Alignment of optical waveforms and stimulus markers in the illustrations was done manually using Corel Draw X5 (Corel Corp, Canada). Unless indicated otherwise, all data are presented as grand means across preparations ± S.E.M.

RESULTS

Optical recordings of calcium responses from individual SPNs in the intermediate motor column of the thoracic segments were obtained in a total of 74 animals (T2, T4, T6, T8 and T12, n = 3 for each, and T10, n = 65). Recordings were made from ipsilateral SPNs (n = 44 animals) and/or contralaterally SPNs (n = 42 animals). In 9/74 animals, recordings were obtained from SPNs in more than one segment (T2, T6 and T12, n = 3; T4, T8 and T10, n = 3; T2 and T4 (n = 3). In 6 out the 65 animals where T10 SPNs were recorded, we also recorded from the somatic MNs in the medial motor column of the same segment. A total of 470 neurons (422 SPNs and 48 somatic MNs) were analyzed in the present study.

Determination of effective stimulation parameters for VIIIth nerve-evoked responses in SPNs

Stimulation of the VIIIth nerve with 5 s trains at 5Hz readily evokes reproducible Ca^{2+} responses in somatic MNs of the thoracic cord in the neonatal mouse (Kasumacic et al 2010). To determine whether these parameters are also effective in evoking responses in SPNs, we systematically varied stimulation parameters (Figure 1B and C). With 5 s train stimulation, the magnitudes of the evoked responses in the SPNs increased with increasing stimulus frequency (Figure 1B). While 5 s trains at 1Hz were often sufficient to evoke Ca2+ responses in SPNs, the responses were usually small (sometimes falling below the detection level) and required high threshold currents (200 - 320 μA, mean = 273 ± 32 μA, Figure 1B). In contrast, 5 s trains at 5Hz always evoked easily detectable responses and required substantially lower threshold currents (100 – 150 μA, mean = 110 ± 13 μA). Further increase in stimulus frequency to 10 or 20 Hz did not substantially decrease the threshold current. Stimulation at twice the current threshold (2T) for evoking a measurable increase in CGDA fluorescence (as defined in Methods), showed that 5 s trains were more effective than trains of shorter duration

(shown as individual white circles in Figure 1C). Since increasing the train duration to 10s only increased response magnitudes by about 30%, we settled on 5 s as an appropriate train length.

Altogether these experiments indicate that 2T stimulation of the VIIIth nerve with 5 s trains at 5 Hz reliably produces responses in SPNs (as in somatic MNs) and therefore all experiments described below were performed using these specific stimulus parameters.

Pattern and latency of responses in SPNs

As shown in Figure 3, vestibular nerve stimulation evoked Ca2+ responses in ipsilateral and contralateral SPNs in all the thoracic segments investigated (total of 422 SPNs). Response magnitudes tended to increase with more caudal segmental location. To examine this further, in 6 preparations where SPNs were labeled in multiple thoracic segments (see above), we compared the response magnitudes in the SPNs of the most rostral segment (T2 or T4, pooled) to those in the most caudal segment (T10 or T12, pooled). The response magnitudes in the SPNs of T10 and T12 were significantly larger than those in the SPNs of T2 and T4 (Mann-Whitney, $U = 15$, $P = 0.010$).

To estimate the latencies of the vestibular-evoked responses in SPNs, we recorded them at a higher temporal resolution (100 frames/sec rather than 4 frames/sec, n = 10 animals) and measured the time from the onset of the stimulation train to the onset of the responses. As shown in Figure 4, the vestibular-evoked responses had a mean latency of 131 ± 13 ms in ipsilateral SPNs (n = 4 animals for a total of 11 SPNs, black dots in Figure 4A1 and top trace in Figure 4A2) and 132 ± 21 ms in contralateral SPNs (n = 4 animals for a total of 13 SPNs, black dots in Figure 4B1 and top trace in Figure 4B2). The difference in response latencies

between the ipsilateral and contralateral SPNs was not statistically significant (Mann–Whitney, $U = 72$, $P = 0.976$). In addition to their long latencies, the responses in SPNs rose slowly, reaching peak amplitude several seconds after the onset of stimulation. These features suggested that vestibular-evoked responses in thoracic SPNs were mediated predominantly by polysynaptic pathways.

We then compared the latencies of the responses in SPNs and the responses in the somatic MNs of the same segment. Mean response latencies were 67 ± 4.1 ms in ipsilateral somatic MNs (n = 4 for a total of 12 MNs, gray dots in Figure 4A1 and bottom trace in Figure 4A2) and 72 ± 3.8 ms in contralateral somatic MNs (n = 5 for a total of 16 MNs, gray dots in Figure 4B1 and bottom trace in Figure 4B2). These response latencies in ipsilateral and contralateral somatic MNs were not statistically different (Mann-Whitney, $U = 112$, $P = 0.47$), but both were shorter than the response latencies in the SPNs of the same side (Mann-Whitney, $U = 2$, $P < 0.0001$ for ipsilateral SPNs vs MNs and $U = 13$, $P < 0.0001$ for contralateral SPNs vs MNs). The difference in response latency between SPNs and somatic MNs suggested that separate descending pathways mediated the responses in these two classes of thoracic neurons.

Mephenesin applied selectively to the spinal cord abolishes vestibulosympathetic responses

To investigate further the polysynapticity of the descending connections mediating the vestibulosympathetic responses, we examined the effects of mephenesin, a drug that diminishes the efficacy of transmission in polysynaptic pathways (Kaada 1950; Pinco and Lev-Tov 1994; Vinay et al 1995; Shreckengost et al 2010). The aim of the experiments was to determine whether the spinal portion of the pathway is polysynaptic. In four animals, the

brain stem was isolated from the spinal cord by a Vaseline barrier at C1 and vestibular-evoked responses in T10 SPNs were recorded before and after applying mephenesin (1 mM) selectively to the spinal cord. As shown in Figure 5A, mephenesin completely eliminated the responses in both ipsilateral and contralateral SPNs (total of 17 SPNs). As a positive control for the selective action of mephenesin on polysynaptic connections, in three of the preparations we also examined the effect of mephenesin on the vestibular-evoked responses in T10 somatic MNs. Responses in somatic MNs were substantially diminished but not completely eliminated by mephenesin (Figure 5B, total of 32 MNs, see also Kasumacic et al 2010). These results substantiate the idea that vestibulosympathetic responses in thoracic SPNs are mediated predominantly if not exclusively by polysynaptic vestibulospinal pathways, and indicate that the spinal portion of the pathway is itself polysynaptic.

Vestibulosympathetic responses are mixed excitatory/inhibitory

It has been suggested that the descending pathways that mediate the vestibulosympathetic responses in SPNs involve combined inhibitory and excitatory inputs (Kerman et al 2000b). However, this has been deduced from extracellular recordings of sympathetic nerve fiber activity without substantiation at the synaptic level. Calcium imaging of the SPNs more directly reveals synaptic connections. Excitatory synaptic connections are revealed by postsynaptic depolarization and subsequent activation of voltage-sensitive Ca2+ channels. Convergent inhibitory synaptic connections counteract excitatory synaptic potentials and diminish Ca2+ responses, and can be revealed by the increase of Ca2+ response that occurs in the presence of inhibitory neurotransmitter receptor blockers. Thus, to test for vestibular-mediated inhibitory inputs onto SPNs, we examined the effects of the GABA-A receptor antagonists bicuculline and picrotoxin and the glycinergic receptor antagonist strychnine on the responses evoked in SPNs of the T10 segment (n = 18 animals). As shown in Figure 5A

and B, biccuculine (20 μM) and picrotoxin (40 μM) each increased the response magnitudes in ipsilateral SPNs by more than 100% (Mann-Whitney, biccuculine: U = 29, P = 0.03, picrotoxin: U = 16, P = 0.01) whereas strychnine (0.2 μM) had no significant effect (Mann-Whitney, strychnine: U = 11, P = 0.65). Figure 6A and C show similar effects on the responses evoked in contralateral SPNs (Mann-Whitney, biccuculine: U = 29, P = 0.04, picrotoxin: U = 16, P = 0.01, strychnine: U = 8, P = 0.55). These data demonstrate a clear contribution from GABAergic inhibitory synaptic inputs. Recordings at 100 frames/sec (not shown) showed no significant difference in the latencies of the responses before and after blockade of GABAergic inputs (ipsilateral SPNs: Mann-Whitney, biccuculine: U = 18, P = 0.04, picrotoxin: U = 20, p = 0.18, strychnine: U = 20, P = 0.61, contralateral SPNs: biccuculine: U = 18, P = 0.16. picrotoxin: U = 20, P = 0.2, strychnine: U = 20, P = 0.73).

Pathways mediating the vestibulosympathetic responses

It cannot be assumed that network architecture in newborn mammals is the same as in adults. To investigate the axonal pathways that mediate the vestibulosympathetic responses in the neonatal mouse, we first considered whether, in contrast to adult mammals, there might be direct vestibulospinal projections to SPNs by assessing the extent to which direct stimulation of the LVST generated responses in ipsilateral SPNs (Figure 7). We then investigated the effects of various types of lesions in the brain stem and cervical cord on responses in ipsilateral and contralateral SPNs (Figure 8).

To directly stimulate the LVST, we inserted a stimulation electrode into the LVN where the LVST group, source of the LVST, resides. Electrode placement was made based on external landmarks that we had correlated with the location of the LVST group in earlier anatomical and physiological studies of embryonic and neonatal mice (Pasqualetti et al 2007, Kasumacic

et al 2010). Stimulation sites were marked by electrolytic lesions and in a few preparations we confirmed correct electrode placement by retrogradely labeling the LVST group at the end of the experiment. Since the LVST group lies in close proximity to and partly overlaps the VIIIth nerve entry zone, stimulation of the group also risks stimulating vestibular afferents, an obvious confounding factor. Thus, we first asked whether direct stimulation of the LVST group generated the same response pattern as VIIIth nerve stimulation in thoracic segments. We found that stimulation within the LVST group generated responses in somatic MNs of similar magnitude and duration to those generated by VIIIth nerve stimulation, but smaller and shorter responses in SPNs relative to VIIIth nerve stimulation. This suggested straightaway that the pathways mediating vestibular nerve-mediated responses in somatic MNs and SPNs must differ, as has been shown in adult mammals, since LVST stimulation mimicked VIIIth nerve stimulation for somatic MN responses but not for SPN responses. Because the small SPN responses could have been due either to activation of the LVST or of a small number of passing afferents, we next sought to stimulate the LVST group while blocking all excitatory synaptic transmission within the brain stem with kyurenic acid. This would be expected to eliminate any afferent contribution to the responses. We found that kyurenic acid (5 mM) applied selectively to the brain stem completely eliminated the small SPN responses to LVST stimulation, and diminished but did not eliminate the somatic MN responses. However, washout of the kyurenic acid was capricious, and in only 1 of 4 experiments were we able to reverse these effects completely. These experiments suggested that if a direct LVST-to-SPN connection exists, it provides only a minor contribution.

Since direct LVST stimulation provided little support for a direct vestibulospinal component, we performed the following lesions to better characterize the nature of what obviously was predominantly an indirect projection (Figures 2 and 8): 1) ipsi- or contralateral cervical

hemisection at C1, which interrupted transmission along all ipsi- or contralaterally descending pathways (n = 4), 2) midline lesion at T9-T10, which interrupted transmission along segmental, midline-crossing axons or dendrites (n = 4), 3) bilateral MLF lesion at medullary levels, which interrupted transmission via the medial vestibulospinal tracts (iMVST and cMVST) and all other MLF-projecting descending pathways originating from above the level of the lesion (n = 20 animals), and 4) medullary lesions designed to eliminate brainstem circuitry encompassing the CVLM and RVLM as well as descending projections from the RVLM on both sides, but to preserve descending projections from the ipsilateral LVST (as well as from the iMVST and raphe nuclei, n = 4). Figure 7 shows examples of responses in ipsilateral and contralateral SPNs before and after these various lesions.

Ipsilateral SPNs. Vestibular-mediated responses in ipsilateral SPNs decreased by 66 ± 7 % (n = 4) after ipsilateral hemisection at C1 and by 12 ± 13 % (n = 4) after contralateral hemisection at C1 (Figure 7B). The responses were not affected by either bilateral MLF (103 ± 12 %, n = 4) or thoracic midline (105 ± 2 %, n = 4) lesions. These results indicate that vestibular-evoked responses in ipsilateral SPNs are mediated primarily by ipsilaterally descending pathways and to some extent by contralaterally descending pathways lateral to the MLF, with little or no contribution from MLF-projecting descending pathways including the iMVST or from commissural projections at the thoracic level. The medullary lesions designed to assess whether the responsible descending projections derive from the RVLM or from a direct LVST projection, were made in two steps. The first, which removed nearly the entire contralateral medulla, produced an SPN response decrement similar to that seen after C1 contralateral hemisection (n = 4). The second, which removed the lateral part of the ipsilateral medulla (and hence the entire ipsilateral CVLM, most if not all of the ipsilateral RVLM, as well as projections into and out of these regions), led to a complete loss of all SPN responses

but did not eliminate responses in somatic MNs (n = 4). This showed that the ipsilaterally descending projection must include elements within the region that contains the CVLM and RVLM and that neither the ipsilateral raphespinal nor the LVST projection is sufficient to elicit SPN responses.

To summarize, the vestibular-evoked responses in ipsilateral SPNs were mediated by an ipsilateral, and to a lesser extent a contralateral, indirect descending pathway that includes the region containing the CVLM and RVLM.

Contralateral SPNs. Vestibular-mediated responses in *contralateral* SPNs were decreased substantially by all lesions except bilateral MLF lesions. Ipsilateral hemisection at C1, contralateral hemisection at C1, thoracic midline lesion and the first medullary lesion that removed the contralateral medulla decreased the responses in contralateral SPNs by 28 ± 13% (n = 4), 51 ± 11% (n = 4), 26 ± 2% (n = 4), and 65 ± 14 % (n = 4), respectively (Figure 6C). The second medullary lesion that ablated in addition the region containing the ipsilateral CVLM and RVLM led to a complete loss of contralateral SPN responses, as for the ipsilateral SPN responses (Figure 6C).

Altogether these data indicate that, as for ipsilateral SPNs, both ipsilaterally and contralaterally descending pathways contribute to the responses in contralateral SPNs but that in this case the contralateral pathway predominates. Moreover, as for responses in ipsilateral SPNs, the projection involved in mediating responses in contralateral SPNs must involve the region containing the CVLM and RVLM (Figure 8) and do not depend on direct raphespinal or LVST projections. However, in contrast to the responses in ipsilateral SPNs, excitatory

commissural projections at thoracic levels also contribute. This may arise from commissural collaterals from descending axons, excitatory commissural interneurons or both.

DISCUSSION

Using calcium imaging, we have shown that vestibulosympathetic synaptic connections are present in the mouse, and are already functional at birth. We have further shown that the projections are organized as in the adult mammal, in the sense that they involve circuitry within the brain stem critically dependent on neurons present in the region containing the CVLM and RVLM, with no obvious contribution from direct vestibulospinal pathways (although see below). A novel finding not previously documented in adult mammals is the polysynaptic nature of the spinal component of the pathway, which we have demonstrated through selective pharmacological treatment of the spinal cord with mephenesin. This accords with the longer latencies of responses in SPNs as compared to thoracic somatic MNs, which in the neonatal mouse evidently receive both monosynaptic and polysynaptic vestibulospinal inputs. Lastly, we show that the vestibulosympathetic responses are mixed excitatory/inhibitory, as previously deduced (but not directly demonstrated) in the adult mammal.

Technical considerations related to latency measurements

Several technical issues regarding the use of Ca2+ imaging to characterize synaptic connectivity have been addressed in our previous studies of brain stem-spinal cord projections (Szokol at al 2008; Szokol and Perreault 2009; Kasumacic et al 2010, Szokol et al 2011) and will not be discussed here. However, there is one point that warrants additional discussion. By using relatively high frame rate imaging (100 frames/sec) we have been able to estimate the latencies of the evoked responses with an error of +/- 10 msec. Although this does not permit us to definitively gauge the number of synapses involved in polysynaptic responses, as might be possible with electrophysiological approaches, it does allow us to distinguish clearly the response latencies of SPNs (about 130 msec) from those of somatic MNs (about 70 msec).

We can therefore conclude that the former must involve more synaptic relays or longer total conduction times or both. Because a residual response is seen in somatic MNs but not SPNs after selective treatment of the spinal cord with mephenesin, at least part of the difference evidently lies in a greater degree of spinal polysynapticity for vestibulosympathetic connections. But undoubtedly much of the longer response latency is explained by the more complex brainstem circuitry involved in the vestibulosympathetic responses.

Although we saw no change in response latencies following selective GABA-A receptor blockade in the spinal cord, the temporal uncertainty of the response latency measurements does not allow us to preclude the possibility that inhibitory events (which can be invisible to Ca2+ recording if occurring in isolation) might precede excitatory events, as seen in a few instances in the adult cat (Kerman et al 2000). Thus, our latency measurements may be overestimates if the actual responses involve inhibitory inputs that fall within about 10 msec before excitatory inputs.

Comparing vestibulosympathetic responses in the newborn mouse and adult mammals

Response latencies

We have recorded responses in ipsilateral and contralateral sympathetic MNs during electrical stimulation of the VIIIth nerve, with response latencies averaging about 130 and 140 ms, respectively. These latencies are similar to those that have been recorded from the splanchnic nerve of the adult cat during VIIIth nerve stimulation (Yates et al 1993), but are substantially longer than those recorded from the splanchnic nerve of the adult rat during VIIIth nerve stimulation (about 45 ms, Pan et al 1991). In general, longer latencies are to be expected in neonates due to lack of myelination and immaturity of synapses. The large discrepancy between latencies recorded in adult cats and adult rats could in principle be explained by

different conduction distances (about 4-fold longer in cats than rats) if the descending axons involved are slowly conducting. Indeed, Deuschars et al (1995) have estimated that conduction velocities in the RVLM-SPN pathway in the rat are within the range for C fibers (about 0.5 m/sec). This feature deserves a closer inspection in both cats and rodents as better information is obtained about the descending axons that mediate the reflex.

Pathways mediating vestibulosympathetic responses

Based on work in the cat, Yates (1996) has proposed a model for vestibulosympathetic circuitry in which head pitch-sensitive receptors activate neurons in the medial and inferior vestibular nuclei, which then via a relay in the caudal ventrolateral medulla activate neurons in the autonomic control center in the RVLM, which have been shown to project to the spinal cord and synapse onto SPNs (Figure 9). Much of the foundation for this model is based on the attempted elimination of various parts of the brain stem through electrolytic or neurochemical lesions (Pan et al 1991; Yates and Miller 1994; Yates et al 1995). Although very indicative, the use of lesions has several caveats. First, since it is hard to control the extent of lesions in vivo, it can be difficult to conclude that the observed effects are due to damage to the target region or nucleus and not other nearby structures. Second, lesioned regions that do not result in changes in the vestibulosympathetic responses cannot, without further investigation, be excluded as potential components of the reflex if the reflex involves parallel pathways. The lateral vestibular nucleus (LVN), for example, has been excluded as a potential component of the vestibulo-sympathetic reflex based on lesion studies, a conclusion supported by the argument that the MVN and rostral IVN are more suitable candidates since they have a somewhat larger proportion of pitch-sensitive cells than the LVN (Yates 1996). However, Lee et al (2007), using transynaptic labeling with pseudorabies virus to trace the source of

supraspinal inputs to SPNs, found labeling in the LVN that looked no less direct (based on labeling latency) than the labeling they found in the RVLM (see figure 2 in their paper).

Because brainstem-spinal cord circuitry may not be mature in newborn mammals, we carried out a series of lesion experiments to assess the pathways involved in the vestibulosympathetic responses in the neonatal mouse. In particular, we wanted to test whether direct vestibulospinal connections to SPNs exist. Our findings provide no support for the involvement of a direct vestibulospinal projection. Direct stimulation of the LVN/LVST produces only very short and small responses in SPNs, and lesions that spare the LVST but eliminate the CVLM and RVLM abolish the responses. MVST axons do not reach the thoracic cord and do not evoke responses in thoracic somatic MNs in the neonatal mouse (Kasumacic et al 2010), but could in principle engage propriospinal interneurons to activate SPNs. However, lesions of the iMVST and cMVST do not affect the responses. We have not stimulated directly the raphe nuclei but according to Iiagawa et al. (2007) only few raphespinal neurons, if any, have functional synaptic connections with SPNs in the neonatal rat.

Thus, as in adult mammals, the vestibulosympathetic control of SPNs in the neonatal mouse involves predominantly, if not exclusively, indirect projections that are channeled to the spinal cord through the region that contains the CVLM and RVLM.

Vestibulosympathetic responses are clearly bilateral in adult cat, adult rat and neonatal mouse. This is likely due in part to commissural collaterals from RVLM axons to the intermediolateral region of the thoracic spinal cord, as shown in the adult rat (Moon et al 2002 and see below). Our lesion experiments indicate in addition a bilateral influence within the

brain stem, since ipsilateral hemisection at C1 did not abolish responses in contralateral SPNs. Clearly, there must be a commissural connection at some level of the brainstem vestibulosympathetic circuit that channels activity from vestibular afferents to the contralateral RVLM. This could occur either through vestibulo-vestibular connections (which, however, are thought to be primarily inhibitory), connections between the two sides of the lateral reticular formation, connections between the two RVLMs, or commissural connections across these levels. A more comprehensive set of lesion experiments could be envisioned to test these possibilities once sufficient information about the trajectories of the relevant axons is available.

We show further that mephenesin, when applied to the spinal cord, completely abolishes the vestibular-evoked responses in SPNs, but not in somatic MNs. This indicates that the pathways mediating vestibulosympathetic responses and vestibulosomatic responses must differ, with the latter relying strongly on direct vestibulospinal projections. This is consistent with the findings of Miyazawa and Ishikawa (1985), who showed that a lesion of laterally descending fibers at the T3 level in the adult cat abolished vestibulosomatic responses without affecting vestibulosympathetic responses.

It has been reported from experiments in the adult cat that vestibulosympathetic responses are composed of inhibitory as well as excitatory components (Kerman et al 2000). We find that application of biccuculine and picrotoxin, but not strychnine, selectively to the spinal cord leads to an increase in the magnitude of vestibulosympathetic responses. This indicates the presence of an inhibitory component in the vestibulosympathetic pathway mediated by GABA (through $GABA_A$ receptors) but not glycine. Whether this inhibitory component is a direct

GABAergic projection from the brain stem from RVLM or mediated by intercalated GABAergic spinal interneurons remains to be determined.

Segmental distribution

Several studies have shown that vestibulosympathetic effects are larger in hindlimb than forelimb vasculature, indicating a regional pattern within the vestibulosympathetic reflex (Kerman et al 2000; Wilson et al 2006, Sugiyama et al 2011). The way this is achieved in the spinal cord is not well understood, but could involve the well characterized segmental mapping of sympathetic outflow in which more caudal thoracic segments contain greater proportions of SPNs projecting caudally within the sympathetic trunk (reviewed in Forehand et al 1994). This topographic efferent arrangement can be easily accessed by descending axons through the distinctive intrasegmental segregation within each segmental cohort of SPNs projecting rostrally versus caudally in the sympathetic trunk (Forehand et al 1994, 1998). Here, we have shown that vestibulosympathetic responses as assessed with Ca2+ imaging are larger in caudal than in rostral thoracic segments; indeed there appears to be a trend of increasing magnitude that suggests a rostrocaudal gradient of inputs to SPNs. Such a gradient could clearly contribute to a larger response in the hindlimb. It will be important in this respect to investigate how these different response magnitudes are generated, including assessing the density of RVLM-derived axon collaterals and synaptic terminals and characterizing electrophysiologically the synaptic drive in the different thoracic segments.

Spinal circuitry involved in mediating vestibulosympathetic responses

Our mephenesin experiments indicate that transmission of vestibular information to SPNs involves multiple synapses within the spinal cord. The potential role of spinal interneurons in vestibulosympathetic circuitry has recently been addressed by Miller et al (2009), who found

interneurons in the thoracic region that respond to vestibular nerve stimulation and to head tilts. Whether these interneurons are necessary or sufficient components of the vestibulosympathetic reflex circuit has not been demonstrated. It is not clear from our experiments, for example, whether the mixed excitatory/inhibitory nature of the vestibulosympathetic responses arises through convergence of excitatory and inhibitory descending projections or through the engagement of excitatory and inhibitory spinal interneurons by purely excitatory descending projections. Further investigation of RVLM inputs to spinal interneurons is therefore warranted.

Our finding that midline lesion of the thoracic spinal cord effectively reduces responses in contralateral SPNs implies in addition that a proportion of the ipsilaterally descending RVLM axons either extend collaterals across the midline at the thoracic level or innervate spinal commissural interneurons (CINs) which relay the effects to the opposite side. Anatomical evidence exists for commissural axon collaterals (Moon et al 2002), but the connectivity of RVLM axons to spinal interneurons including CINs has yet to be investigated.

Future perspectives

Although it is clear that there are functional synaptic connections between the vestibular system and SPNs in the mouse already at birth, it is not clear whether the vestibulosympathetic reflex has achieved a mature organization at birth. Future studies should be aimed at investigating the physiological function of the reflex in the newborn mouse *in vivo*, as has been done in the adult cat (Doba and Reis, 1974). Moreover, the specific connectivity of the brainstem and spinal cord circuitry involved is not yet fully worked out, a challenge that can be addressed advantageously in the neonatal mouse through combined anatomical, transgenic and optical approaches that target specific neuron populations.

References (47 references)

Abe C, Tanaka K, Awazu C, Morita H. (2008) Impairment of vestibular-mediated cardiovascular response and motor coordination in rats born and reared under hypergravity. Am J Physiol Regul Integr Comp Physiol. 2008 Jul;295(1):R173-80

Balaban CD and Porter JD (1998) Neuroanatomic substrates for vestibulo-autonomic interactions. J Vestib Res. 1998 Jan-Feb;8(1):7-16.

Bent LR, Bolton PS, Macefield VG (2006) Modulation of muscle sympathetic bursts by sinusoidal galvanic vestibular stimulation in human subjects. Exp Brain Res 174:701-711.

Buckey JC, Jr., Lane LD, Levine BD, Watenpaugh DE, Wright SJ, Moore WE, Gaffney FA, Blomqvist CG (1996) Orthostatic intolerance after spaceflight. J Appl Physiol 81:7-18.

Burke PG, Neale J, Korim WS, McMullan S, Goodchild AK (2011) Patterning of somatosympathetic reflexes reveals nonuniform organization of presympathetic drive from C1 and non-C1 RVLM neurons. Burke PG, Neale J, Korim WS, McMullan S, Goodchild AK.

Carter JR and Ray CA (2008) Sympathetic responses to vestibular activation in humans. Am J Physiol Regul Integr Comp Physiol. 2008 Mar;294(3):R681-8

Díaz C, Glover JC, Puelles L, Bjaalie JG (2003). The relationship between hodological and cytoarchitectonic organization in the vestibular complex of the 11-day chicken embryo. J Comp Neurol. 2003 Feb 24;457(1):87-105

Doba N, Reis DJ (1974) Role of the cerebellum and the vestibular apparatus in regulation of orthostatic reflexes in the cat. Circ Res 40:9-18.

Deuchars SA, Morrison SF, Gilbey MP (1995) Medullary-evoked EPSPs in neonatal rat sympathetic preganglionic neurones in vitro. J Physiol. 1995 Sep 1;487 (Pt 2):453-63.

Deuchars SA, Spyer KM, Gilbey MP. (1997) Stimulation within the rostral ventrolateral medulla can evoke monosynaptic GABAergic IPSPs in sympathetic preganglionic neurons in vitro. J Neurophysiol. 1997 Jan;77(1):229-35.

Etard O, Reber A, Quarck G, Normand H, Mulder P, Denise P (2004). Vestibular control on blood pressure during parabolic flights in awake rats. Neuroreport. 2004 Oct 25;15(15):2357-60.

Forehand CJ, Ezerman EB, Rubin E, Glover JC. (1994) Segmental patterning of rat and chicken sympathetic preganglionic neurons: correlation between soma position and axon projection pathway. J Neurosci. 14:231-241.

Forehand CJ, Ezerman EB, Goldblatt JP, Skidmore DL, Glover JC. Segment-specific pattern of sympathetic preganglionic projections in the chicken embryo spinal cord is altered by retinoids. Proc Natl Acad Sci U S A. 95:10878-10883.

Friedrich VL Jr, Martinelli GP, Prell GD, Holstein GR. (2007) Distribution and cellular localization of imidazoleacetic acid-ribotide, an endogenous ligand at imidazol(in)e and adrenergic receptors, in rat brain. J Chem Neuroanat. 2007 Jan;33(1):53-64.

Glover JC (1995) Retrograde and anterograde axonal tracing with fluorescent dextran-amines in the embryonic nervous system. Neuroscience Protocols: Elsevier Science.

Gotoh TM, Fujiki N, Matsuda T, Gao S, Morita H. (2004) Roles of baroreflex and vestibulosympathetic reflex in controlling arterial blood pressure during gravitational stress in conscious rats. Am J Physiol Regul Integr Comp Physiol. 2004 Jan;286(1):R25-30

Holstein GR, Martinelli GP, Friedrich VL (2011) Anatomical observations of the caudal vestibulo-sympathetic pathway. J Vestib Res. 2011;21(1):49-62.

Kaada BR (1950) Site of action of myanesin in the central nervous system. J Neurophysiol 13:89-104.

Kasumacic NK, Glover JC, Perreault M-C (2009) Vestibular influence on somatic and autonomic thoracic motoneurons in the neonatal mouse.

Kasumacic NK, Glover JC, Perreault M-C (2010) Segmental patterns of vestibular-mediated synaptic inputs to axial and limb motoneurons in the neonatal mouse assessed by optical recording. J Physiol. 2010 Dec 15;588(Pt 24):4905-25.

Kerman IA, Yates BJ, McAllen RM (2000b) Anatomic patterning in the expression of vestibulosympathetic reflexes. Am J Physiol Regul Integr Comp Physiol 279:R109-R117.

Kerman IA, McAllen RM, Yates BJ (2000a) Patterning of sympathetic nerve activity in response to vestibular stimulation. Brain Res Bull. 2000 Sep 1;53(1):11-6.

Lee TK, Lois JH, Troupe JH, Wilson TD, Yates BJ (2007) Transneuronal tracing of neural pathways that regulate hindlimb muscle blood flow. Am J Physiol Regul Integr Comp Physiol. 2007 Apr;292(4):R1532-41.

Martinelli GP, Friedrich VL Jr, Prell GD, Holstein GR. (2007) Vestibular neurons in the rat contain imidazoleacetic acid-ribotide, a putative neurotransmitter involved in blood pressure regulation. J Comp Neurol. 2007 Apr 1;501(4):568-81.

Miller DM, Reighard DA, Mehta AS, Mehta AS, Kalash R, Yates BJ. (2009) Responses of thoracic spinal interneurons to vestibular stimulation. Exp Brain Res. 2009 May;195(1):89-100. Epub 2009 Mar 13.

Miyazawa T and Ishikawa T. (1983) Cerebellar inhibitory action on vestibulo-sympathetic responses. J Auton Nerv Syst. 1983 Feb;7(2):185-9.

Miyazawa T and Ishikawa T. (1985) Separation of the medullo - spinal descending pathway for somatic and autonomic outflow in the cat. Brain Research, 334 (1985) 297-302

Moon EA, Goodchild AK, Pilowsky PM. (2002) Lateralisation of projections from the rostral ventrolateral medulla to sympathetic preganglionic neurons in the rat. Brain Res. 2002 Mar 8;929(2):181-90.

Pan PS, Zhang YS, Chen YZ (1991) Role of the nucleus vestibularis medialis in vestibulo-sympathetic response in rats. Sheng Li Xue Bao 43:184-188.

Pasqualetti M, Diaz C, Renaud JS, Rijli FM, Glover JC (2007) Fate-mapping the mammalian hindbrain: segmental origins of vestibular projection neurons assessed using rhombomere-specific Hoxa2 enhancer elements in the mouse embryo. J Neurosci 27:9670-9681.

Paxinos G, Halliday G, Watson C, Koutcherov Y & Wang HQ (2007). Atlas of the Developing Mouse Brain at E17.5, P0, and P6. Academic Press, Elsevier

Pinco M, Lev-Tov A (1994) Synaptic transmission between ventrolateral funiculus axons and lumbar motoneurons in the isolated spinal cord of the neonatal rat. J Neurophysiol 72:2406-2419.

Porter JD, Balaban CD. (1997) Connections between the vestibular nuclei and brain stem regions that mediate autonomic function in the rat. J Vestib Res. 1997 Jan-Feb;7(1):63-76.

Ray CA, Monahan KD (2002) Aging attenuates the vestibulosympathetic reflex in humans. Circulation 105:956-961.

Ray CA, Carter JR (2003) Vestibular activation of sympathetic nerve activity. Acta Physiol Scand 177:313-319.

Shreckengost J, Calvo J, Quevedo J, Hochman S (2010) Bicuculline-sensitive primary afferent depolarization remains after greatly restricting synaptic transmission in the mammalian spinal cord. J Neurosci 30:5283-5288.

Sugiyama Y, Suzuki T, Yates BJ. (2011) Role of the rostral ventrolateral medulla (RVLM) in the patterning of vestibular system influences on sympathetic nervous system outflow to the upper and lower body. Exp Brain Res. 2011 May;210(3-4):515-27.

Szokol K, Glover JC, Perreault MC. (2008) Differential origin of reticulospinal drive to motoneurons innervating trunk and hindlimb muscles in the mouse revealed by optical recording. J Physiol. 2008 Nov 1;586(Pt 21):5259-76.

Szokol K, Glover JC, Perreault MC. (2011) Organization of functional synaptic connections between medullary reticulospinal neurons and lumbar descending commissural interneurons in the neonatal mouse. J Neurosci. 2011 Mar 23;31(12):4731-42.

Szokol K and Perreault MC (2009) Imaging synaptically mediated responses produced by brainstem inputs onto identified spinal neurons in the neonatal mouse. J Neurosci Methods 180:1-8.

Tanaka K, Gotoh TM, Awazu C, Morita H. (2006) Roles of the vestibular system in controlling arterial pressure in conscious rats during a short period of microgravity. Neurosci Lett. 2006 Apr 10-17;397(1-2):40-3.

Vinay L, Cazalets JR, Clarac F (1995) Evidence for the existence of a functional polysynaptic pathway from trigeminal afferents to lumbar motoneurons in the neonatal rat. Eur J Neurosci 7:143-151.

Voustianiouk A, Kaufmann H, Diedrich A, Raphan T, Biaggioni I, Macdougall H, Ogorodnikov D, Cohen B (2006) Electrical activation of the human vestibulo-sympathetic reflex. Exp Brain Res 171:251-261.

Wilson TD, Cotter LA, Draper JA, Misra SP, Rice CD, Cass SP, Yates BJ (2006) Vestibular inputs elicit patterned changes in limb blood flow in conscious cats. J Physiol. 2006 Sep 1;575(Pt 2):671-84

Yates BJ (1992) Vestibular influences on the sympathetic nervous system. Brain Res Brain Res Rev 17:51-59.

Yates BJ and Bronstein AM (2005) The effects of vestibular system lesions on autonomic regulation: observations, mechanisms, and clinical implications. J Vestib Res. 2005;15(3):119-29.

Yates BJ, Jakus J, Miller AD (1993) Vestibular effects on respiratory outflow in the decerebrate cat. Brain Res 629:209-217.

Yates BJ, Miller AD (1994) Properties of sympathetic reflexes elicited by natural vestibular stimulation: implications for cardiovascular control. J Neurophysiol 71:2087-2092.

Yates BJ (1996) Vestibular influences on the autonomic nervous system. Ann N Y Acad Sci 781:458-473.

Yates BJ, Sinaia MS and Miller AD (1995) Descending pathways necessary for vestibular influence on sympathetic and inspratory outflow. Am J Physiol Regulatory Integrative Comp Physiol 268:1318-1385, 1995

Zhang F, Aravanis AM, Adamantidis A, de Lecea L, Deisseroth K. (2007) Circuit-breakers: optical technologies for probing neural signals and systems. Nat Rev Neurosci. 2007 Aug;8(8):577-81.

FIGURE LEGENDS

Figure 1. Brainstem-spinal cord preparation and effective stimulation parameters

A) Schematic representation of the brainstem-spinal cord preparation indicating the segments and neuron groups studied. Inset shows an image of the glass suction electrode placed on the proximal end of the cut VIIIth nerve for electrical stimulation. Shown to the right are schematic illustrations of the obliquely cut spinal cord with the transverse surface facing up towards the objective. Inset shows an image of CGDA-labeled SPNs, pseudocolored as described in Methods, in a transverse section of the T10 segment. Scale bars: 100 μm, M = medial, D = dorsal. **B** and **C)** Effective stimulation parameters for evoking Ca2+ responses in SPNs in T10. The graph in B displays the magnitudes of the responses produced by stimulating the VIIIth nerve at threshold current (T) with a 5 s train as a function of frequency. Each response is an average of 4 experiments (4-8 SPNs per experiment). The graph in C displays the magnitude-frequency curves when stimulating at 2T with a 5 s train and the response magnitudes as a function of the train duration when stimulating at 2T and 5 Hz (individual open circles). Each response is an average (total of 4 experiments 4-9 SPNs per experiment) and is expressed as a percentage of the response at 5 Hz. All values are means ± standard deviations.

Figure 2. Summary of lesions in the medulla and upper spinal cord used to assess vestibulosynpathetic pathways

A. Lesions designed to interrupt 1) all axons descending into one or the other side of the spinal cord, 2) all axons descending on either side of the MLF from above the level of the vestibular nuclei, 3) commissural axons (and dendrites) at thoracic levels, and 4) removal of the region containing the CVLM and RVLM, extended in figure B.

B. Lesions designed to eliminate the region containing the CVLM and RVLM (and any descending axons originating from the RVLM) but spare axons descending in the LVST. 1)

Examples of the two successive lesions (contralateral first, ipsilateral second) as seen in wholemount. 2) Transverse sections (50 μm) stained with methylene blue (Sigma) to show the extent of the remaining tissue through which the LVST projects.

Figure 3. Responses evoked in SPNs in different spinal segments

Responses recorded at 4 frames/sec of ipsilateral (right) and contralateral (left) SPNs in segments T2, T4, T6, T8, T10 and T12 during train stimulation of the vestibular nerve. Each waveform shows the average of recordings from 4 SPNs.

Figure 4. Latencies and waveforms of vestibular-mediated responses in thoracic SPNs and somatic MNs

Cumulative distribution of latencies measured in ipsilateral (A1) and contralateral (B1) SPNs (black circles) and somatic MNs (grey circles) recorded at 100 frames/sec. Both ipsilateral and contralateral somatic MNs responded with significantly shorter latencies then their sympathetic counterparts. There was no significant difference in the reponses of ipsilateral vs contralateral somatic MNs or ipsilateral vs contralateral SPNs (see main text for statistics). A2 Waveforms of Ca2+ responses recorded in ipsilateral SPNs (top, black waveform) and somatic MNs (bottom, grey waveform) in T10 during nerve VIII stimulation. Each waveform is the average of responses from 6 neurons. B2) Waveforms of Ca2+ responses recorded in contralateral SPNs (top, black waveform) and somatic MNs (bottom, grey waveform) in T10 during nerve VIII nerve stimulation.

Figure 5. Mephenesin applied to the spinal cord abolishes vestibulosympathetic responses

A) Responses evoked in T10 SPNs by vestibular nerve stimulation (2T, 5s, 5Hz) before (control) and after application of 1 mM mephenesin to the thoracolumbar spinal cord. Responses were recorded at 4 frames/sec and each waveform is the average of responses from 5 SPNs.

B) Response magnitudes during mephenesin application normalized to control (n = 4 preparations). Each circle represents the average response from a single preparation.

Figure 6. Effect of biccuculine, picrotoxin and strychnine applied to the spinal cord on vestibulosympathetic responses

A) Waveforms showing responses recorded at 4 frames/sec in ipsilateral (top) and contralateral (bottom) SPNs in T10 before and during application of 20μM biccuculine, 40μM picrotoxin or 0.2μM strychnine to the thoracolumbar spinal cord. Each waveform is an average of responses in 5 SPNs.

B) and **C)** Response magnitudes in ipsilateral (B) and contralateral (C) T10 SPNs during application of biccuculine, picrotoxin or strychnine normalized to control responses. Biccuculine and picrotoxin lead to an increase in response magnitudes on both sides, whereas strychnine has no effect (see main text for statistics).

Figure 7. Effect of spinal cord, MLF and medullary lesions on vestibulosympathetic responses

A) Effects of ipsilateral and contralateral hemisections, midline spinal lesions, bilateral MLF lesion and medullary lesions on responses in ipsilateral and contralateral SPNs in T10 segment. Responses were recorded at 4 frames/sec. Each waveform is an average of responses in 5 SPNs.

B and **C)** Response magnitudes in ipsilateral (B) and contralateral (C) T10 SPNs following spinal cord, MLF or medullary lesions, normalized to control responses. The spinal cord

lesions had differential effects on the ipsilateral and contralateral SPNs, the MLF lesion had no effect on responses on either side, the contralateral medullary lesion alone had an effect similar to that of the contralateral hemisection, and the combined contralateral plus ipsilateral medullary lesions abolished responses (for details see main text).

Figure 8. Direct stimulation of the LVST group within the LVN evokes small responses in SPNs that are blocked by kynurenic acid applied selectively to the brainstem

A1-A2) Frontal sections showing the distribution of vestibulospinal neurons and axons labeled retrogradely with RDA from C1, and the location of an electrolytic lesion (white arrow) used to determine the location of the stimulation site in one of the preparations in which the LVST was stimulated directly. A3) Schematic showing the distribution of all stimulation sites (black squares) relative to retrogradely labeled LVST group neurons. Scale bars: 50 μm.

B) Responses evoked in ipsilateral SPNs (black) by stimulation (5s, 5hz) within the LVST group. The responses were smaller in magnitude and shorter in duration relative to responses elicited by stimulation of the VIIIth nerve. These responses were blocked by 5 mM kynurenic acid. Responses in the ipsilateral somatic MNs (gray) were similar relative to the responses elicited by stimulation of the VIIIth nerve. These responses were not blocked by 5 mM kyurenic acid.

C) Latencies of responses in SPNs (black circles) and somatic MNs (grey circles) elicited by stimulation within the LVST group.

Figure 9. Summary diagram of brainstem vestibulosympathetic circuitry supported by the present experiments

Summary of the brainstem circuit believed to underly the vestibulosympathetic reflex (A), its relationship to the LVST group and tract (B) and the impact of the medullary lesions

described under Figure 2B on the various projections involved (C). Flow of impulse traffic is shown by arrows, with dotted lines indicating connections that are not well characterized in the literature (CVLM to RVLM) or only postulated from our results (RVLM to RVLM). The precise descending trajectory of spinally projecting RVLM neurons has not been described; it is shown here in the MLF but may lie further lateral. Vestibulosympathetic impulses derive from neurons in the MVN and IVN, but only the MVN is shown here for simplicity. In B, the LVST group and the proximal portion of its derivative tract lie dorsal to the medullary reticular formation. The vestibular afferents have been removed from B and C for clarity. In C, although not shown here, the ipsilateral lesion actually extends down to the border between cervical segments C2 and C3.

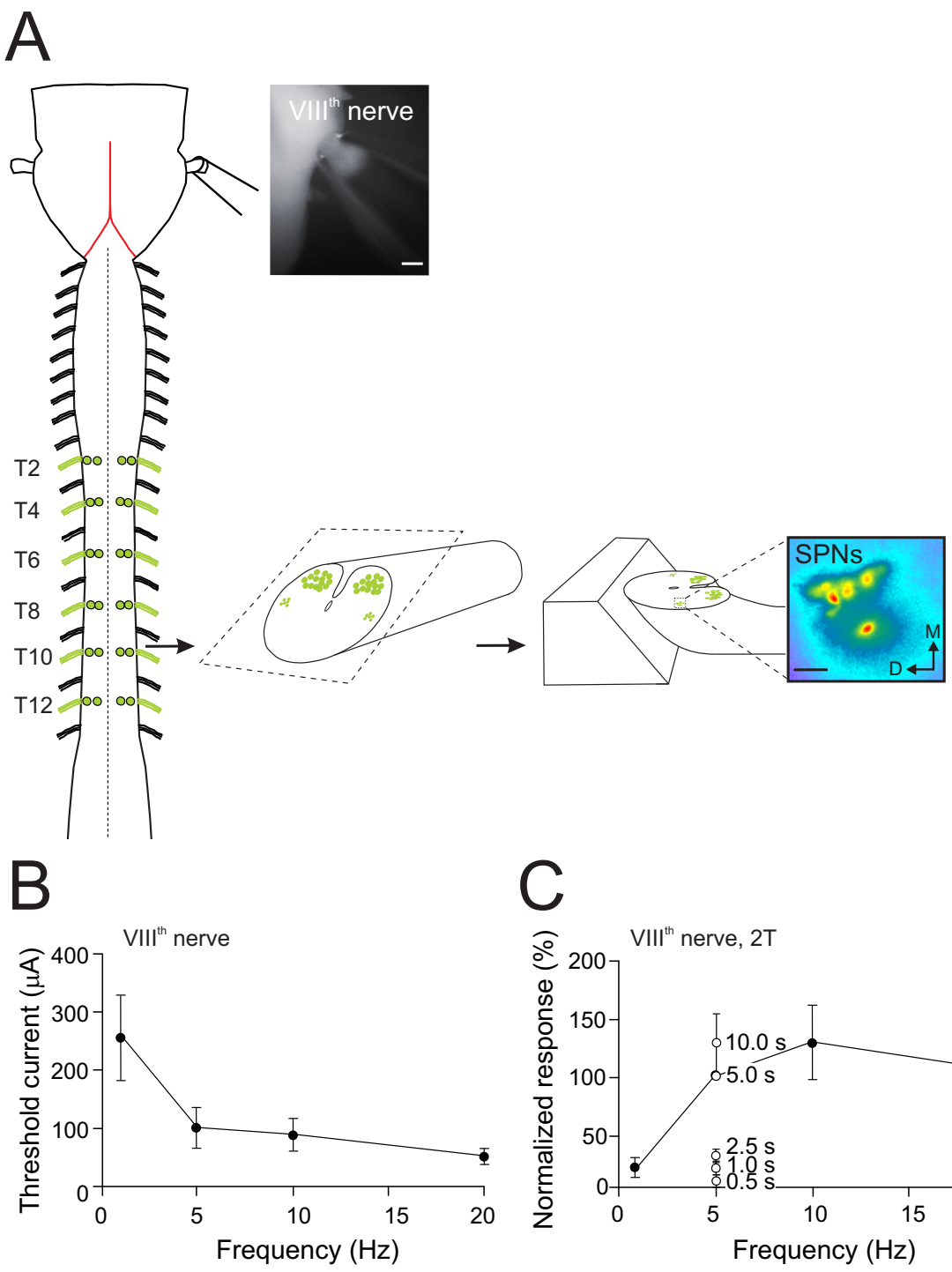
A
VIII^th nerve
T2
T4
T6
T8
T10
T12
SPNs
M
D
B
VIII^th nerve
Threshold current (μA)
400
300
200
100
0
0
5
10
15
20
Frequency (Hz)
C
VIII^th nerve, 2T
Normalized response (%)
200
150
100
50
0
10.0 s
5.0 s
2.5 s
1.0 s
0.5 s
0
5
10
15
20
Frequency (Hz)

Figure 1

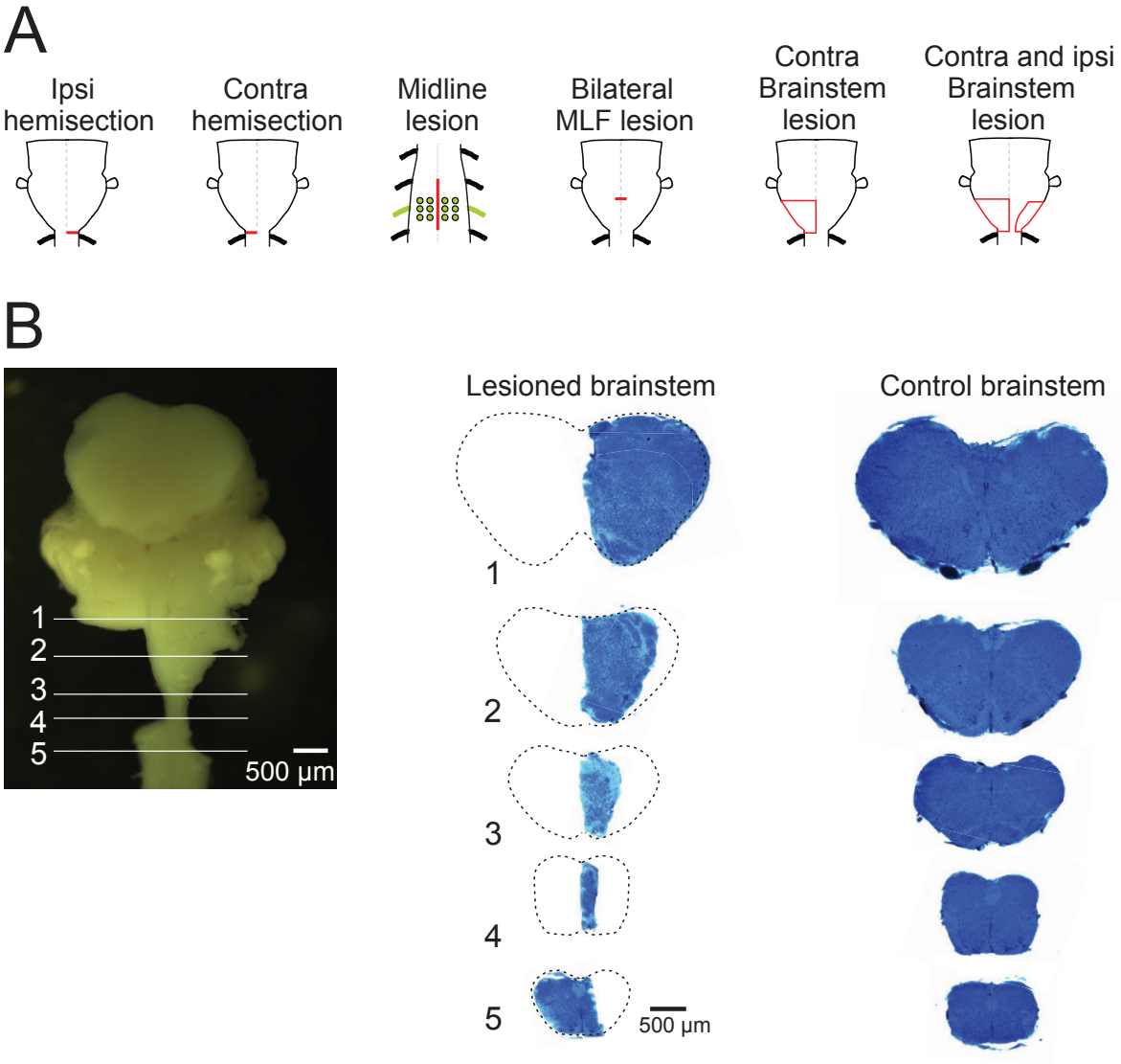
A
Ipsi hemisection
Contra hemisection
Midline lesion
Bilateral MLF lesion
Contra Brainstem lesion
Contra and ipsi Brainstem lesion
B
1
2
3
4
5
500 µm
Lesioned brainstem
Control brainstem
1
2
3
4
5
500 µm

Figure 2

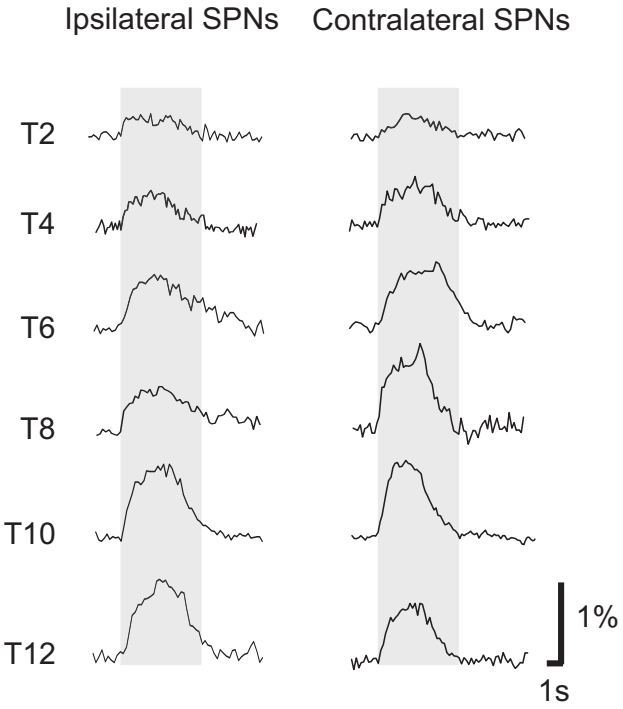

Figure 3

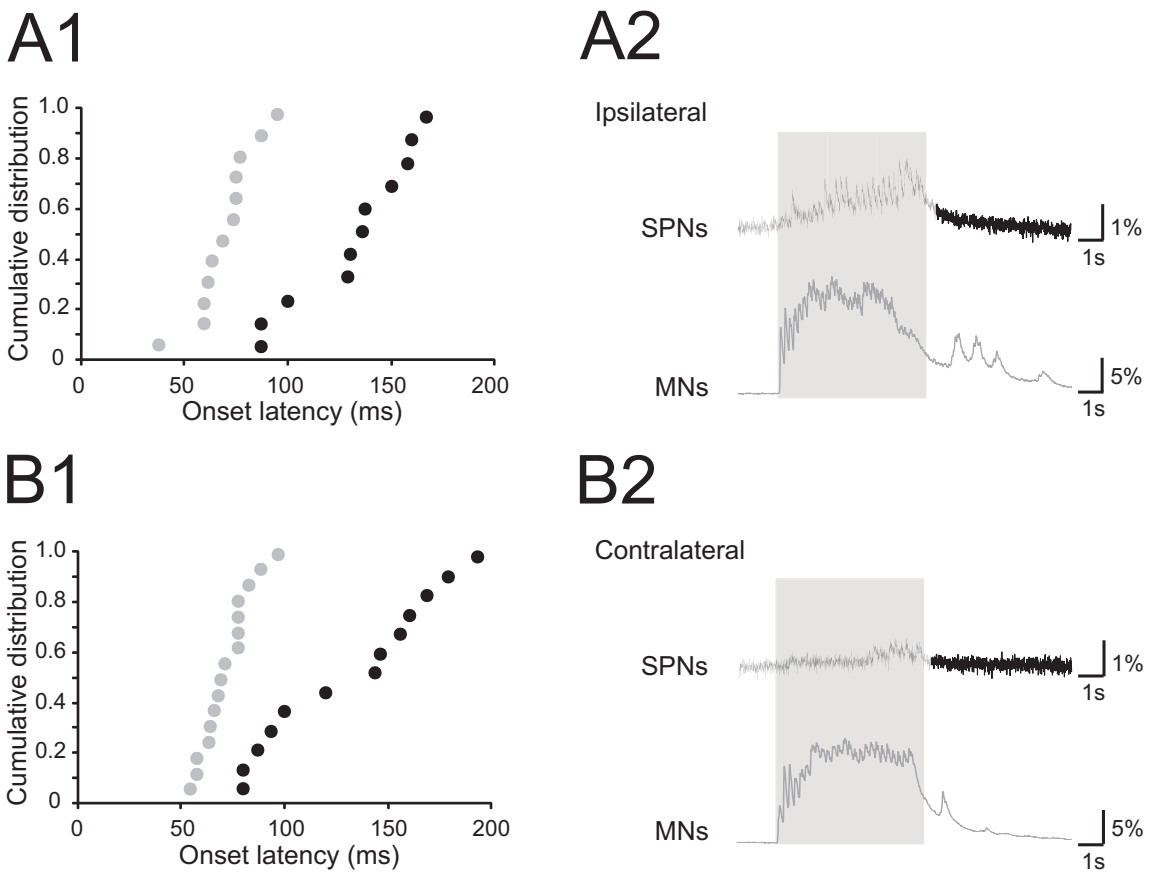
A1
Cumulative distribution
1.0
0.8
0.6
0.4
0.2
0
0
50
100
150
200
Onset latency (ms)
A2
Ipsilateral
SPNs
1%
1s
MNs
5%
1s
B1
Cumulative distribution
1.0
0.8
0.6
0.4
0.2
0
0
50
100
150
200
Onset latency (ms)
B2
Contralateral
SPNs
1%
1s
MNs
5%
1s

Figure 4

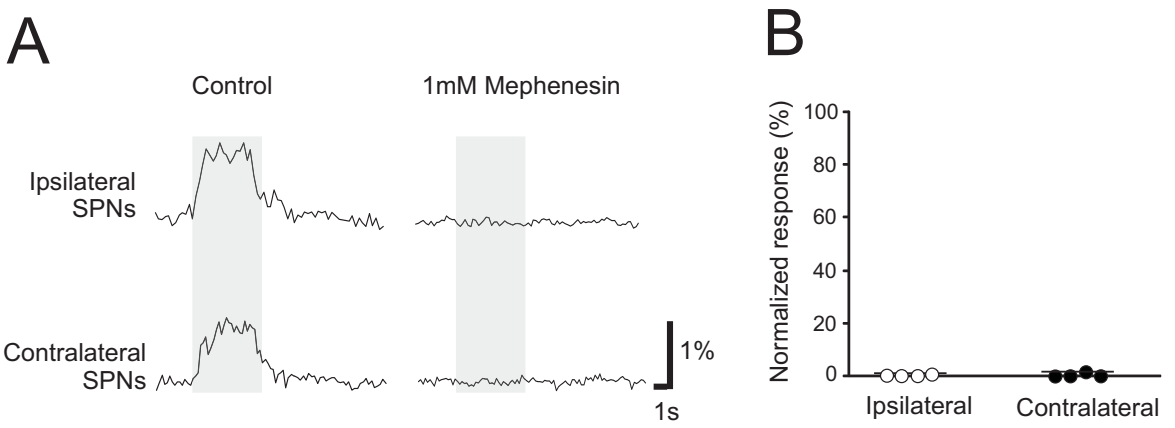
A
Control
1mM Mephenesin
Ipsilateral SPNs
Contralateral SPNs
1%
1s
B
Normalized response (%)
100
80
60
40
20
0
Ipsilateral
Contralateral

Figure 5

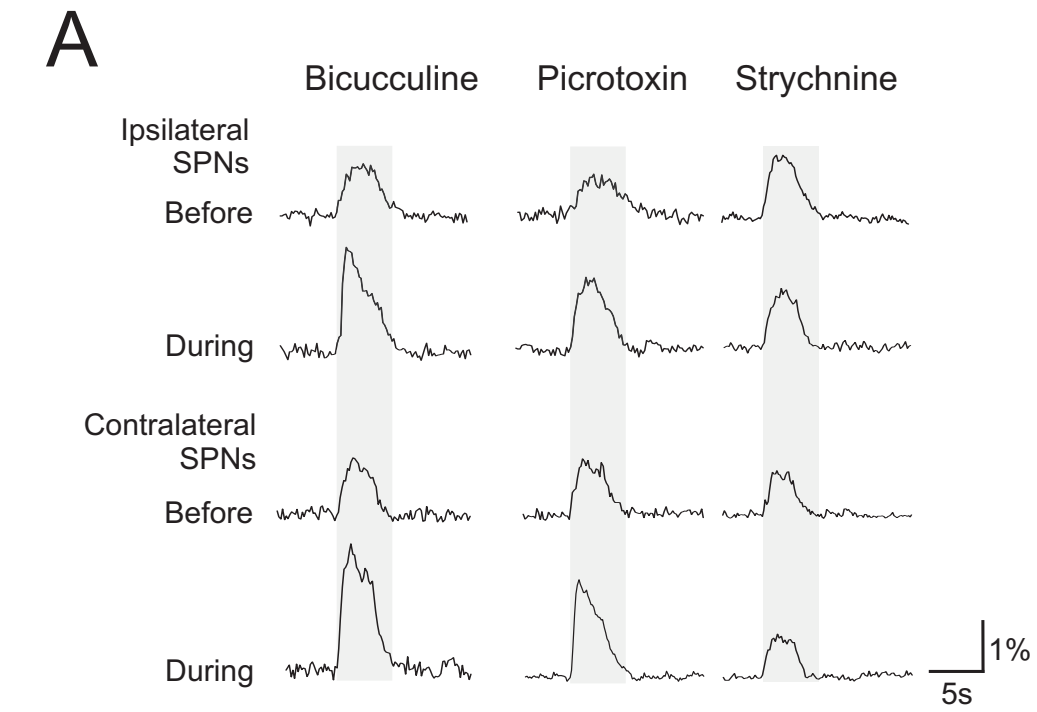
A
Bicucculine
Picrotoxin
Strychnine
Ipsilateral SPNs
Before
During
Contralateral SPNs
Before
During
1%
5s

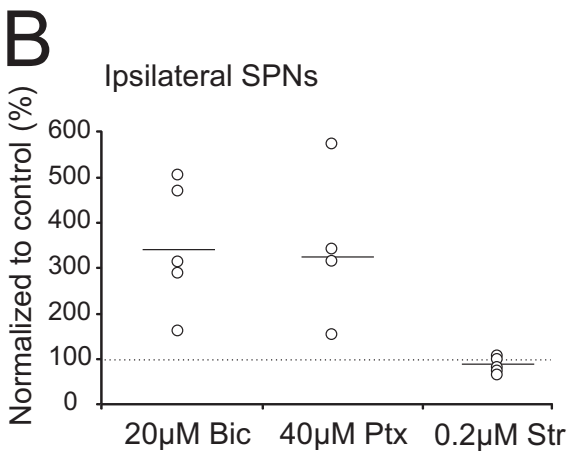
B
Ipsilateral SPNs
Normalized to control (%)
600
500
400
300
200
100
0
20μM Bic
40μM Ptx
0.2μM Str

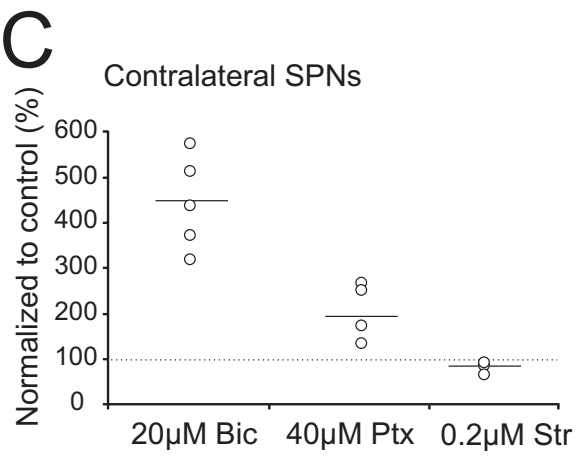
C
Contralateral SPNs
Normalized to control (%)
600
500
400
300
200
100
0
20μM Bic
40μM Ptx
0.2μM Str

Figure 6

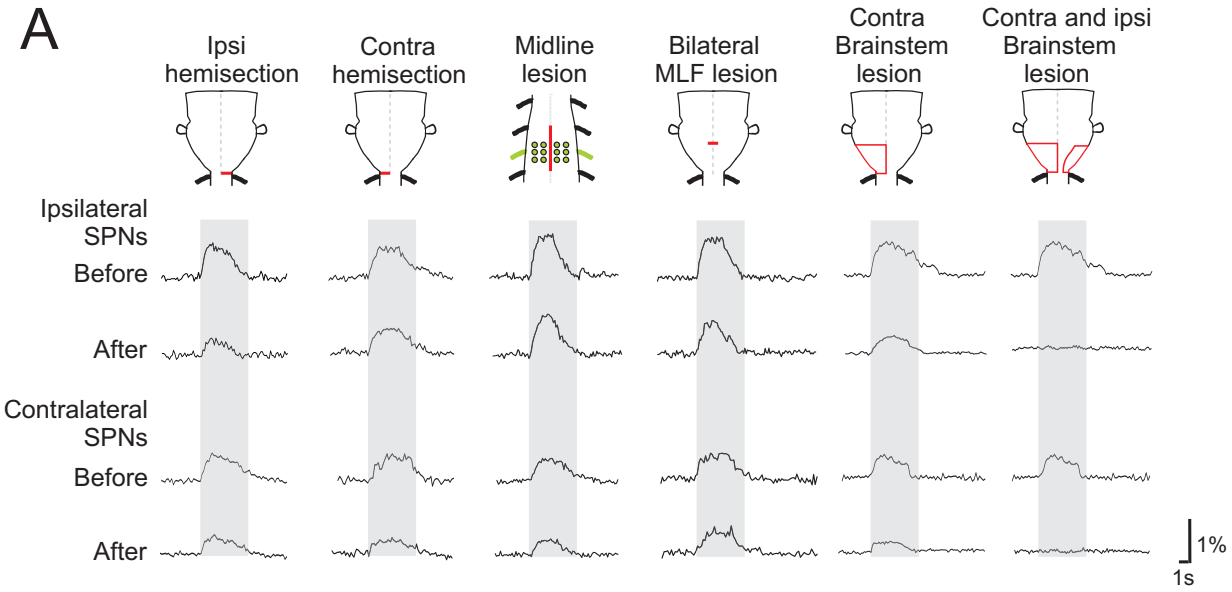
A
Ipsi hemisection
Contra hemisection
Midline lesion
Bilateral MLF lesion
Contra Brainstem lesion
Contra and ipsi Brainstem lesion
Ipsilateral SPNs
Before
After
Contralateral SPNs
Before
After
1%
1s

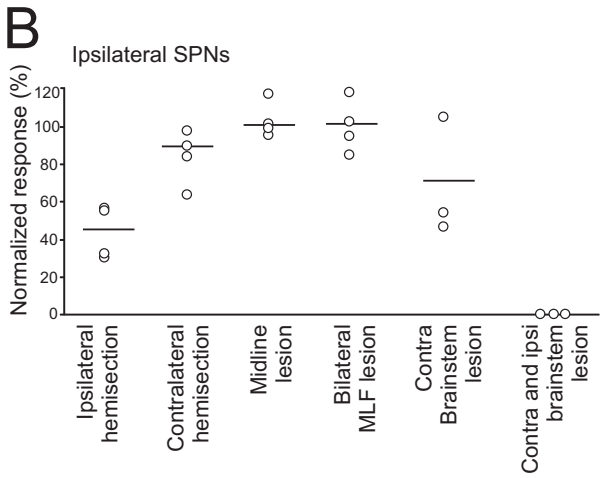
B
Ipsilateral SPNs
Normalized response (%)
0
20
40
60
80
100
120
Ipsilateral hemisection
Contralateral hemisection
Midline lesion
Bilateral MLF lesion
Contra Brainstem lesion
Contra and ipsi brainstem lesion

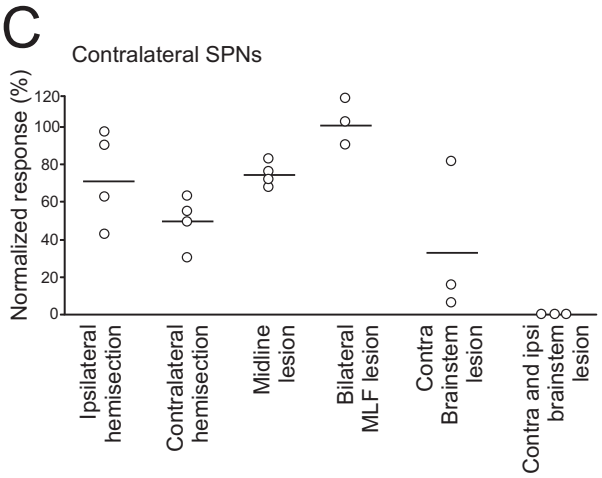
C
Contralateral SPNs
Normalized response (%)
0
20
40
60
80
100
120
Ipsilateral hemisection
Contralateral hemisection
Midline lesion
Bilateral MLF lesion
Contra Brainstem lesion
Contra and ipsi brainstem lesion

Figure 7

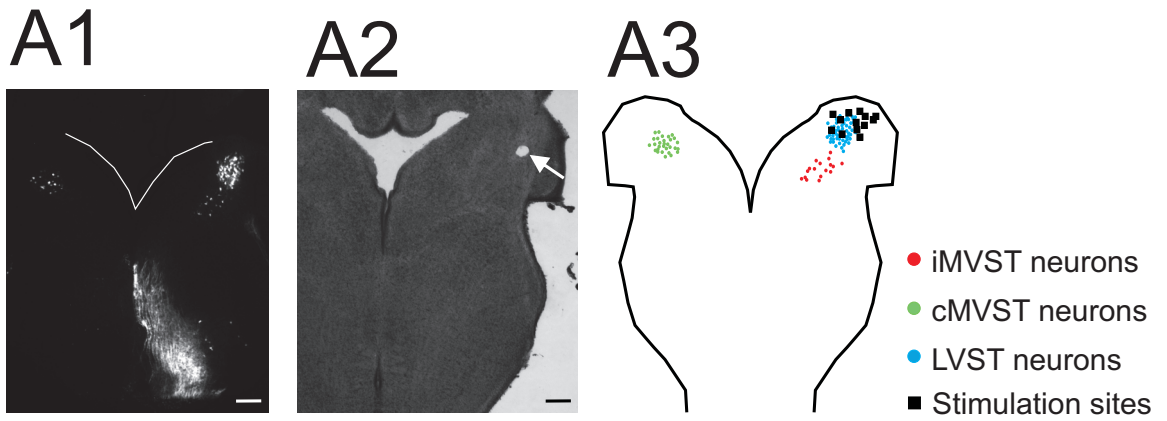
A1
A2
A3
iMVST neurons
cMVST neurons
LVST neurons
Stimulation sites

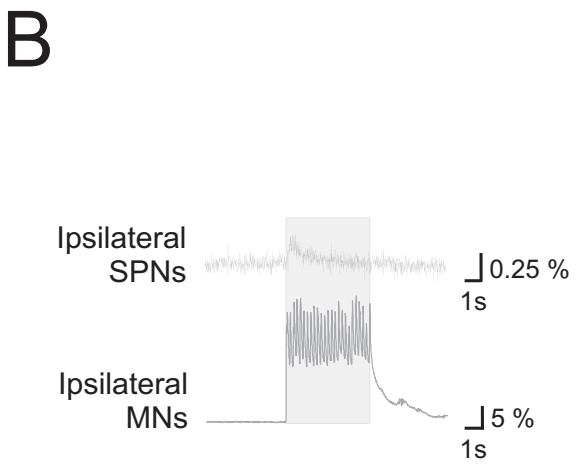
B
Ipsilateral SPNs
0.25 %
1s
Ipsilateral MNs
5 %
1s

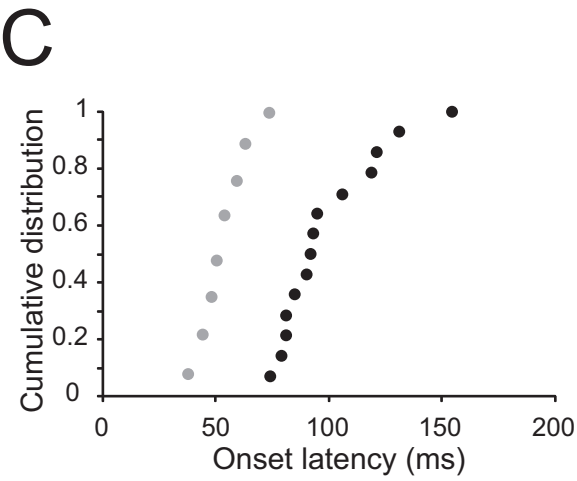
C
Cumulative distribution
1
0.8
0.6
0.4
0.2
0
0
50
100
150
200
Onset latency (ms)

Figure 8

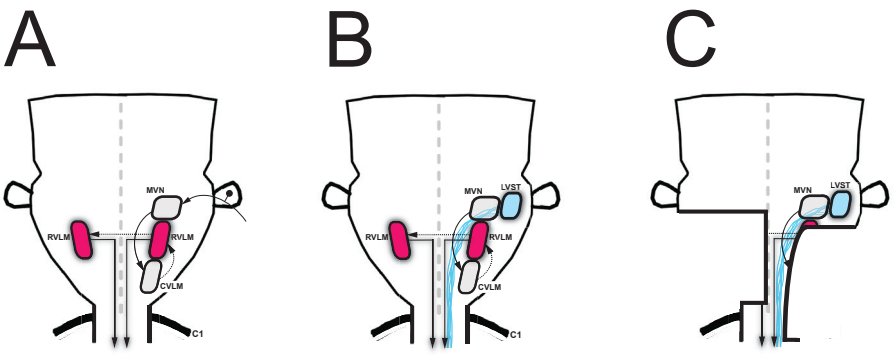

Figure 9

III

Differential distribution of vestibulospinal inputs to descending commissural interneurons in thoraco-lumbar spinal cord segments in the neonatal mouse

Nedim Kasumacic[1], Joel C. Glover[1,2]* and Marie-Claude Perreault[1,2]*

1. Laboratory of Neural Development and Optical Recording (NDEVOR), Department of Physiology, Institute of Basic Medical Sciences, University of Oslo, N-0317 Oslo, Norway

2. Norwegian Center for Stem Cell Research, Department of Immunology and Transfusion Medicine, Oslo University Hospital-Rikshospital

Running head: Imaging vestibulospinal inputs to commissural interneurons

Number of Figures: 6
Number of Tables: 1
Number of supplementary figures: 2

Keywords: SupraspinalControl, Descending Motor Pathways, Spinal Network, Calcium Imaging,

***Co-communicating authors to whom correspondence should be addressed:**
Joel C. Glover, Laboratory of Neural Development and Optical Recording (NDEVOR), Department of Physiology, Institute of Basic Medical Sciences, University of Oslo, N-0317 Oslo, Norway
Email: joel.glover@medisin.uio.no

Marie-Claude Perreault, Department of Physiology, Emory University School of Medicine, Whitehead Biomedical Research Building, 615 Michael Street, Atlanta, GA, USA.
Email: m-c.perreault@emory.edu

Acknowledgements
We are grateful to Kobra Sultani and Marian Berge Andersen for technical assistance and to Magne Sand Sivertsen for help with figures. This work was supported by grants from the Medical Faculty of the University of Oslo and from the Norwegian Research Council to M-C.P. and J.C.G.

ABSTRACT

Vestibulospinal pathways activate contralateral motoneurons (MNs) in the thoraco-lumbar spinal cord of the neonatal mouse exclusively via axons descending ipsilaterally in the lateral vestibulospinal tract (LVST) (Kasumacic et al. 2010). Transmission in the LVST pathway to the contralateral spinal cord must rely on either locally crossing LVST axon collaterals, midline-crossing MN dendrites, ipsilateral commissural interneurons (CINs), or some combination of these. To test the potential mediation by CINs, we examined the effect of mephenesin on LVST-evoked responses in contralateral MNs and recorded LVST-evoked responses in descending CINs (dCINs) in the T7, L2 and L5 segments, using calcium imaging in a brainstem-spinal cord neonatal mouse preparation (Szokol et al. 2008; Szokol and Perreault 2009; Kasumacic et al 2012).

LVST-mediated calcium responses in contralateral MNs of the T7, L2 and L5 segments were virtually abolished by mephenesin, consistent with a predominantly polysynaptic pathway. In agreement with this, a large proportion of ipsilateral dCINs exhibited LVST-mediated calcium responses, although the proportion differed strikingly in the T7, L2 and L5 segments (93%, 38% and 93%, respectively). LVST-mediated inputs to dCINs in T7, L2 and L5 also exhibited strikingly different spatial distributions, with responsive dCINs in T7 and L5 distributed throughout the ventral region of the spinal cord and responsive dCINs in L2 limited to the ventral-most half of that region.

The results indicate a differential distribution of LVST-mediated inputs to thoraco-lumbar dCINs in a pattern that could provide the vestibulospinal system with a substrate for coordinating contralateral trunk and hindlimb movements.

INTRODUCTION

The vestibulospinal system plays a central role in the control of posture and movement. Vestibulospinal axons running in the medial vestibulospinal tracts (iMVST and cMVST) are involved in coordinating upper trunk and head movements (Wilson and Yoshida 1969; Akiake et al 1973; Shinoda et al 2006) and coordinating these with eye movements, whereas vestibulospinal axons running in the lateral vestibulospinal tract (LVST) are involved in coordinating trunk and limb movements (Lund and Pompeiano 1968; Wilson and Yoshida 1969; Grillner et al 1970; Wilson et al 1970; Hongo et al 1971; Abzug et al 1974; Kasumacic et al 2010). The connectivity of vestibulospinal axons to different spinal motoneuron (MN) and interneuron (IN) populations is only superficially understood. We recently demonstrated the presence of LVST-mediated inputs both to axial MNs in the medial motor column (MMC) and to hindlimb MNs in the lateral motor column (LMC) of the cervical, thoracic and lumbar spinal cord in the neonatal mouse (Kasumacic et al 2010). In the lumbar cord, LVST-mediated inputs were targeted to MMC MNs only on the contralateral side but to LMC MNs on both sides. The concerted action of LVST-mediated inputs on both axial and limb MNs provides a potential substrate for coordinating lower trunk and hindlimb movements, and the asymmetry of MMC activation suggests an essential midline-crossing element in that coordination.

We showed previously that LVST axons descend only on the ipsilateral side of the spinal cord, and that the activation of contralateral lumbar MNs by the LVST depends on an intact lumbar commissure (Kasumacic et al 2010). The activation of contralateral MNs thus may be mediated either by locally crossing LVST axon collaterals, midline-crossing MN dendrites or excitatory commissural interneurons (CINs) or some combination of these. Anatomical studies in the cat have shown that LVST axon collaterals can cross the midline, but this appears to be restricted to the upper cervical cord (Kuze et al 1999).

Midline-crossing dendrites extending from MMC MNs have been described in several species (rat: Huang and Goshgarian 2009; frog: Rose and Collins 1985; mouse: our unpublished results) but dendro-dendritic synapses between MMC MNs on either side of the midline have yet to be demonstrated. Stimulation of the lateral vestibular nucleus, from which most LVST axons originate, produces monosynaptic and disynaptic responses in last-order ipsilateral CINs of the L4-L5 segments in the adult cat (Krutki et al 2003). Although all of these findings are compatible with a role for CINs, little information is available about the segmental and intrasegmental distribution of LVST inputs onto thoracolumbar CINs and how this may relate to activation of contralateral trunk and hindlimb MNs.

Reticulospinal neurons have established functional synaptic connections with CINs already by birth in the mouse (Szokol et al. 2011), but it has not been determined whether this is also the case for vestibulospinal neurons. The goal of the present study was first to test for the presence of functional vestibulospinal connections to CINs in the newborn mouse and then to examine their distribution in different thoracolumbar segments. We have used optical recording of synaptically mediated activity visualized with calcium-sensitive retrograde tracers to assess these features. Of the four projection classes of CINs that can be identified in the mouse (Nissen et al 2005, Restrepo et al 2009), we have chosen to focus on the subpopulation that has descending axons (dCINs). This choice is based mainly on the fact that dCINs can be labeled retrogradely with calcium-sensitive tracers without compromising the integrity of vestibulospinal projections. Since we previously reported on reticulospinal inputs to dCINs, this also facilitates a comparison of the effects of these two descending systems.

Vestibulospinal connections to dCINs are assessed here in preparations of the brain stem and spinal cord of the neonatal mouse (Szokol et al. 2008; Szokol and Perreault 2009;

Kasumacic et al 2010, 2012; Szokol et al. 2011). We first show that application of mephenesin to the spinal cord dramatically reduces LVST-mediated postsynaptic Ca2+ responses in contralateral lumbar MNs, indicating that these connections are predominantly polysynaptic. Second, we demonstrate LVST-mediated responses in ipsilateral dCINs of the T7, L2 and L5 segments, implicating these in the polysynaptic pathway. We also see LVST-mediated responses in contralateral dCINs, indicating that the influence of the LVST on the contralateral lumbar cord is more complex than a simple pathway from LVST to ipsilateral dCINs to contralateral MNs. Finally, we show that LVST-mediated inputs are differentially distributed onto ipsilateral dCINs both segmentally and intrasegmentally, indicating that LVST-mediated activity is channeled to the contralateral spinal cord by dCIN subpopulations in a segment-specific manner. Preliminary accounts of the present work have appeared previously (Perreault et al., 2009; Kasumacic et al 2011).

MATERIALS AND METHODS

Animals and brainstem-spinal cord preparation

Experiments were performed on ex vivo preparations of the brain stem and spinal cord of newborn mice of the ICR strain (n = 41) at postnatal days (P) 0 – 5. Mice were deeply anesthetized with isoflurane (Abbott, Scandinavia AB), decerebrated at the level of the superior colliculus, after which the brain stem and spinal cord were rapidly dissected and removed using the same procedure as described in Kasumacic et al (2010). All efforts were made to minimize the number of animals used in accordance with the European Communities Council directive 86/609/EEC and the National Institutes of Health

Guidelines for the Care and Use of Animals. All procedures were approved by the National Animal Research Authority in Norway (Forsøksdyrutvalget).

Retrograde labeling of dCINs with fluorescent calcium indicator

After dissection the preparation was placed in oxygenated artificial cerebrospinal fluid (aCSF) containing in mM: NaCl 128, KCl 3, D-glucose11 CaCl2 2.5, MgSO4 1, NaH2PO4 1.2, HEPES 5, and NaHCO3 25. Descending commissural interneurons (dCINs) in T7 were labeled by applying crystals of Calcium Green 1-conjugated Dextran-Amine(CGDA, 3000 MW, Invitrogen) to the cut ventral and ventrolateral funiculi (VF and VLF) at the level of T8 on the contralateral side (Glover 1995). L2 and L5 dCINs were labeled by CGDA applications to the VF and VLF of segments L3 and L6, respectively (Figure 1). Retrograde labeling was allowed to continue in aCSF at room temperature (22 – 25°C) in the dark for 4 hours.

Optical recording of calcium transients in CGDA-labeled dCINs

Preparations were then transferred to a sylgard-coated chamber and pinned down with stainless steel (Minuten) pins ventral side up. The bath containing the brainstem-spinal cord preparation was perfused with oxygenated aCSF at a rate of 7.5 ml/min, giving a total volume exchange every 2 minutes. Labeled dCINs were visualized through an obliquecut made through the relevant segment (see Szokol and Perrault 2009 and Kasumacic et al 2012) using a 40x water immersion objective (LUMPlanFl, 0.8 NA, Olympus, Norway) on an upright epi-fluorescence microscope (Axioskop FS 2, Carl Zeiss, Oberkochen, Germany) equipped with a 100 W halogen lamp driven by a DC

power supply (PAN35-20A, Kikusui Electronics Corporation, Japan) and excitation and emission filters (BP 450-490 nm and LP 515 nm, respectively). Fluorescence changes associated with neuronal activity, which we refer to hereafter as " Ca^{2+} responses", were registered using a cooled CCD camera (Cascade 650 or Evolve:512, Photometrics, Texas Instruments, USA) mounted on a video zoom adaptor, using the image-processing software Metamorph 5.0 (Universal Imaging Corporation, Molecular Devices, USA). Image series were acquired at 4 frames/second (binning factor 2) or 150 frames/second (binning factor 6). In experiments where we compared the magnitude of a response in a given cell prior, during and after an intervention (lesion or drug application) imaging series were acquired at 4 frames/second rather than 150 frames/second to minimize bleaching.

Electrical stimulation of the vestibular nerve, ventrolateral funiculus and dorsal roots

The entire eighth cranial nerve was stimulated electrically with a borosilicate glass suction electrode (Harvard Apparatus, Cat. #: 30-0056) coupled to a digital stimulator (WPI, DS 8000). Nerve stimulation consisted of 5 sec trains of 200 μsec pulses at 5 Hz, with a current strength between 80 - 300 μA. These stimulation parameters were chosen because they had already been shown to be the most effective in eliciting responses in lumbar MNs (Kasumacic et al 2010). In some experiments, we also stimulated the peeled ventrolateral funiculus (VLF) or the dorsal roots (DR) using a 5 sec, 5 Hz train (10-20 μA current). Throughout this paper, stimulation strengths are expressed in multiples of the current threshold (T) for evoking a detectable increase in CGDA fluorescence (see data analysis section below).

Data analysis and statistics

Circular digital apertures of identical size and shape, termed regions of interest (ROIs) in the MetaMorph software, were placed manually over individual dCIN somata. To compensate for variability in the CGDA labeling intensity, the Ca2+ responses in each ROI were quantified as changes in fluorescence ΔF divided by the baseline fluorescence F0 before the stimulation (ΔF/F0 = (F-F0)/F0). A detectable response was defined as a continuous positive deflection exceeding a detection limit of two standard deviations above the mean of the baseline. Response magnitude was defined as the area under the waveform above the detection limit. Unless indicated otherwise, all data are presented as grand means across preparations.

Pseudocolor representations of responses such as shown in Figures 1, 3, 4 and Supplementary Figure 1 were made by filtering the complete image series of the recording session in Metamorph with a low pass 3 x 3 filter and then converting greyscale values to colors using a rainbow index, with transition from blue to red to white representing increasing response size. In some cases moderate adjustments in brightness and contrast were performed on the entire image series prior to this conversion using the auto-levels function. Data are presented as means and standard errors of the mean. Student's T-test was used to test the significance of differences in cumulative plots of dorsoventral positions.

RESULTS

Effect of mephenesin on LVST-mediated responses in contralateral MNs

We have shown previously that a midline lesion encompassing T6 to T8 or L1 to L6 eliminates LVST-mediated responses in the contralateral MNs of respectively T7 and L2 and L5 (Kasumacic et al 2010), suggesting that locally crossing excitatory connections play an important role in mediating these responses. To test the potential role of ipsilateral CINs in mediating this crossed pathway, we first examined the effects of 1 mM mephenesin, a drug that reduces polysynaptic transmission in sensory (Kaada, 1950; Ziskind-Conhaim, 1990; Lev-Tov &Pinco, 1992) and descending (Floeter and Lev-Tov, 1993) pathways, applied selectively to the spinal cord. Within 10 min of mephenesin application, LVST-mediated responses in contralateral MNs of the T7, L2 and L5 segments virtually disappeared (Figure 2A) with response magnitudes decreased to 2-7% of control in the different MN populations (Figure 2B). This indicates an overwhelmingly polysynaptic LVST-mediated input to contralateral MNs of the thoracolumbar cord.

As an additional test of polysynaptic connections, we measured the onset latencies of the LVST-mediated responses in T7, L2 and L5 MNs. Latency measurements were performed with a frame rate of 150 Hz (6.7 msec temporal resolution, Figure 2C) which was more than adequate to determine the onset of responses because the earliest latencies observed, as calculated from the start of the train stimulation, were substantially greater than 7 msec. The ranges of latencies are shown in Figure 2D as five separate cumulative plots for T7 MMC (n = 4, 22 MNs), L2 MMC and LMC (n = 4, 26 MNs for both) and L5 MMC and LMC (n = 3, 18 MNs for both). As shown, contralateral MNs examined in T7 and L5 segments responded within latency ranges of 50-125 msec and 47-220 msec, respectively. In L2, the latencies of the responses were generally longer and contralateral MNs responded within a latency range of 60-350 msec. Altogether these results indicate

that LVST-mediated inputs to contralateral MNs are polysynaptic and thus channeled through spinal interneurons.

LVST-mediated inputs to ipsilateral dCINs

The presence of LVST-mediated inputs was investigated in a total of 395 dCINs in 18 animals (83 dCINs in T7, 163 dCINs in L2 and 149 dCINs in L5). In T7 and L5, nearly all of the ipsilateral dCINs examined (77/83, 93% and 138/149, 93%, respectively) responded to activation of the LVST (Table 1). Typically, the responses had sharp rising phases followed by, in T7, a plateau of similar magnitude and a slow falling phase that started approximately halfway through the 5 sec stimulus train, or, in L5, just the falling phase with an earlier onset (Figure 3 A). In contrast, in L2, only 38% (61/160) of the dCINs responded to activation of the LVST (Figure 3B, Table 1). The responses in L2 dCINs were similar to those in L5 in waveform and magnitude, except that the falling phase was more rapid.

Since T7, L2, and L5 dCINs were recorded in different preparations, we wanted to test whether the lack of response to VIIIth nerve stimulation in the majority of L2 dCINs was genuine by checking how the non-responsive dCINs responded to other sources of inputs. Stimulation of the ipsilateral VLF at C6 to activate multiple descending pathways or of the ipsilateral L2 dorsal root to activate sensory afferents both elicited responses in those ipsilateral dCINs that did not respond to LVST stimulation (Supplementary Figure 1).

To assess the relative timing of activation of ipsilateral dCINs versus contralateral MNs, we measured the response latencies in a sample of the responsive dCINs in T7 (n= 4 animals, 37 dCINs), L2 (n=6 animals, 38 dCINs) and L5 (n=6 animals, 38 dCINs) using high frame rate recording (150Hz, Figure 5A). Consistent with ipsilateral dCINs being activated prior to contralateral MNs, the minimum onset latencies of the dCINs were

shorter than those of the MNs with latencies ranging from 32-140 ms in T7, 32-98 ms in L2 and 56-130 ms in L5 (Figure 5B). These findings are compatible with the idea that, as part of a crossed vestibulospinal pathway, dCINs contribute to LVST-mediated responses in contralateral MNs.

Spatial distribution of responsive ipsilateral dCINs

Using the central canal and the midline as landmarks in the oblique plane, we determined the positions of all ipsilateral dCINs recorded and analyzed in the transverse plane of T7 (83 dCINs), L2 (163 dCINs) and L5 (149 dCINs). For each dCIN, we measured the radial distance from the middle of the central canal and the angle from the vertical represented by the midline, scaled these linearly to project the obliquely cut surface to a vertically cut surface, and plotted the resultant values on a standard transverse section. Figure 6A-C shows for each segment the locations of the LVST-responsive dCINs (green circles) and LVST-unresponsive dCINs (red circles). In all three segments, most dCINs were located ventral to the midpoint of the central canal, with a spatial distribution similar to that previously reported for dCINs in the mouse embryo (Nissen et al., 2005) and neonate (Szokol et al. 2011). A striking feature in all three segments was the pronounced skewing of non-responsive and responsive dCINs to respectively dorsal and ventral locations. In T7 and L5, where nearly all dCINs responded to activation of the LVST, the few unresponsive dCINs were all restricted to approximately the dorsalmost third of the range. In L2, where the responsive dCINs were the minority, the unresponsive dCINs dominated the dorsal half of the range. To quantitate this, we display the dorsoventral locations of the L2 dCINs with respect to the central canal in a cumulative plot (Supplementary Figure 2). As shown, the non-responsive and responsive populations had

clearly distinct cumulative distributions with dorsoventral positions ranging from -285µm to +260 µm (average of 38µm) for the non-responsive dCINs and from -5µm to +334 µm (average of 168µm) for the responsive dCINs (Student's t-test, $p< 0.0001$). To give a rough approximation of the segregation of the two dCIN populations, about 50% of responsive dCINs but only 8% of non-responsive dCINs were located ventral to the 160 µm line whereas 50% of non-responsive dCINs but only 4% of responsive dCINs were located dorsal to the 30µm line (Figure 6D).

Altogether, these results show that ipsilateral dCINs in thoracolumbar segments receive LVST-mediated inputs in a segment-specific pattern, with a numerically and spatially much more restricted responsive subpopulation in L2 relative to T7 and L5.

LVST-mediated inputs to contralateral dCINs

To determine whether the influence of the LVST on the contralateral thoracolumbar spinal cord is limited to activation of contralateral MNs, we tested for LVST-mediated responses in contralateral dCINs (T7: 145 dCINs, L2: 148 dCINs, L5: 142 dCINs) in a total of 18 animals (6 animals for each segment). Responsive contralateral dCINs were found in all three segments, comprising 79% (115/145) of recorded contralateral dCINs in T7, 34% (50/148) of recorded contralateral dCINs in L2, and 93% (132/142) of recorded contralateral dCINs in L5 (Figure 4 and Table 1). Thus, the segment-specific proportional pattern was similar to that of ipsilateral dCINs. The shapes of the responses elicited in contralateral dCINs were also similar to those of ipsilateral dCINs, exhibiting the same segment-specific characteristics such as the pronounced plateau in T7 but not in L5 (Figure 5C). The latencies of the responses in contralateral dCINs were 87 ms ± 3.5 ms in T7 (range 57 – 140 ms, n = 5 animals, 31 neurons), 69 ms ± 2.4 ms in L2 (range 56

– 140 ms, n = 5 animals, 24 neurons) and 93 ms ± 3.7 ms in L5 (range 46 – 151 ms, n = 6 animals, 38 neurons) (Figure 5D).

The spatial distribution of non-responsive and responsive contralateral dCINs was remarkably similar to that of ipsilateral dCINs, with clear skewing of non-responsive and responsive dCINs towards respectively dorsal and ventral locations in all 3 segments, and a pronounced ventral restriction of responsive contralateral dCINs in L2 (Figure 6D, E and F).

DISCUSSION

We have shown that the LVST in the newborn mouse elicits synaptic responses in dCINs on both sides of the thoracolumbar spinal cord. Response latencies in ipsilateral dCINs suggest that at least some of these are presynaptic to and mediate the polysynaptic responses elicited in contralateral thoracolumbar MNs by activation of the LVST. Our findings can be summarized as follows: 1) mephenesin, which reduces polysynaptic transmission, diminishes LVST-evoked responses in contralateral MNs by over 90%, 2) activation of the LVST elicits responses in ipsilateral dCINs with shorter absolute and average minimal latencies than for responses in contralateral MNs, 3) activation of the LVST also elicits responses in contralateral dCINs, 4) both ipsilateral and contralateral dCINs show a segment-specific activation pattern in which a vast majority of LVST-responsive dCINs respond in T7 and L5 but only 30-40% respond in L2, 5) nearly all responsive dCINs in all 3 segments are found ventral to the central canal, but in L2 the responsive population is even more restricted within the transverse plane, with a clear segregation of more ventral responsive dCINs and more dorsal unresponsive dCINs.

Indirect pathway from the LVST to the contralateral spinal cord

LVST axons are known in the adult cat to make both monosynaptic and polysynaptic connections onto ipsilateral and contralateral lumbar MNs, with polysynaptic connections predominating (Wilson and Yoshida 1969; Wilson et al 1970; Grillner et al 1970). Excitatory and inhibitory polysynaptic connections are primarily to extensor and flexor MNs, respectively. LVST axon terminals are found in the ipsilateral lamina VIII and medial parts of ipsilateral lamina VII (Nyberg-Hansen and Mascitti 1964; Erulkar et al 1966), with only a few terminals seen contralaterally (Erulkar et al 1966; Kuze et al

1999). Thus, dCINs, which densely populate lamina VIII (Bannatyne et al 2003, Nissen et al 2005), are prime candidates for mediating polysynaptic connections onto contralateral MNs.

Our results show that the LVST has a widespread influence on contralateral neurons, with polysynaptic inputs both to contralateral MNs and nearby contralateral dCINs. Potentially, these inputs may be disynaptic and directly mediated by ipsilateral dCINs, but since we cannot definitively assess the number of synapses involved using calcium imaging, this will have to be resolved in future experiments. A critical experiment in this regard will be to selectively block the activation of the ipsilateral dCINs in specific segments and assess the effects on contralateral MN and dCIN responses. Of particular interest is the presence of LVST-mediated responses in a similarly restricted intrasegmental subset of contralateral dCINs as seen for the presynaptic ipsilateral dCINs. This indicates a highly specific channeling of LVST-mediated signals from ipsilateral to contralateral sides, in a double-crossed pathway that is expected to recurrently influence the ipsilateral side.

Segmental differences in the proportion of LVST-responsive dCINs

The substantially lower proportions of responsive dCINs in L2 relative to T7 and L5 suggests a functional relationship between the segmental addresses of dCINs and the channeling of vestibular information by the LVST to MNs and muscles. Of particular interest in this regard is that L2 and L5 are populated primarily by flexor and extensor MNs, respectively. Thus, the difference between L2 and L5 in the proportion of responsive dCINs may be related to flexor versus extensor activation. It is known that the LVST activates primarily extensor MNs on the contralateral side and that some dCINs in

L2 are presynaptic to extensor MNs in L4 (Butt and Kiehn 2003). Thus, one intriguing possibility is that the restricted population of LVST-responsive dCINs in L2 is extensor-related and potentially premotor to extensor MNs in L2 and more caudal segments. Seen in this light, it may be that the LVST-responsive dCIN populations in T7 and L5 are larger and more dispersed dorsoventrally because they are more heterogeneous with respect to the types of MNs they innervate. For example, the LVST-responsive T7 dCINs may not innervate hindlimb MNs at all but rather trunk MNs, and the LVST-responsive L5 dCINs may innervate contralateral extensor as well as flexor MNs in that segment as well as tail MNs in more caudal segments.

Ipsilateral limb MNs in L5 and L2 are also distinctive in the timing of their responses relative to LVST stimulation. Ipsilateral L5 LMC MNs respond strongly during the stimulation whereas ipsilateral L2 LMC MNs respond strongly only after the stimulation is terminated (Kasumacic et al 2010). Both types of response are produced and modulated by convergent excitatory and inhibitory connections, since blocking GABA-A receptors increases the magnitude of the response in L5 and reveals a subjugated ”during stimulation” response in L2. The situation is more complex in contralateral limb MNs. Here, the response is during stimulation in L2, and both during and after stimulation in L5 (Kasumacic et al 2010).

The overall picture is one in which ipsilateral L2 and L5 MN responses to LVST stimulation are reciprocal and L2 responses on opposite sides are reciprocal. It is not difficult to envision a scheme in which monosynaptic connections from excitatory and inhibitory spinal INs including dCINs could sculpt these different responses from descending LVST inputs. It will therefore be of great interest to identify the specific MN targets of the LVST-responsive dCINs in the various lumbar segments and place this into the context of the crossed, reciprocally organized extensor activation and flexor inhibition

that characterizes the vestibulospinal reflexes. Moreover, it will be of equally great interest to investigate whether the LVST-responsive dCINS are also involved in setting up the same crossed, reciprocal organization that characterizes locomotion, as this would represent a direct overlap between descending motor control and the functional organization of the locomotor CPG.

The significance of differential dorsoventral distribution: developmental implications

Examples abound of spatial segregation within neuron populations in the motor system, to the extent that it is now commonly believed that the specific anteroposterior and dorsoventral positions both of MNs and of premotor INs and projection neurons is part of a developmental scheme by which the coarse strokes of motor connectivity are established (see Glover 2000 for review). This is also true in the vestibular system (Glover 2003). It is appealing in this regard to see that the specific LVST-responsive dCIN population in L2 is strikingly segregated from the non-responsive dCIN population along the dorsoventral axis. Providing dCINs with different outputs with different spatial addresses provides vestibulospinal (and other descending) axons presynaptic to the dCINs the opportunity to establish functionally appropriate polysynaptic pathways simply by targeting their collateral branches to different regions of the ventromedial spinal cord. Since the pattern has been set up by birth, it will be extremely interesting to follow the ingrowth of LVST axons during the end of fetal life to see whether such targeting occurs, and whether the connections to specific dCIN populations obtains from the outset.

References

Abzug C, Maeda M, Peterson BW and Wilson VJ. (1974) Cervical branching of lumbar vestibulospinal axons. *J Physiol. 1974 243:499-522.*

Akaike T, Fanardjian VV, Ito M, Kumada M and Nakajima H. (1973) Electrophysiological analysis of the vestibulospinal reflex pathway of rabbit. I. Classification of tract cells. *Exp Brain Res. 1973 17:477-96.*

Bannatyne BA, Edgley SA, Hammar I, Jankowska E, Maxwell DJ. (2003) Networks of inhibitory and excitatory commissural interneurons mediating crossed reticulospinal actions. *Eur J Neurosci. 2003 18:2273-84.*

Butt SJ, Kiehn O. (2003) Functional identification of interneurons responsible for left-right coordination of hindlimbs in mammals. *Neuron. 2003 38:953-63.*

Erulkar SD, Sprague JM, Whitsel BL, Dogan S and Jannetta PJ. (1966) Organization of the vestibular projection to the spinal cord of the cat. *J Neurophysiol. 1966 29:626-64.*

Floeter MK, Lev-Tov A. (1993) Excitation of lumbar motoneurons by the medial longitudinal fasciculus in the in vitro brain stem spinal cord preparation of the neonatal rat. *J Neurophysiol. 1993 70:2241-50.*

Glover JC. (1995) Retrograde and anterograde axonal tracing with fluorescent dextran-amines in the embryonic nervous system. *NeurosciProt 1995 30, 1–13.*

Glover JC. (2000) Development of specific connectivity between premotor neurons and motoneurons in the brain stem and spinal cord. *Physiol Rev. 2000 80:615-47.*

Glover JC. (2003) The development of vestibulo-ocular circuitry in the chicken embryo. *J Physiol Paris. 2003 97:17-25.*

Grillner S, Hongo T and Lund S. (1970) The vestibulospinal tract. Effects on alpha-motoneurones in the lumbosacral spinal cord in the cat. *Exp Brain Res. 197010:94-120.*

Hongo T, Kudo N and Tanaka R. (1971) Effects from the vestibulospinal tract on the contralateral hindlimbmotoneurones in the cat. *Brain Res. 1971 31:220-3.*

Huang Y, Goshgarian HG. (2009) Identification of the neural pathway underlying spontaneous crossed phrenic activity in neonatal rats. *Neuroscience. 2009 163:1109-18.*

Kaada BR. (1950) Site of action of myanesin in the central nervous system. *J Neurophysiol 13:89-104.*

Kasumacic N, Glover JC, Perreault MC. (2010) Segmental patterns of vestibular-mediated synaptic inputs to axial and limb motoneurons in the neonatal mouse assessed by optical recording.*J Physiol. 2010 588:4905-25*

Kasumacic N, Glover JC, Perreault MC. (2011) Vestibulospinal inputs to thoracolumbar commissural interneurons in the neonatal mouse assessed with optical recording. *Annual meeting of the Society for Neuroscience 809.03/PP21*

Krutki P, Jankowska E and Edgley SA. (2003) Are crossed actions of reticulospinal and vestibulospinal neurons on feline motoneurons mediated by the same or separate commissural neurons? *J Neurosci. 2003 23:8041-50.*

Kuze B, Matsuyama K, Matsui T, Miyata H, Mori S. (1999) Segment-specific branching patterns of single vestibulospinal tract axons arising from the lateral vestibular nucleus in the cat: A PHA-L tracing study. *J Comp Neurol. 1999 414:80-96.*

Lev-Tov A, Pinco M. (1992) In vitro studies of prolonged synaptic depression in the neonatal rat spinal cord. *J Physiol. 1992 447:149-69.*

Lund S and Pompeiano O. (1968) Monosynaptic excitation of alpha motoneurones from supraspinal structures in the cat. *ActaPhysiol Scand. 1968 73:1-21.*

Nissen UV, Mochida H, Glover JC. (2005) Development of projection-specific interneurons and projection neurons in the embryonic mouse and rat spinal cord.
J Comp Neurol. 2005 483:30-47.

Nyberg-Hansen R, Mascitti TA. (1964) Sites and mode of termination of fibers of the veestibulospinal tract in the cat. An experimental study with silver impregnation methods.
J Comp Neurol. 1964 122:369-83.

Perreault MC, Kasumacic N, Glover JC and Szokol K. (2009) Bulbospinal control of lumbar motor networks in the neonatal mouse. *Breathe, Walk and Chew: The Neural Challenge 31st annual symposium 2009 Montreal*

Restrepo CE, Lundfald L, Szabó G, Erdélyi F, Zeilhofer HU, Glover JC, Kiehn O. (2009) Transmitter-phenotypes of commissural interneurons in the lumbar spinal cord of newborn mice. *J Comp Neurol. 2009 517:177-92.*

Rose RD, Collins WF (1985). Crossing dendrites may be a substrate for synchronized activation of penile motoneurons. *Brain Res. 1985 337:373-7.*

Shinoda Y, Sugiuchi Y, Izawa Y, Hata Y. (2006) Long descending motor tract axons and their control of neck and axial muscles. *Prog Brain Res. 2006;151:527-63.*

Szokol K, Glover JC, Perreault MC. (2008) Differential origin of reticulospinal drive to motoneurons innervating trunk and hindlimb muscles in the mouse revealed by optical recording. *J Physiol. 2008 586:5259-76.*

Szokol K and Perreault MC. (2009) Imaging synaptically mediated responses produced by brainstem inputs onto identified spinal neurons in the neonatal mouse. *J Neurosci Methods 180:1-8.*

Szokol K, Glover JC and Perreault MC. (2011) Organization of functional synaptic connections between medullary reticulospinal neurons and lumbar descending commissural interneurons in the neonatal mouse. *J Neurosci. 2011 31:4731-42.*

Wilson VJ and Yoshida M. (1969) Comparison of effects of stimulation of Deiters' nucleus and medial longitudinal fasciculus on neck, forelimb, and hindlimb motoneurons.*J Neurophysiol. 1969 32:743-58.*

Wilson VJ, Yoshida M and Schor RH. (1970) Supraspinal monosynaptic excitation and inhibition of thoracic back montoneurons. *Exp Brain Res. 1970 11:282-95.*

Ziskind-Conhaim L. (1990) NMDA receptors mediate poly- and monosynaptic potentials in motoneurons of rat embryos. *J Neurosci. 1990 1:125-35.*

FIGURE LEGENDS

Figure 1. Right: schematic overview of the brainstem-spinal cord preparation with indications of the labeling protocol for the different dCIN groups studied. Upper inset: photograph of the vestibular nerve inserted into a glass suction electrode, scale bar 100 µm. Lower inset: photograph of the obliquely cut transverse surface of L2 segment. dCINs to the right, dIINs to the left. Lower schematic show the position of the spinal cord during imaging, rightmost: pseudocolor image of dCINs, scale bar 50µm, D: dorsal direction, M: medial direction. The pseudocolor image was produced by filtering with a 3x3 low pass filter, and assigning the colors to a rainbow index.

Figure 2. A and B show the effect of application of 1mM Mephenesin to the spinal cord in a split brainstem-spinal cord bath at C1. A: Waveforms of responses recorded at 4 frames/second before and after application of Mephenesin. Grey bars represent the 5 second 5 Hz stimulation train. B: Normalized response magnitudes (mephenesin/control) in individual motor columns. C: 150frames/second recording from individual MNs in the different motor columns. D: Cumulative distribution of latencies in individual MNs. Vertical bars represent averages for individual motor columns. Color-coded to match waveforms in C.

Figure 3. Response in ipsilateral dCINs of T7 (A), L2 (B) and L5 (C) recorded at 4 frames/second. The pseudocolor image was produced by filtering with a 3x3 low pass filter, and assigning the magnitudes grey-scale values that were then converted to a

rainbow color index. Scale bars: 50 μm. Grey bars represent the 5 second 5 Hz stimulation train. In B, n = 3 for each segment

Figure 4. Responses in contralateral dCINs of T7 (A), L2 (B) and L5 (C) recorded at 4 frames/second. The pseudocolor image was produced by filtering with a 3x3 low pass filter, and assigning the magnitudes to a rainbow color index as for Figure 3. Scale bars: 50 μm. Grey bars represent the 5 second 5 hz stimulation train.

Figure 5. High frame rate (150 frames/second) recording from individual ipsi (A) and contra (C) dCINs in segments T7, L2 and L5. Gray bars represent the 5 second 5 hz stimulation train. B and D: Cumulative distribution of latencies in individual ipsi (B) and contra (D) dCINS in segments T7, L2 and L5. Vertical bars represent average for individual motor columns. Color coded to match waveforms in A and C.

Figure 6. Distributions of ipsi (A-C) and contra (D-F) dCINs in T7, L2 and L5 in the transverse plane. Green dots: neurons responsive to vestibular nerve stimulation, red dots: neurons not responding to vestibular nerve stimulation. Scalebar: 250 μm.

Table 1. Numbers and proportions of recorded, responsive and non-responsive ipsilateral and contralateral dCINs in T7, L2 and L5 segments.

Supplementary Figure 1. Comparative responsiveness of L2 dCINs to VIIIth nerve, VF and dorsal root stimulation.100 frames/second recordings from L2 dCINs that were not responsive during vestibular nerve stimulation. These neurons responded to stimulation of the ipsilateral L2 dorsal root, and ipsilateral ventral funiculus stimulated at the level of C4. In all cases, the stimulation was delivered in the form of a 5 second 5 Hz train.

Supplementary Figure 2. Cumulative distributions of the dorsoventral positions of LVST-responsive and non-responsive ipsilateral dCINs in L2. Calculated positions of ipsilateral dCINs relative to the central canal. Positive values indicate ventral direction and negative values indicate dorsal direction. T-test shows that the ventral skewing of the responsive neurons is statistically significant, $p<0.0001$.

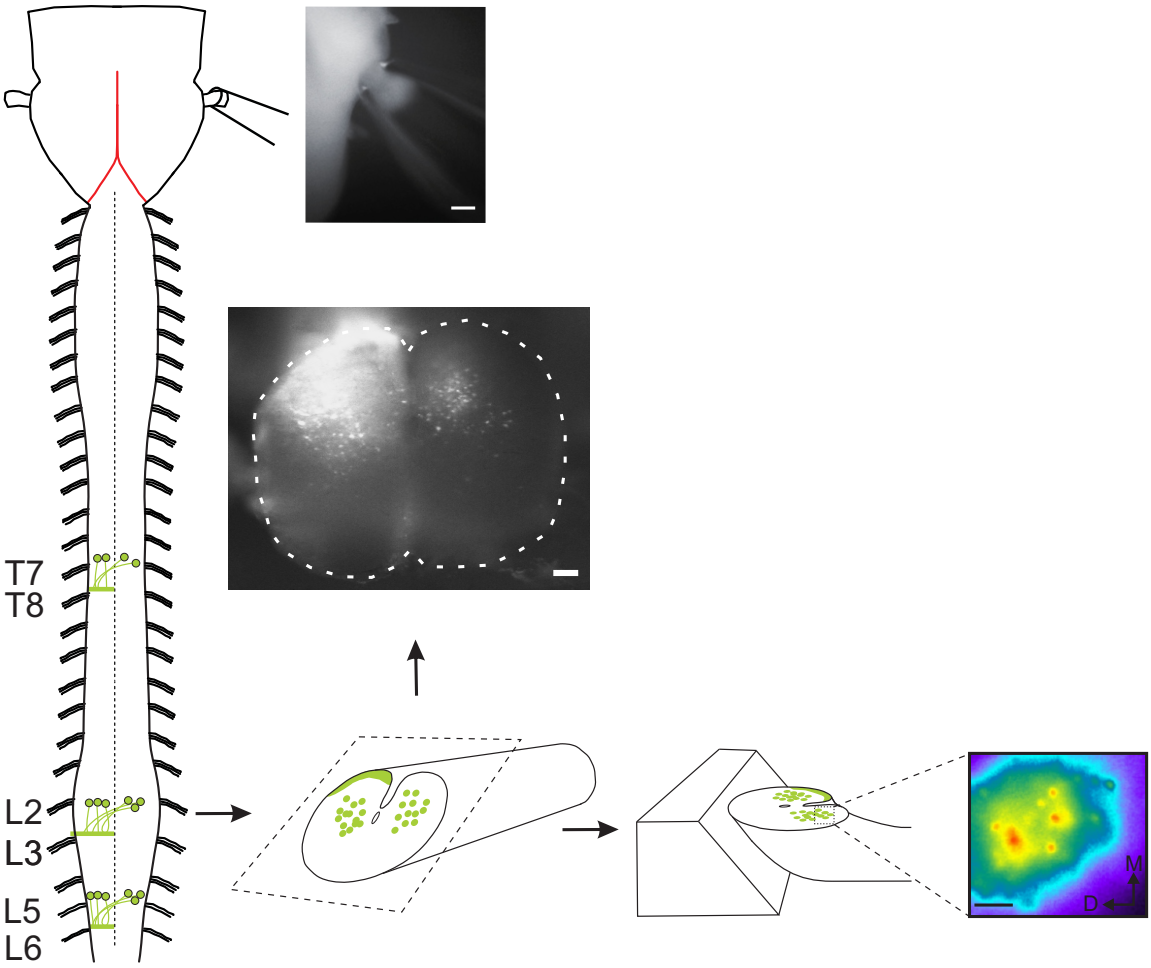

Figure 1

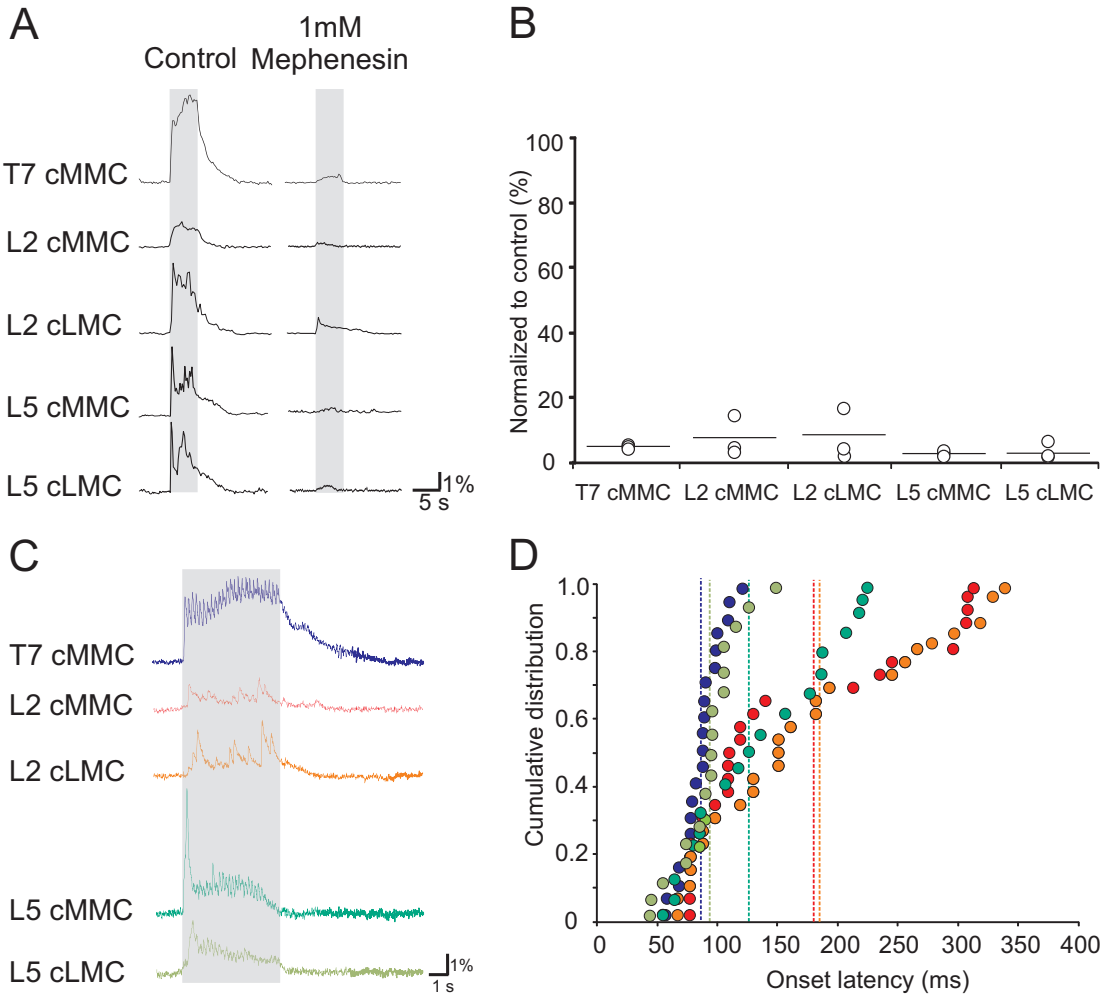
A
Control
1mM
Mephenesin
T7 cMMC
L2 cMMC
L2 cLMC
L5 cMMC
L5 cLMC
1%
5 s
B
Normalized to control (%)
100
80
60
40
20
0
T7 cMMC
L2 cMMC
L2 cLMC
L5 cMMC
L5 cLMC
C
T7 cMMC
L2 cMMC
L2 cLMC
L5 cMMC
L5 cLMC
1%
1 s
D
Cumulative distribution
1.0
0.8
0.6
0.4
0.2
0
0
50
100
150
200
250
300
350
400
Onset latency (ms)

Figure 2

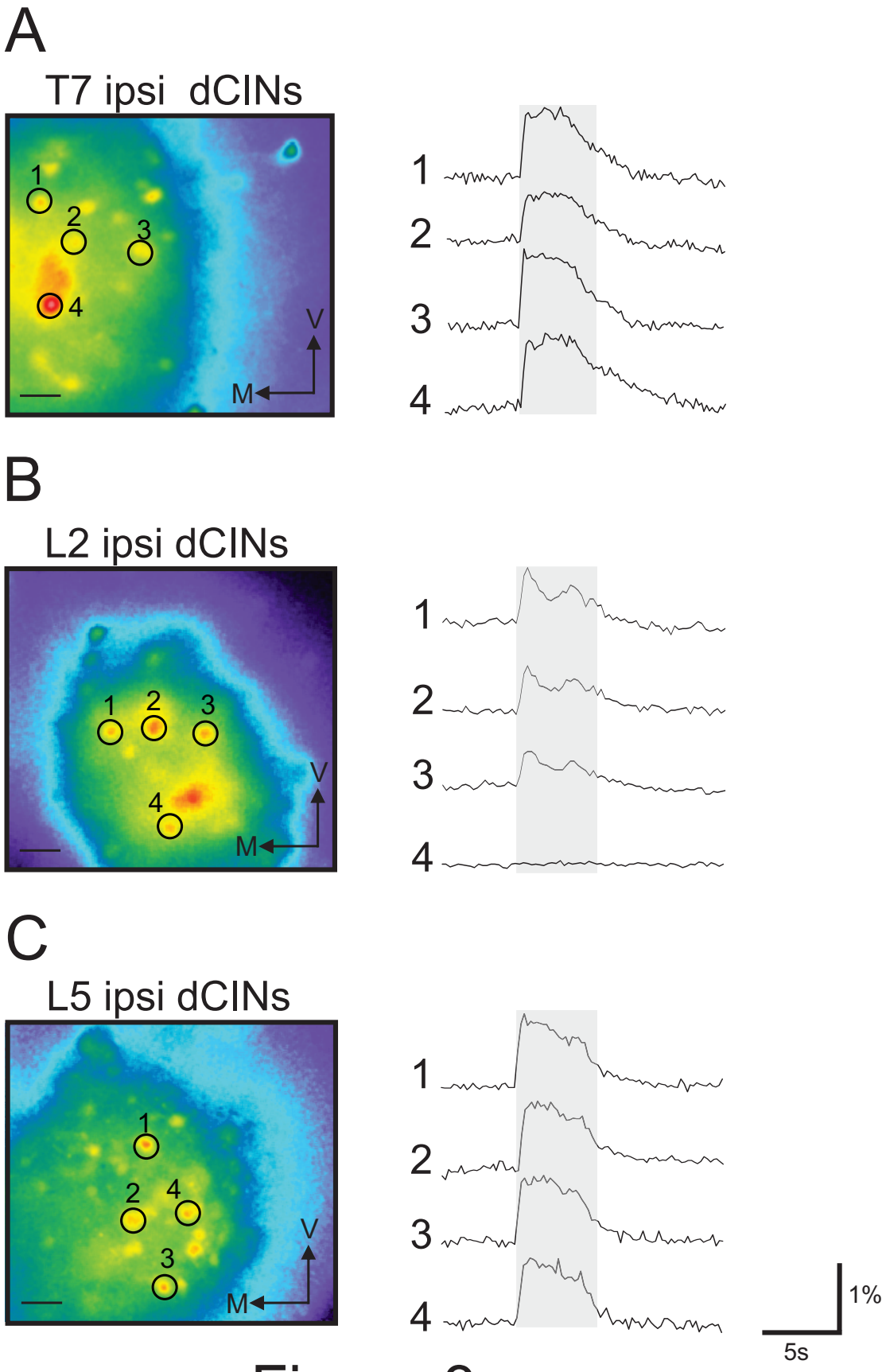
A
T7 ipsi dCINs
1
2
3
4
V
M
1
2
3
4
B
L2 ipsi dCINs
1
2
3
4
V
M
1
2
3
4
C
L5 ipsi dCINs
1
2
4
3
V
M
1
2
3
4
1%
5s

Figure 3

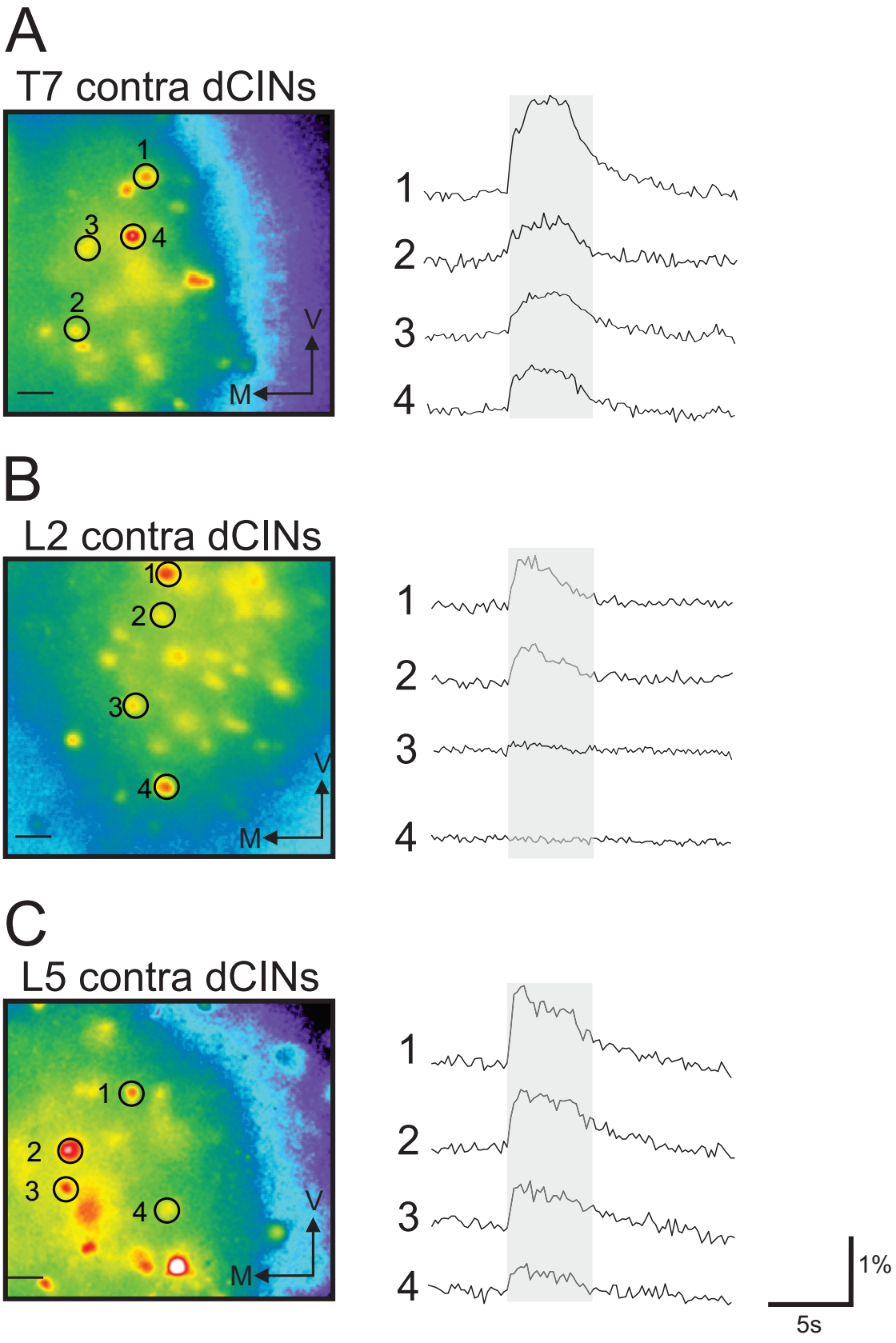
A
T7 contra dCINs
1
3
4
2
V
M
1
2
3
4
B
L2 contra dCINs
1
2
3
4
V
M
1
2
3
4
C
L5 contra dCINs
1
2
3
4
V
M
1
2
3
4
1%
5s

Figure 4

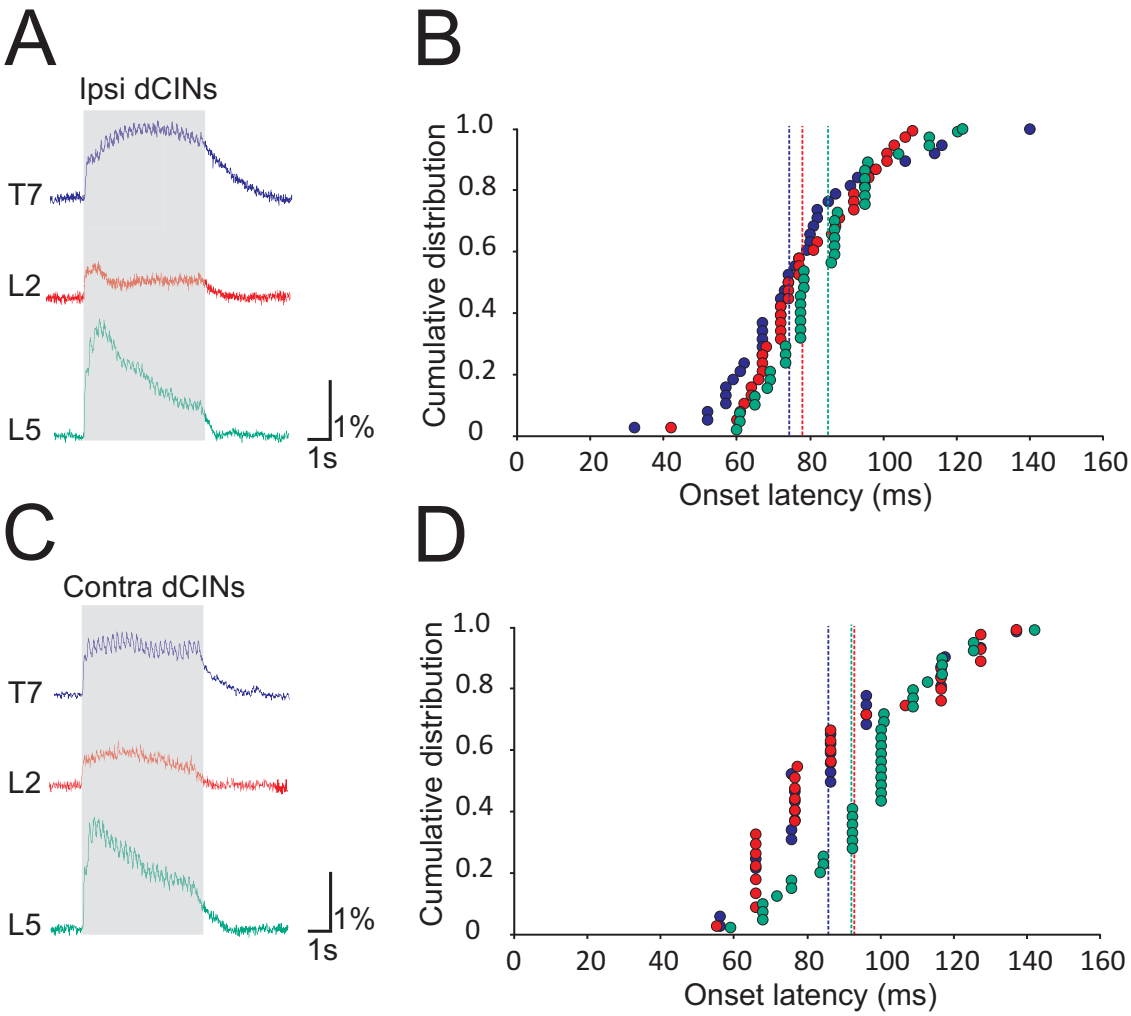
A
Ipsi dCINs
T7
L2
L5
1%
1s
B
Cumulative distribution
1.0
0.8
0.6
0.4
0.2
0
0
20
40
60
80
100
120
140
160
Onset latency (ms)
C
Contra dCINs
T7
L2
L5
1%
1s
D
Cumulative distribution
1.0
0.8
0.6
0.4
0.2
0
0
20
40
60
80
100
120
140
160
Onset latency (ms)

Figure 5

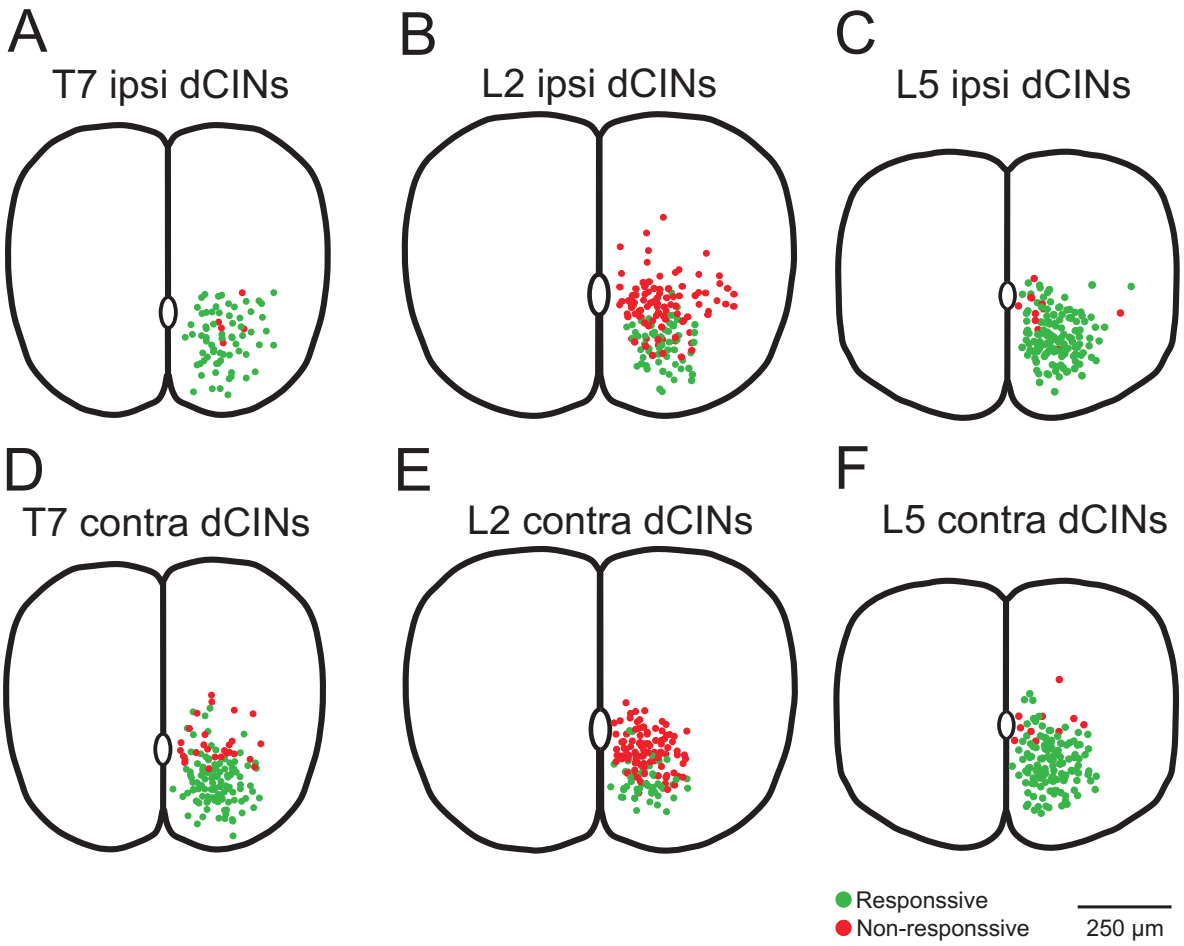
A
T7 ipsi dCINs
B
L2 ipsi dCINs
C
L5 ipsi dCINs
D
T7 contra dCINs
E
L2 contra dCINs
F
L5 contra dCINs
Responssive
Non-responssive
250 µm

Figure 6

	Ipsi			Contra		
	T7	**L2**	**L5**	**T7**	**L2**	**L5**
# dCINs recorded	83	160	149	145	148	142
# dCINs responsive	77	58	138	115	50	132
% dCINs responsive	92.8 %	36.3 %	92.6 %	79.3 %	33.8 %	92.9 %

Table 1

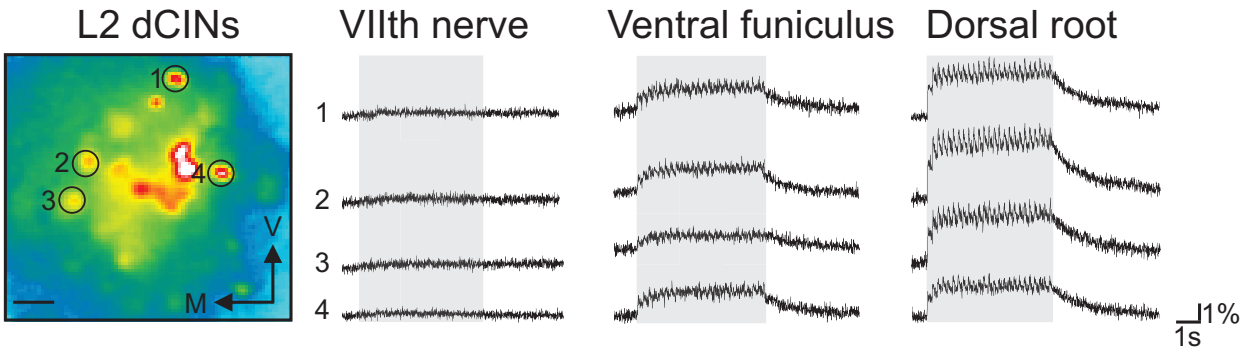

Supplementary figure 1

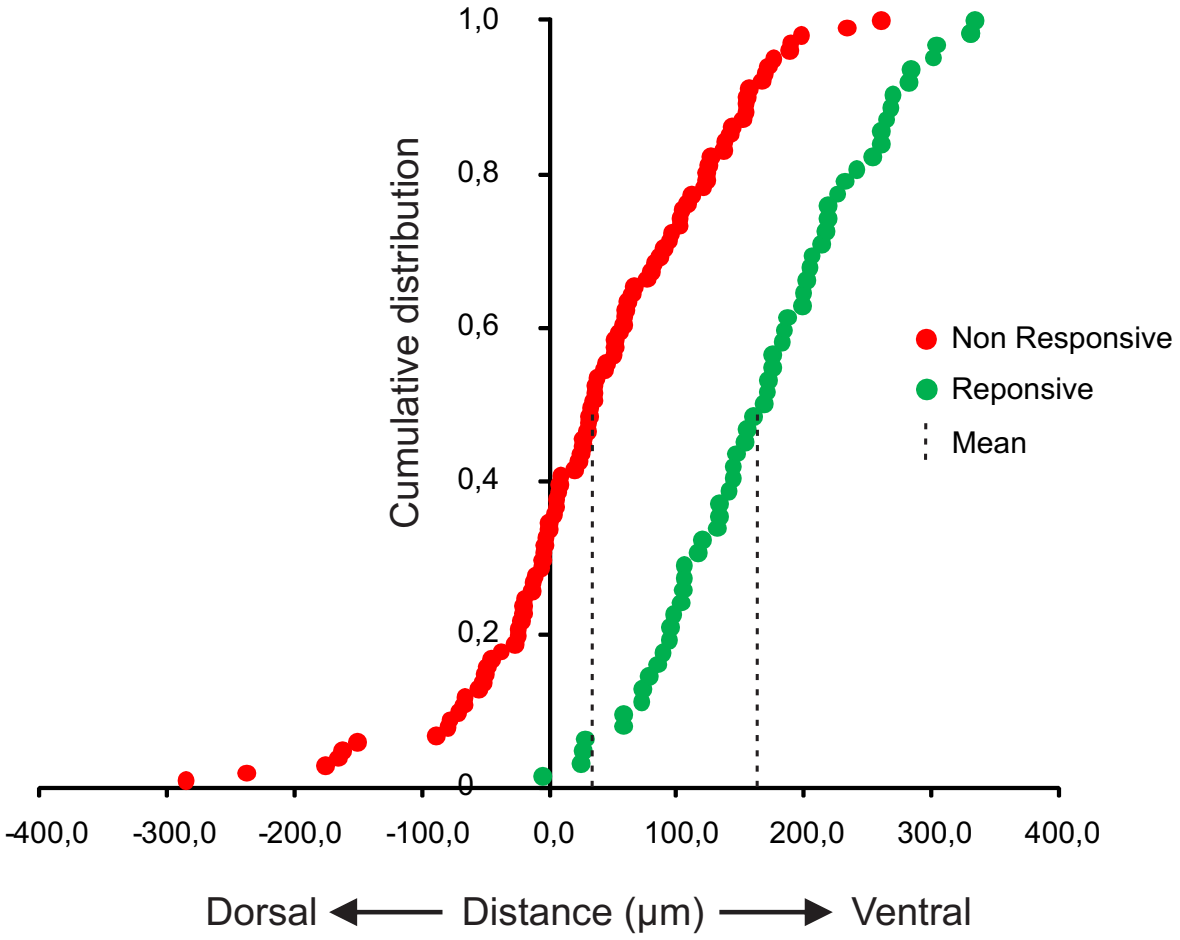

Supplementary figure 2